NASA CONTRACTOR REPORT

NASA CR-1234

A LUNAR GRAVITY SIMULATOR

VOLUME II

by Richard J. Morgen

Prepared by
CASE WESTERN RESERVE UNIVERSITY
Cleveland, Ohio
for Langley Research Center

NATIONAL AERONAUTICS AND SPACE ADMINISTRATION • WASHINGTON, D. C. • DECEMBER 1968

NASA CR-1234

A LUNAR GRAVITY SIMULATOR

VOLUME II

By Richard J. Morgen

From a thesis entitled "The Design of a Vertical Lunar Gravity Simulator" submitted to Case Institute of Technology in partial fulfillment of the requirement for the Degree of Master of Science in Mechanical Engineering.

Prepared under Contract No. NAS 1-7459 by
CASE WESTERN RESERVE UNIVERSITY
Cleveland, Ohio

for Langley Research Center

NATIONAL AERONAUTICS AND SPACE ADMINISTRATION

For sale by the Clearinghouse for Federal Scientific and Technical Information
Springfield, Virginia 22151 – CFSTI price $3.00

ABSTRACT

The design of a vertical lunar gravity simulator is presented. The simulation technique involves negating the various limb segments spearately using constant-force negator springs. Overhead support is provided by magnetic air pads which offer negligible resistance to horizontal movement. The torso harness that is used provides for six degrees of freedom over a wide range of movements.

The dynamic behavior of the lunar gravity simulator is considered. Indications are that low fatigue-life negator coils mounted back-to-back will be suitable as constant-force, long-deflection springs. A conical drum, adjustable-force negator unit is optimized for minimum weight. A technique for determing the mass and center of mass of the various body segments is also presented. An analysis to determine the correct attachment points for negating the limbs and torso is presented. It is recommended that negator coils of the lowest rated fatigue life be used as constant-force, long-deflection spring elements.

TABLE OF CONTENTS

	Page
ABSTRACT	iii
TABLE OF CONTENTS	v
LIST OF FIGURES	vii
LIST OF SYMBOLS	ix
1.0 INTRODUCTION	1
1.1 Introduction	1
1.2 Types Of Simulators	2
1.3 General Description of Case Simulator	5
2.0 DESIGN EQUATIONS FOR NEGATOR UNITS	9
Introduction	9
2.1 Force Vs. Extension	11
2.1.1 Simple extension type	11
2.1.2 Torque motor type	24
2.2 Fatigue Life Characteristics	31
2.2.1 Force to weight ratio vs. fatigue life	31
2.2.2 Adjustability	33
3.0 SIMULATOR DYNAMICS	38
3.1 Simple Approximate Solutions	38
3.2 One-Dimensional Simulator Dynamics	41
3.3 Two-Dimensional Simulator Dynamics	48
4.0 NEGATOR UNIT DESIGN	53

Page

4.1 Design Techniques 54

4.1.1 Width alternation 54

4.1.2 Backwound-frontwound techniques 55

4.1.3 Adjustment 56

4.2 Optimum conical drum design 57

5.0 HARNESS DESIGN 74

5.1 Cable Suspension Analysis 74

5.1.1 4-Point torso suspension 75

5.1.2 "L-C brace" torso suspension 75

5.1.3 Limb suspension 76

5.2 Segment Weight Determination 85

6.0 PROTOTYPE SYSTEM 93

6.1 Negator Units 93

6.2 Magnetic Air Pads 96

6.3 Prototype Harness 98

REFERENCES 104

APPENDIX A Two-Dimensional Simulator Dynamics 106

APPENDIX B Computer Programs 121

LIST OF FIGURES

Figure	Title	Page
1.1	Sketch of Inclined-Plane Simulator	3
1.2	4-Point Torso Suspension Vertical Simulator	6
1.3	"L-C Brace" Torso Suspension Vertical Simulator	8
2.1	Negator Simple Extension Coil	10
2.2	Two Negator Coils Mounted Back-To-Back	10
2.3	Sketch of Length of Negator Material	12
2.4	Force Characteristics For H16P38 Negator Coil	20
2.5	Force Characteristics For H20R47 Negator Coil	21
2.6	Force Characteristics for H25S48 Negator Coil	22
2.7	Force Characteristics of Frontwound-Backwound Negator Coil	25
2.8	Torque Characteristics of Torque-Motor	29
2.9	Stress Factor-Fatigue Life Relationship	32
2.10	Functional Relation Between Weight-To-Force Ratio And Rated Fatigue Life Of Negator Coils	34
2.11	Adjustability Function	36
3.1	Typical One-Dimensional Jump	45
3.2	Dynamic Effects of Using Different Fatigue Life Coils	47
3.3	Two-Dimensional Dynamic Jump Showing Air Pad Motion	49

3.4	Dynamic Effects of Using Different Fatigue Life Coils	50
3.5	Dynamic Effects of Increasing Overhead Weight	52
4.1	Adjustable Conical Drum Negator Unit Design	58
4.2	Optimum Force-To-Weight Ratios For SH31U58 Coils Mounted Back-To-Back	69
4.3	Optimum Curves - SH31U58 Coil	70
4.4	Optimum Force-To-Weight Ratios For SL31U69	71
4.5	Optimum Curves For SL31U69 Coil	72
5.1	Segment Weight Determination: Arm Immersion Tank	88
5.2	Segment Weight Determination: Balance Board	90
5.3	Balance Board Showing Load Cell and Pivot	91
6.1	Prototype Back-To-Back Adjustable Conical Drum Negator Unit	94
6.2	Magnetic Air Pad	97
6.3	Magnetic Air Pad Cluster	97
6.4	Prototype Harness	99
6.5	Prototype Harness	100
6.6	Prototype Harness	101
6.7	Prototype Harness: Seat	102
6.8	Prototype Harness: Rear Bearing Pivot Point	103
6.9	Prototype Harness: Side Bearing Pivot Point	103
A1	Lunar Gravity Simulator Model	107

LIST OF SYMBOLS

a	distance from joint (knee or elbow) to cable attachment point
b	spoke thickness
c	$HW^{-1/3}$ (body build index)
d	total body density
d_c	length between negator drums
d_{LA}	density of lower arm plus hand
d_{LL}	density of lower leg plus foot
d_{UA}	density of upper arm
d_{UL}	density of lower leg
	energy
E	Young's modulus of negator material
E_m	Young's modulus of conical section
F	force output of negator coil
F_c	constant negator force
F_2	limb negating force
F_1	reaction force at hip (or shoulder) joint
f	force per unit length
g	acceleration due to earth gravity
H	height of subject
h	spoke width
I	moment of inertia of negator material

I_s	moment of inertia of negator spool
I_c	moment of inertia of coiled portion of negator coil
K	$24\rho_w L/E$
L	total length of negator coil
l	length of unwound portion of negator coil
L_1	length of upper limb
L_2	length of lower limb
l_1	distance to center of mass of upper limb
l_2	distance to center of mass of lower limb
M_1	mass of upper limb
M_2	mass of lower limb
M	mass of test subject
M_n	total mass of negator coils
m	thickness of conical section
P	pressure
P''_{cr}	critical backing load
Q_x	generalized force
q	flange thickness of conical section
R	radius of curvature
R_n	natural radius of curvature of negator coils
R_1	radius of take-up drum for torque-motor
R_2	radius of output drum for torque-motor
R_{io}	radius of take-up drum for negator coil

R_{no}	initial natural radius of curvature of negator coil
R_o	radius of negator take-up drum
r	R_n/R
S_f	stress factor ▫ t/R_n
T	torque output of torque-motor
T_m	kinetic energy of test subject
T_n	kinetic energy of negator
T_1	cable tension at shoulders
T_2	cable tension at hips
T_s	kinetic energy of negator spool
t	thickness of negator coil
W	weight of test subject minus weight of limb
W_t	weight of test subject
w	width of negator coil
x	extension of negator coil
y	distance from neutral axis
α	cone angle
β	buckling load factor
Δ	small increment
ε	strain
θ	angle
μ	Poisson's ratio

ρ	density of negator material
ρ_w	weight density of negator material
σ	stress
σ_{ml}	bending stress at tip of spoke
σ_w	working stress
τ	shear stress
ω	angular velocity
$\dot{(\ )}$	d/dt
$\ddot{(\ )}$	d^2/dt^2
$(\ )_x$	x - direction
$(\ )_y$	y - direction
$(\ )_z$	z - direction

INTRODUCTION

1.1 Introduction

Manned lunar flights will be realized in the near future. Exploration of the lunar surface by man is an essential part of the Appolo lunar mission. Effects of the lunar gravity on the ability of an explorer to perform self-locomotive tasks will probably be appreciable. Because the lunar environment is considerably different from that on the earth, the explorers will have to learn how to adjust their accustomed methods of walking, etc.

There are two major factors affecting a lunar explorer's performance: 1) Lunar gravity is approximately 1/6 earth gravity, and 2) The explorer will be wearing a space suit with life support equipment. To quantitatively evaluate the expected performance of a lunar explorer before the actual Apollo flight, it becomes necessary to simulate realistically the lunar environment. Kinematic and physiological data can then be collected from test subjects performing the required lunar tasks in a simulated lunar environment. Conclusions can be drawn as to how the lunar gravity and spacesuit restrictions will affect the explorer's performance.

1.2 Types Of Simulators

Several types of lunar gravity simulators have been constructed and many others proposed.[19] Langley Research Center has developed a cable suspension, inclined plane simulator[7] that has been used extensively in research programs, (see, for example, reference [11]). In this simulator the test subject is held by cables inclined so that he forms an angle of approximately 9.5° with the floor. (see Figure 1.1). The test subject has 3 degrees of freedom: 1) walking straight ahead, 2) jumping straight up, and 3) rotating forward. The subject cannot move sideways at all, but during normal walking there isn't normally very much sideways movement. The simulator has worked well in self-locomotive studies.

Several types of six degree of freedom simulators have been constructed. Many of these have been used to simulate a zero-gravity situation. Most of them involve a series of gimbals on bearings which allow a test subject to rotate about his center of mass in any rotational direction (see, for example, reference [7], Figure 5, page II-9). When adapted for use as lunar gravity simulators these usually suffer from the fact that the necessary mechanisms involve the addition of a considerable amount of mass to the test

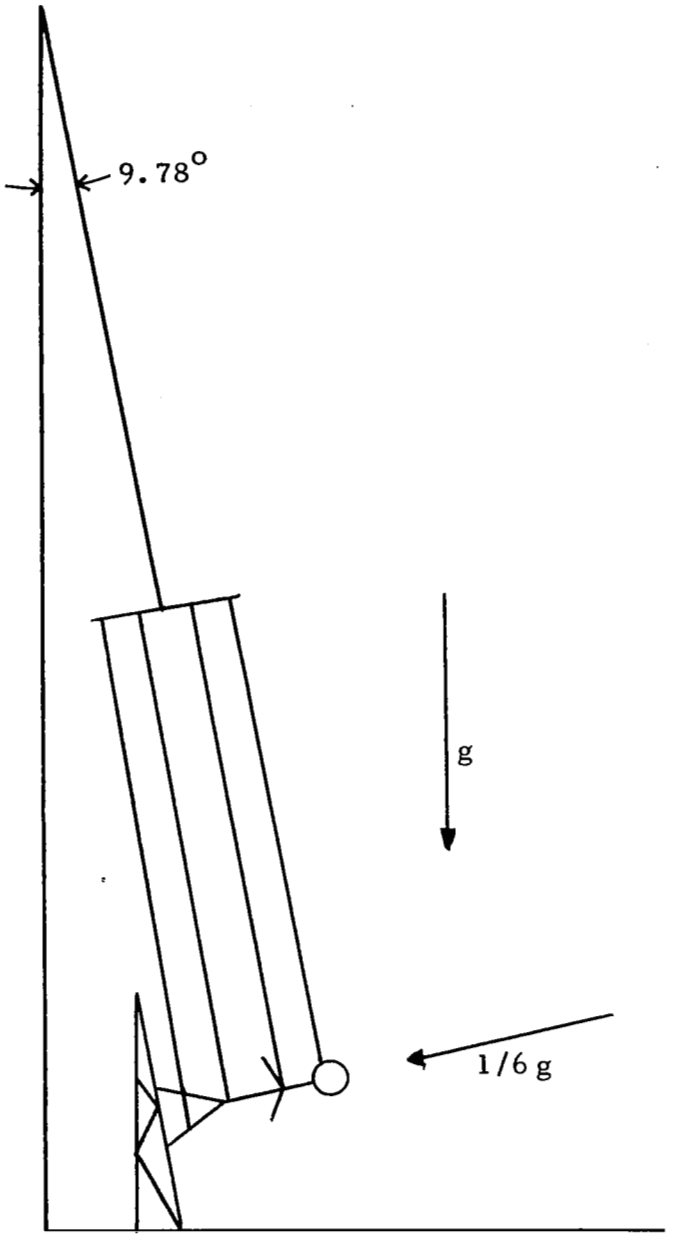

Figure 1.1
Sketch of Inclined-Plane Simulator

subject. This can be at least partly justified because a lunar explorer will be burdened with a great deal of additional mass in the form of a spacesuit and life support equipment. However, during biomedical testing, it becomes necessary to add still more mass in the form of medical data gathering equipment; and the total resultant mass may be more than the lunar explorer will carry while on the moon.

In addition, these simulators may have no provision for negation of the test subject's arms and legs. The main problem is to effectively negate the torso and still allow for true simulation when the subject pivots about his center of mass. However, about 30-35% of the body mass is in the limbs and this fact should not be neglected. The total body center of mass can very appreciably during normal movements,[13] but it is felt that the centers of mass of the individual body segments will not exhibit this same variation. Therefore, if the body segments are negated separately, better simulation should result over a wider range of normal body movements.

1.3 General Description Of Case Simulator

The Initial design work on the Case lunar gravity simulator was based on the following observations:

1) Six degrees of freedom in a simulator would be desirable since even the simplest self-locomotive tasks involve movement that requires six degrees of freedom; and, if these movements are neglected in a simulator, erroneous test results could result. Moreover, various stability problems could be present which would not show-up if the test subject were constrained to less than 6 degrees of freedom.

2) Elementary self-locomotive tasks do not require the full use of all 6 degrees of freedom. One must be able to rotate in any direction, but one need not have the capability to rotate a full 360° in any direction. Rotation in the simulator should be far enough to give the subject an indication of when he has lost his balance.

3) It would be desirable to have the test subject standing upright rather than being held almost horizontal as in the inclined plane simulator.

A preliminary concept of a simulator based on the above observations evolved which involved a test subject being held somewhat like a puppet and standing in an upright position (see Figure 1.2). The desire was to negate the major body

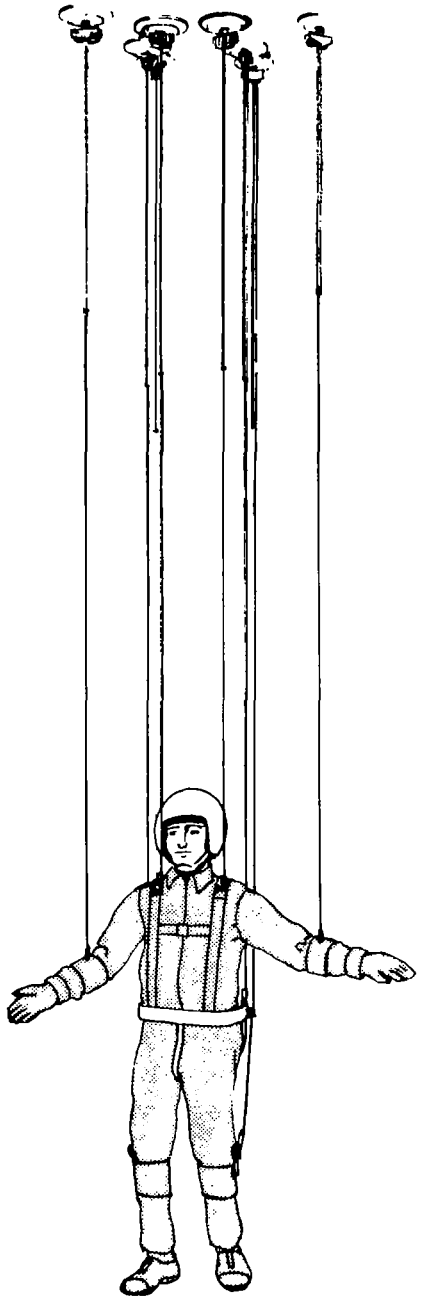

Figure 1.2 - - 4-Point Torso Suspension

components separately in an effort to achieve better simulation. Constant force springs were to be used to negate the body segment's weight. It soon became evident during preliminary investigations (which included a full-size prototype mock-up) that the resultant cable interference was intolerable. It was still felt that the body components should be negated separately, but a better method whould have to be found for achieving this objective.

The concept that eventually evolved is shown in Figure 1.3. The torso is negated by an "L-C" brace which allowed for rotation, and the legs and arms are negated by separate cables. A further innovation was to attach the leg suspension cables directly to the torso harness mechanism in a fashion which allows the cables to remain directly above their attachment points.

The constant force spring elements are negator spring units which are further described in the succeeding sections. Overhead support is provided by magnetic air pads acting against a smooth steel ceiling which exhibit a large holding force while offering negligible resistance to horizontal movement. These air pads are described in another report.[10] The harness design for the Case simulator was done by the Industrial Design Department of the Cleveland Institute of Art working with Case Institute of Technology.

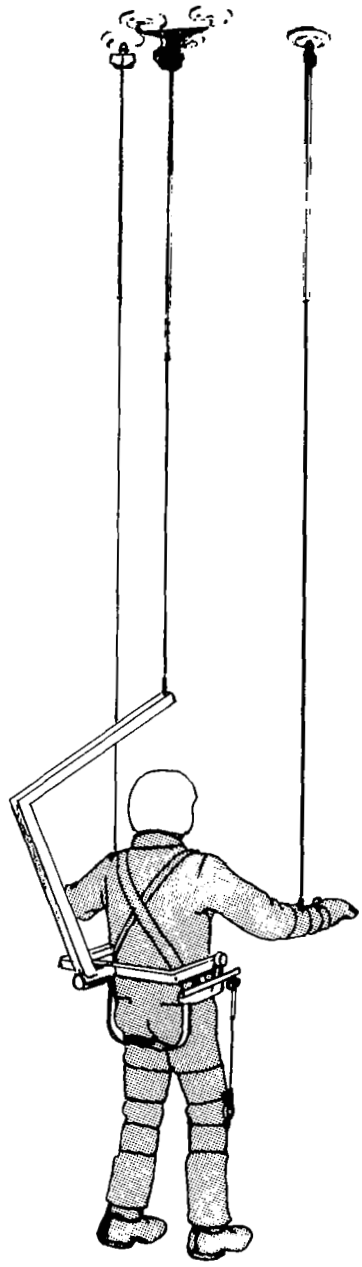

Figure 1.3 - - "L-C Brace" Torso Suspension

DESIGN EQUATIONS FOR NEGATOR UNITS

A negator spring is a device which provides a constant tension for any degree of extension within its designed range. The type proposed for this application is shown in Figure 2.1. It consists of a prestressed strip of flat spring steel, coiled tightly around a bushing. The spring can be uncoiled by applying a force, the magnitude of which depends on the geometry and dimensions of the coil. Figure 2.2 depicts two coils mounted back-to-back in the configuration proposed for use in the lunar gravity simulator.

The force obtained by unwinding a negator coil is almost perfectly constant (i.e., force-extension gradient is zero). Through various methods of manufacturing control, gradients ranging from slightly positive to slightly negative can be achieved.

A dynamic analysis of the proposed system indicates that a negator having a slightly positive force-extension gradient is desirable. The reason for this is that as the negator coil is unwound, an increasing force must be exerted to overcome the weight of the extended portion.

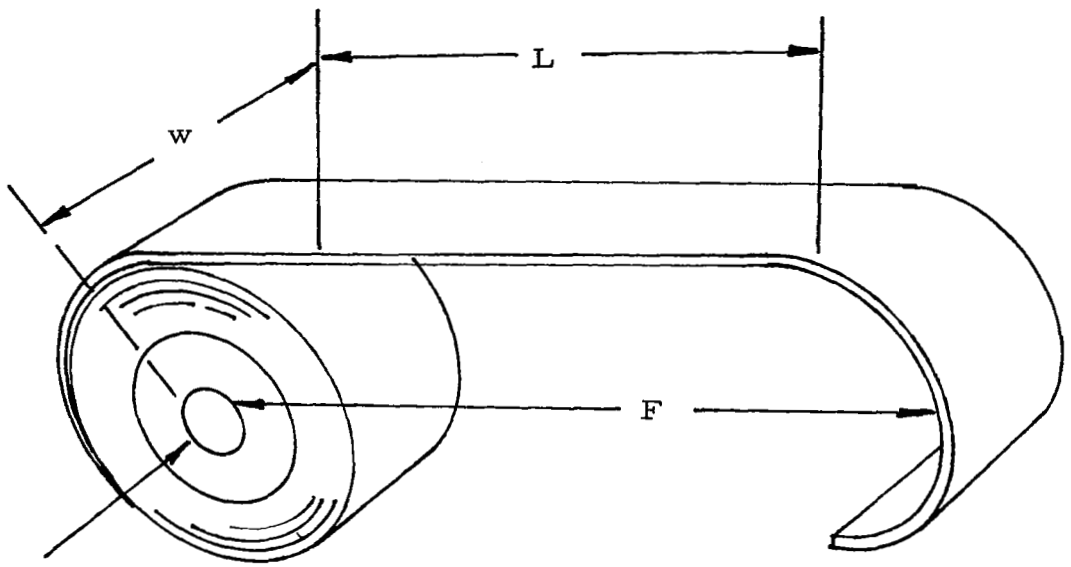

Figure 2.1

Negator Simple Extension Coil

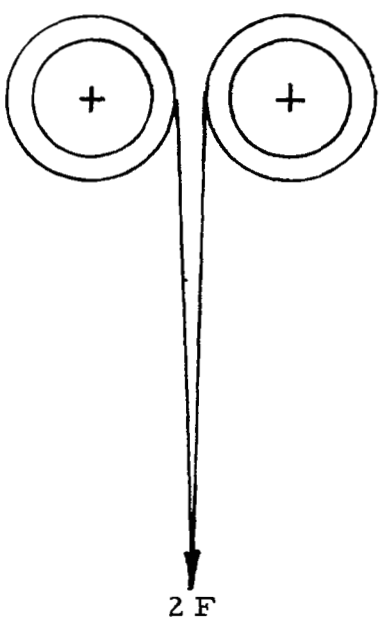

Figure 2.2

Two Negator Coils Mounted Back-To-Back

2.1 Force Vs Extension

2.1.1 Simple extension coil

In this section the equations describing the force verses extension for simple negator coils mounted in a back-to-back configuration will be derived. The derivation is based on a paper by Votta.[18]

First the problem of bending of a thin plate will be considered: A bending moment is applied to a thin plate as shown in Figure 2.3. We will assume that the simple beam formulas apply. Consider a thin plate bent into an arc with a radius of curvature R by a moment M. Using Hooke's Law (assuming $\sigma_y = 0$

$$\varepsilon_x = \frac{1}{E}[\sigma_x - \mu\sigma_z] \qquad (2.1)$$

$$\varepsilon_z = \frac{1}{E}[\sigma_z - \mu\sigma_x] \quad . \qquad (2.2)$$

Now it is observed that for thin plates, there is very little distortion of a cross-section in the y-z plane except at the edges, therefore:

$$\varepsilon_z = 0 \qquad (2.3)$$

and, consequently from Equation 2,

$$\sigma_z = \mu\sigma_x \qquad (2.4)$$

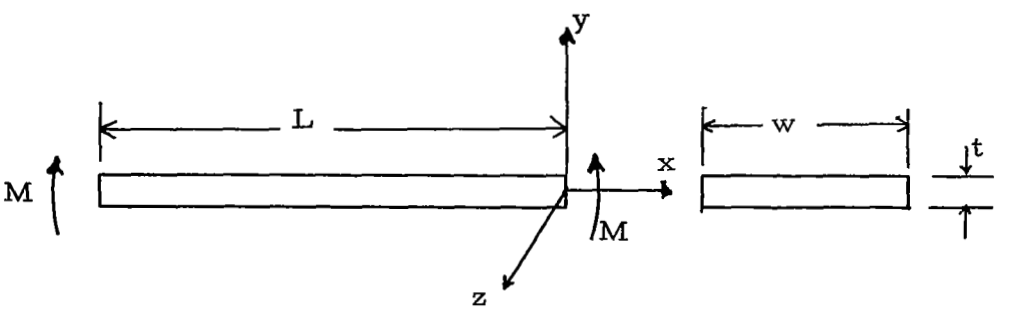

Figure 2.3 - - Sketch Of
Length Of Negator Material

and $$\varepsilon_x = \frac{1}{E}\left[\sigma_x - \mu^2\sigma_x\right] \qquad (2.5)$$

$$\varepsilon_x = \left(\frac{1-\mu^2}{E}\right)\sigma_x \quad . \qquad (2.6)$$

The relation between the resultant radius of curvature and ε_x is:

$$\varepsilon_x = y/R \quad . \qquad (2.7)$$

The end conditions require that:

$$M = \int_{-y/2}^{+y/2} \sigma_x w y dy \qquad (2.8)$$

$$\sigma_x = \frac{E}{1-\mu^2}\frac{y}{R} \qquad (2.9)$$

$$M = \frac{Ewt^3}{12R(1-\mu^2)} \qquad (2.10)$$

since $I = wt^3/12$

$$M = \frac{EI}{(1-\mu^2)R} \quad . \qquad (2.11)$$

However, this equation, (2.11), does not apply to the negator coil because, although the negator material is very thin, the distortion of the cross-section in the y-z plane is servere and Equation (2.3) does not apply. Instead

$$\sigma_z = 0 \qquad (2.12)$$

and

$$\varepsilon_z = -\frac{\mu}{E}\sigma_x \qquad (2.13)$$

$$\varepsilon_x = \frac{1}{E}\sigma_x \quad . \qquad (2.14)$$

The equations analogous to equations 2.8-2.11 are then as follows:

$$M = \int_{-y/2}^{+y/2} \sigma_x w y dy$$

$$\sigma_x = \frac{Ey}{R}$$

$$M = \frac{Ewt^3}{12R}$$

$$M = \frac{EI}{R} \quad . \qquad (2.15)$$

This is the moment-curvature relation, obtained using elementary beam theory.

The negator coil has an initial radius of curvature, R_n. If we apply a moment M:

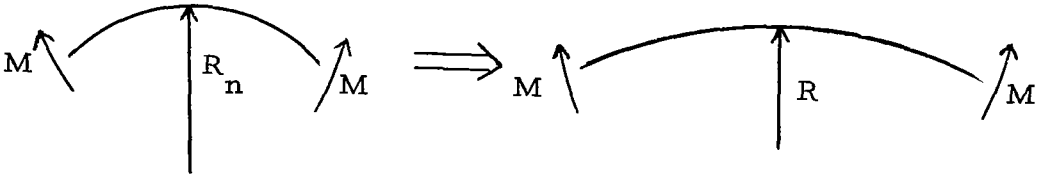

$$M = EI\left(\frac{1}{R_n} - \frac{1}{R}\right) \quad . \tag{2.16}$$

To determine the energy stored in a length of coil L ; consider the following sketch:

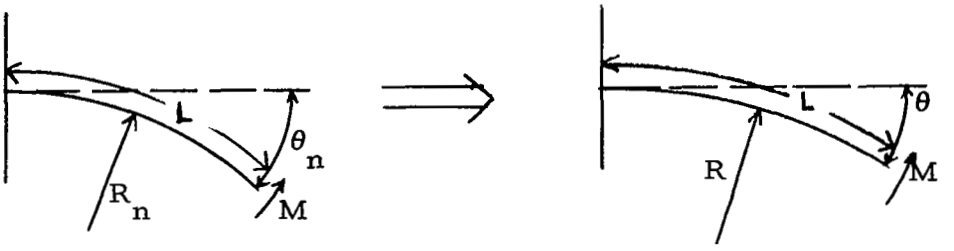

The energy, $\mathcal{E}$, is:

$$\mathcal{E} = -\int_{\theta n}^{\theta} M d\theta$$

$$\theta = \frac{L}{R} \qquad d\theta = \frac{-L}{R^2}\, dR$$

$$\mathcal{E} = +\int_{R_n}^{R} EI\left(\frac{1}{R_n} - \frac{1}{R}\right)\frac{L}{R^2}\, dR \quad . \tag{2.17}$$

Integrating this relation, we obtain:

$$\mathcal{E} = \frac{EIL}{2}\left[\frac{1}{R_n^2} + \frac{1}{R^2} - \frac{2}{R_n R}\right] \quad . \tag{2.18}$$

Now consider the following sketch:

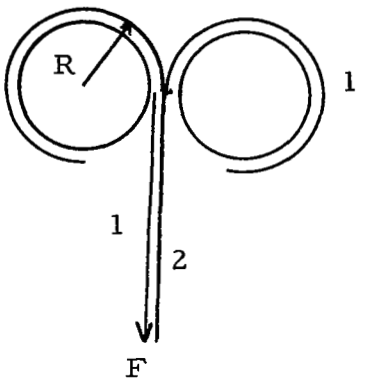

The energy of each coil in state (1) is

$$\mathcal{E}_1 = \frac{EIL}{2}\left[\frac{1}{R^2} + \frac{1}{R_n^2} - \frac{2}{R_n R}\right] \quad .$$

The energy when pulled straight, (2), is

$$\mathcal{E}_2 = \frac{EIL}{2}\left(\frac{1}{R_n}\right)^2 \quad .$$

Since $FL = 2(\mathcal{E}_2 - \mathcal{E}_1)$;

$$F = EI\left[\frac{2}{R_n R} - \frac{1}{R^2}\right] \quad . \qquad (2.19)$$

To find F as a function of L we must find R as a function of L.

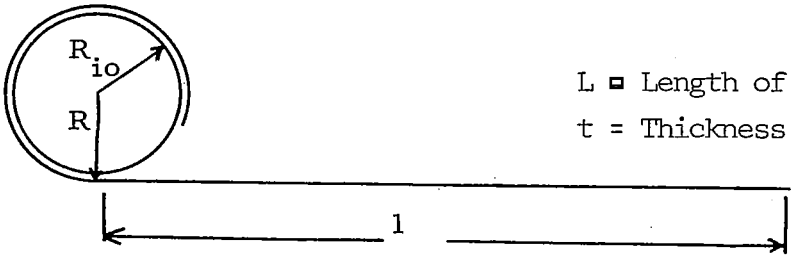

We can write

$$R = [R_{io}^2 + \frac{t}{\pi}(L-1)]^{1/2} \quad .$$

So the force equation becomes:

$$F = \frac{Ewt^3}{12}\left[\frac{2}{R_n[R_{io}^2+\frac{t}{\pi}(L-1)]^{1/2}} - \frac{1}{R_{io}^2+\frac{t}{\pi}(L-1)}\right] \quad . \qquad (2.20)$$

Votta[18] indicated that the natural radius of curvature, R_n, undergoes a change during heat treatment according to the following relation

$$R_n = \frac{13}{15} R_{no} + \frac{2}{15} r \quad . \qquad (2.21)$$

Substituting this into Equation (2.20) we obtain

$$F = \frac{Ewt^3}{12}\left[\frac{2}{[\frac{2}{15}(R_{no}^2+\frac{t}{\pi}(L-1))^{1/2}+\frac{13}{15}R_{no}][R_{io}^2+\frac{t}{\pi}(L-1)]^{1/2}} - \frac{1}{R_{io}^2+\frac{t}{\pi}(L-1)}\right] \quad . \qquad (2.22)$$

Because of the fact that R_n is increased in the outer coils during heat treatment, the negator unit has a different force versus extension characteristic when backwound. It is necessary to substitute l = for $L-l$ in the first term in brackets in Equation (2.22)

$$F_{Bw} = \frac{Ewt^3}{12}\left[\frac{2}{\left[\frac{3}{15}\left(R_{no}^2+\frac{t}{\pi}(l)\right)^{1/2}+\frac{13}{15}R_{no}\right]\left[R_{io}^2+\frac{t}{\pi}(L-l)\right]^{1/2}}\right.$$

$$\left. - \frac{1}{R_{io}^2+\frac{t}{\pi}(L-l)}\right] \quad . \qquad (2.23)$$

One possible way to achieve adjustability of the back-to-back negator arrangement would be to vary the diameter of the drums on which the coils are wrapped. It would be desirable to have an analytical expression for the $\frac{\partial F}{\partial R}$:

We have

$$F = EI\left[\frac{2}{R_n R} - \frac{1}{R^2}\right]. \quad . \qquad (2.24)$$

Differentiating with respect to R

$$\frac{\partial F}{\partial R} = EI\left[\frac{-2}{R_n R^2} + \frac{2}{R^3}\right] \quad . \qquad (2.25)$$

This equation can be written in a different way. If we make the substitutions;

$$R_{n/R} = r \ , \tag{2.26}$$

$$I = \frac{wt^3}{12} \tag{2.27}$$

we have

$$\frac{\partial F}{\partial R} = \frac{Ewt^3}{12R_n^3}[-2r^2 + 2r^3] \tag{2.28}$$

and using $\frac{t}{R_n} = S_f$

$$\frac{\partial F}{\partial R} = \frac{Ew}{6} S_f^3 r^2 (r-1) \quad . \tag{2.29}$$

We now have a simple approximate formula for $\frac{\partial F}{\partial R}$

Computer programs utilizing the above equations were developed in order to get a rapid and accurate theoretical force versus extension characteristic for many different coils.

The force vs. extension characteristics were determined experimentally for three 2500 cycle fatigue life stock negator coil units each with two coils mounted back-to-back. The results are plotted in Figures 2.4 thru 2.6, together with the predicted force characteristics.* The predicted force is higher than the experimentally observed force in every case. There is a corresponding decrease in the difference between the value

* The negator coil numbers refer to a code used by the Hunter Spring Company; Hatfield, Pa.

Figure 2.4 - - Force Characteristics
Of H16P38 Negator Coil

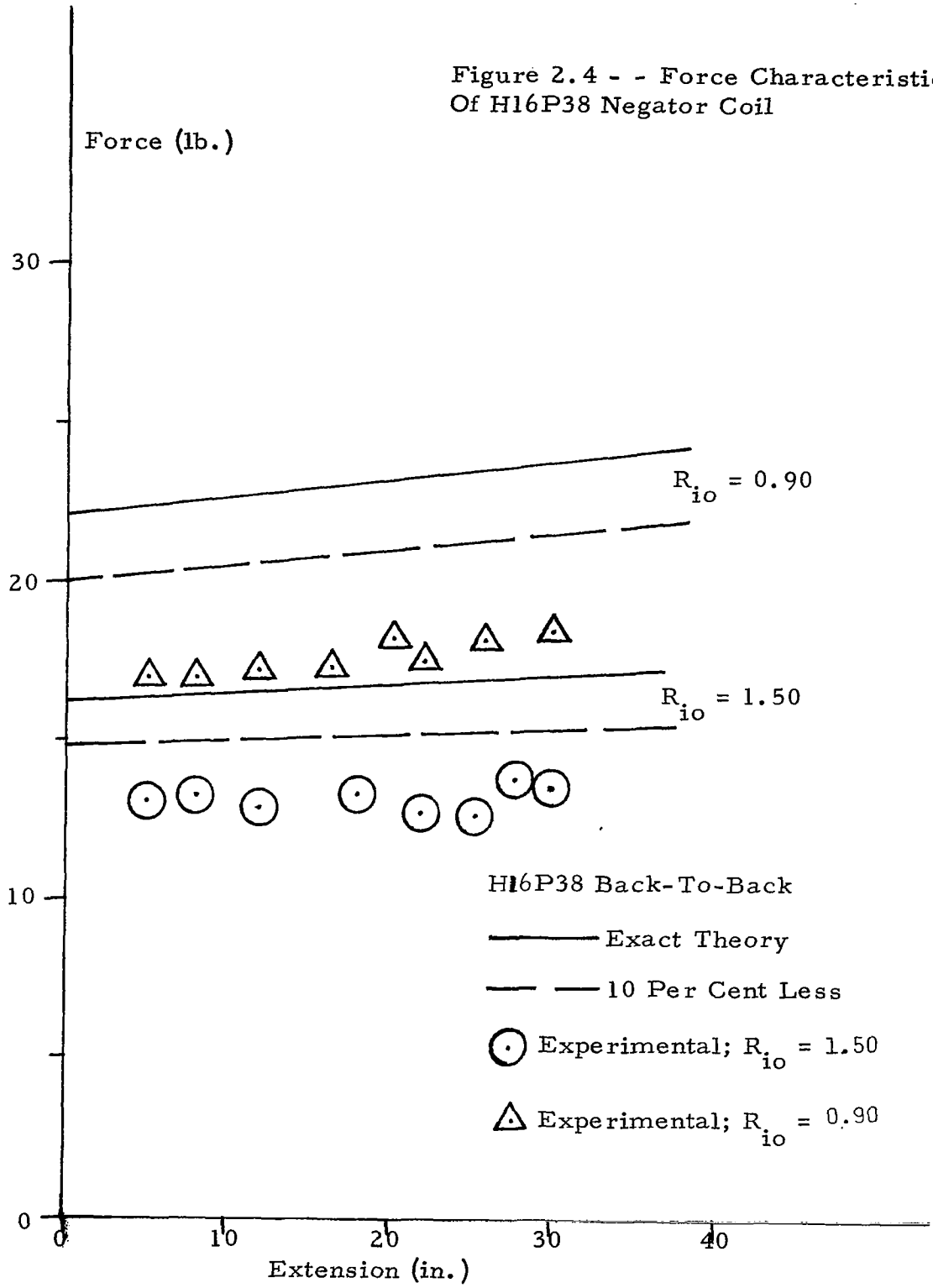

Figure 2.5 - - Force Characteristics
Of H20R47 Negator Coil

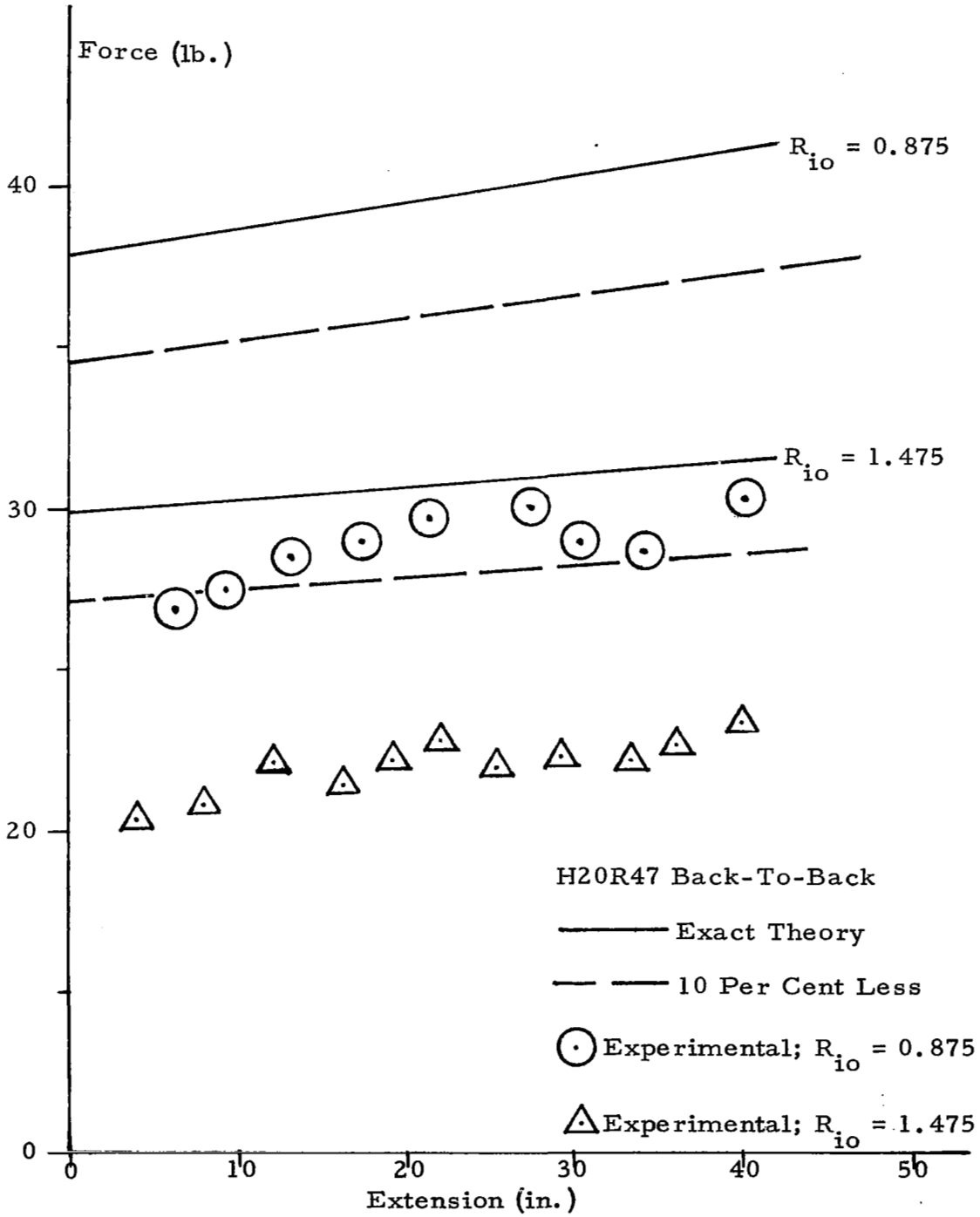

Figure 2.6 - - Force Characteristics
Of H25S48 Negator Coil

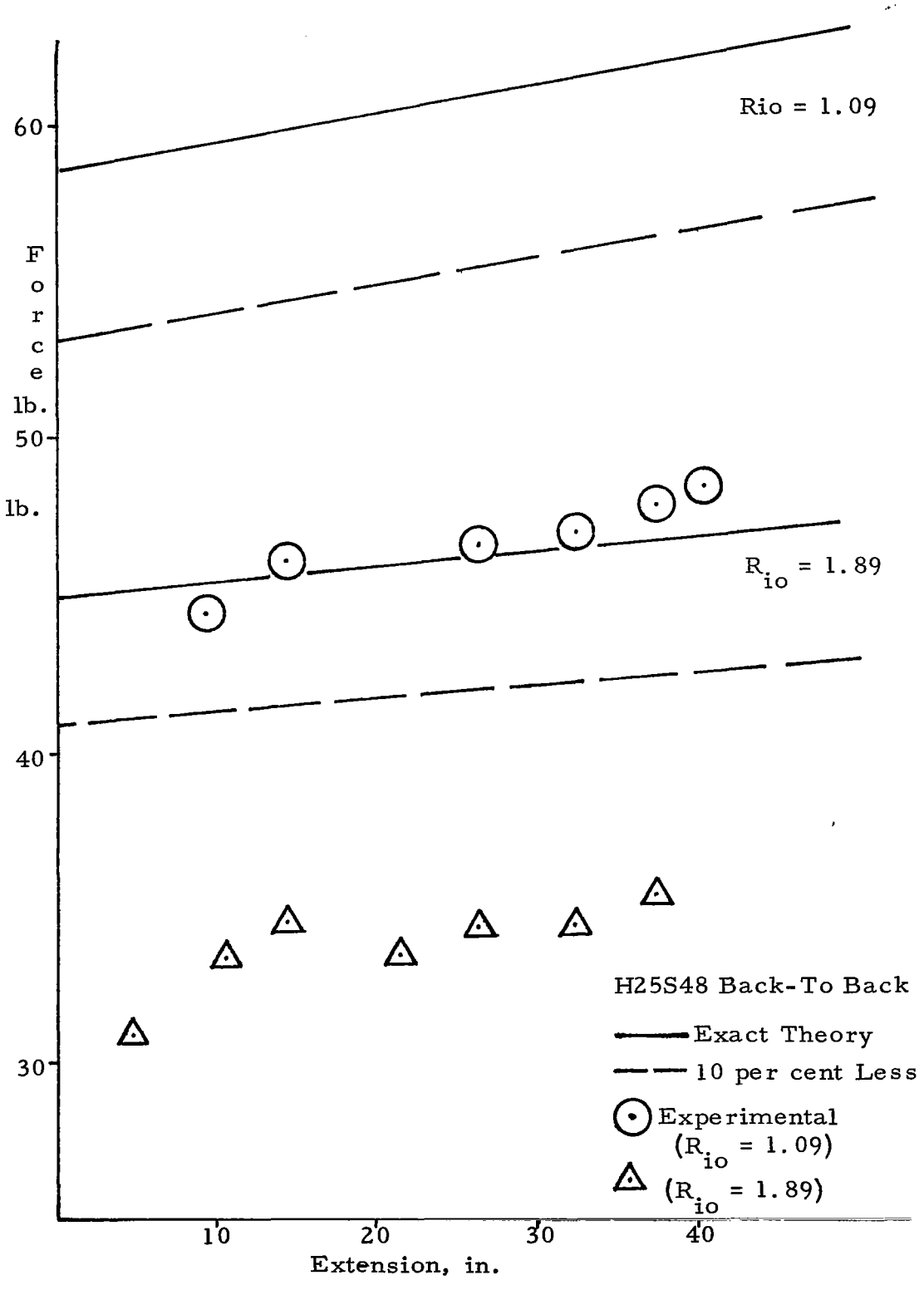

of the force at the high and low values of R_{io}. There are several reasons for this discrepancy. Because the negator coils are mounted on drums which are a finite distance apart, the coils cannot be straightened completely during force measurement. The model on which the force derivation is based assumed that the coils were perfectly straight after leaving the drums. Quantitative evaluation of this effect is very difficult, and is further complicated by the fact that the distance between the drums on which the coils are mounted can vary depending on the diameter of the drums. This is because the force measurements were taken using adjustable drums (see section 4.2).

The curves on the graphs of Figures 2.4 - 2.6 labeled "10% less" represent a force that is 10% less than the derived force labeled "exact theory." Votta[18] has derived a theoretical force for negator coils which is approximately 10% less that the represented by equation 2.19:

$$F = EI\left[\frac{2}{R_n R} - \frac{1}{R^2} \right]$$

The force expression Votta derived is given by :

$$F = (1-\mu^2)EI\left[\frac{2}{R_n R} - \frac{1}{R^2} \right]$$

and since $\mu = 0.3$; $1-\mu^2 = 0.9$ and therefore this force is approximately 10% less than the correct theoretical value.

Another possible reason for the discrepancy between the theoretical and experimental forces is the fact that the coils are sold with a force specification of ±10%. The force is a

strong function of thickness (t^3) so a small variation in thickness could result in large variations in force.

At any rate equation 2.19 can be used for design purpose if one recognized the fact that actual force will probably be lower. If the negator units are designed to be adjustable, it becomes unnecessary to have an exact expression for the force.

When the negator coils are backwound the force output becomes almost constant. Figure 2.7 shows the force characteristics of a typical back-to-back negator unit that is backwound together with the same coils frontwound. It can be seen that the backwound coils exhibit a "flatter" force vs. extension curve.

2.1.2 Torque-Motor

In this section the equations describing the torque output of the "Torque-Motor" configuration will be derived. The configuration to be studied is shown in the following sketch

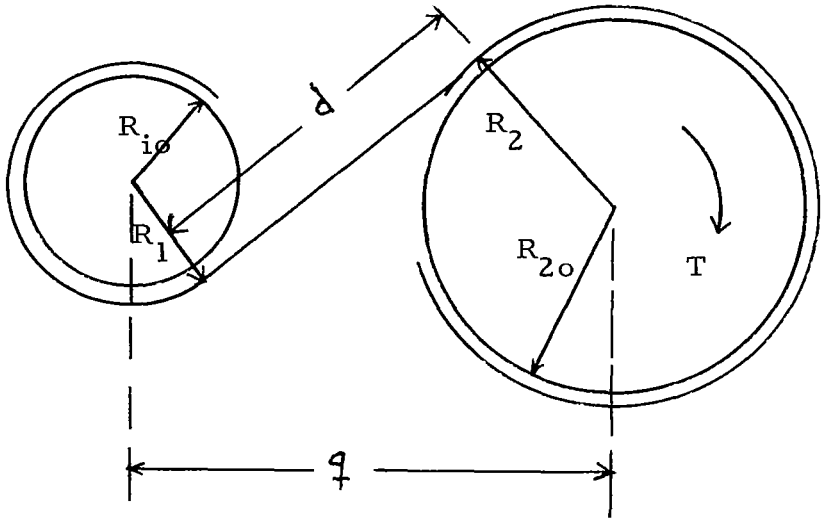

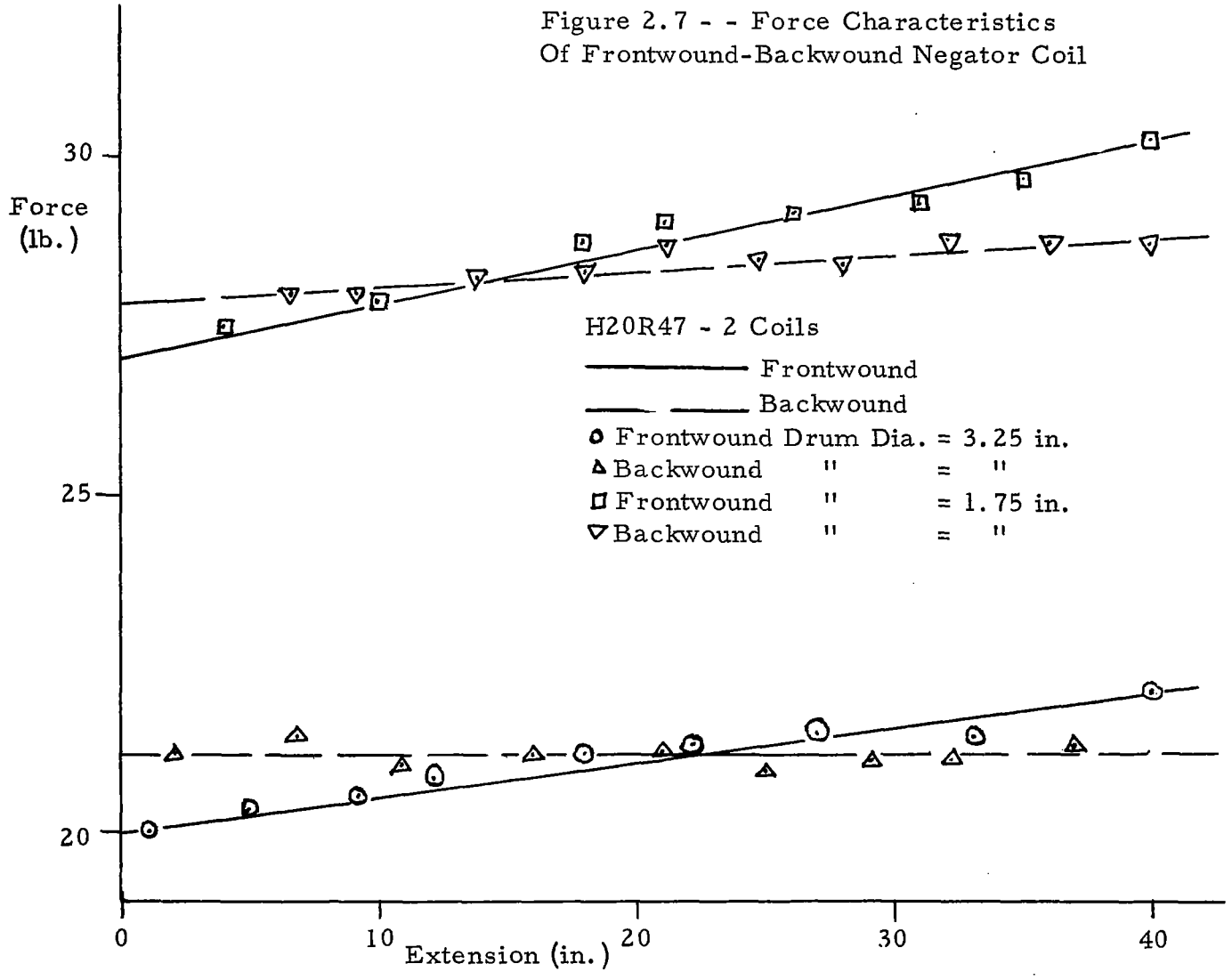

Figure 2.7 - - Force Characteristics
Of Frontwound-Backwound Negator Coil

The coil on drum (1) is in a relaxed state. A torque, T, is developed on drum (2) as the coil is pulled straight through zone d and then wrapped counter to its relaxed curvature on drum (2). To get a force output a 3rd drum could be attached to drum (2), and an output cable wound on the 3rd drum.

The energy $\Delta\mathcal{E}_1$, of a short length of coil, Δl, on drum (1) can be expressed as

$$\Delta\mathcal{E}_1 = \frac{EI}{2}\Delta l\left(\frac{1}{R_n} - \frac{1}{R_1}\right)^2 \quad . \tag{2.32}$$

The corresponding energy, $\Delta\mathcal{E}_2$, of a short length of coil Δl. Wrapped on drum (2) can be written:

$$\Delta\mathcal{E}_2 = \frac{EI\Delta l}{2}\left(\frac{1}{R_n} + \frac{1}{R_2}\right)^2 \quad . \tag{2.33}$$

The change in energy, $\Delta\mathcal{E}$, as a short length of coil Δl passes from drum (1) to drum (2) is

$$\Delta\mathcal{E} = \Delta\mathcal{E}_2 - \Delta\mathcal{E}_1 = \frac{EI\Delta l}{2}\left[\left(\frac{1}{R_n} + \frac{1}{R_2}\right)^2 - \left(\frac{1}{R_n} - \frac{1}{R_1}\right)^2\right] \quad . \tag{2.34}$$

This change in energy can also be written as:

$$\Delta\mathcal{E} = T\Delta\theta \qquad \frac{\Delta l}{\Delta\theta} = R_2 \tag{2.36}$$

Letting $\Delta \rightarrow d$

$$\frac{d\mathcal{E}}{d\theta} = T = \frac{d\mathcal{E}}{dl}\frac{dl}{d\theta} = R_2\frac{d\mathcal{E}}{dl} \tag{2.37}$$

So from (2.34)

$$\frac{d\mathcal{E}}{dl} = \frac{EI}{2}\left[\frac{1}{R_2^2} - \frac{1}{R_1^2} + \frac{2}{R_n}\left(\frac{1}{R_2} + \frac{1}{R_1}\right)\right] \qquad (2.38)$$

and using (2.37)

$$T = \frac{EIR_2}{2}\left[\frac{1}{R_2^2} - \frac{1}{R_1^2} + \frac{2}{R_n}\left(\frac{1}{R_2} + \frac{1}{R_1}\right)\right] \quad . \qquad (2.39)$$

Votta[18] derived a similar expression;

$$T = \frac{EIR_2}{2}\left[\frac{1}{R_n} + \frac{1}{R_2}\right]^2 \qquad (2.40)$$

by assuming that $R_n \square R_1$. It can be seen that Equation (2.39) will reduce to (2.40) if $R_1 \square R_n$. So that R_2 can be related to R_1, it is necessary to find d as a function of q , R_2, and R_1.

We have:

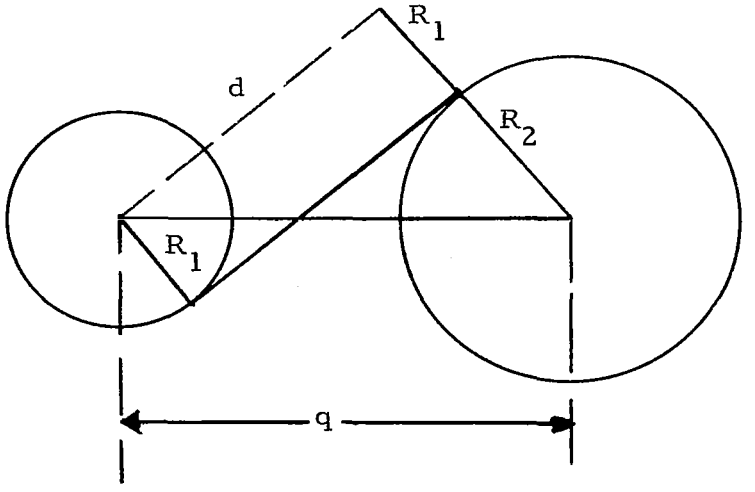

We can see immediately that

$$d^2 + (R_1 + R_2)^2 = q^2 \quad . \tag{2.41}$$

Also, if we denote the length of coil wrapped drum (2) by l and the total coil length by L, we can write:

$$R_2 = [R_{20}^2 + \frac{t}{\pi} l]^{1/2} \tag{2.42}$$

$$R_1 = [R_{10}^2 + \frac{t}{\pi}(L-l-d)]^{1/2} \quad . \tag{2.43}$$

The resulting equations will be greatly simplified if d is replaced by a constant d_c . Let:

$$d_c = [q^2 - (R_{10} + R_{20})^2]^{1/2} \quad . \tag{2.44}$$

Now the Torque equation (2.39) can be used if (2.42), (2.43), and (2.44) are substituted for R_2, R_1, and d.

A fortran computer program was written which used the derived equations to give the output Torque, T , as a function of the number of turns of drum (2). It may be desirable to have a number of take-up drums (1), and so the computer program was written to allow for this.

Computer runs were made for a number of stock "Torque-Motor" coils; utilizing single and multiple take-up drums. The torque output is plotted versus number of output diameters in Figure 2.8 for a typical "Torque-Motor". It is desirable

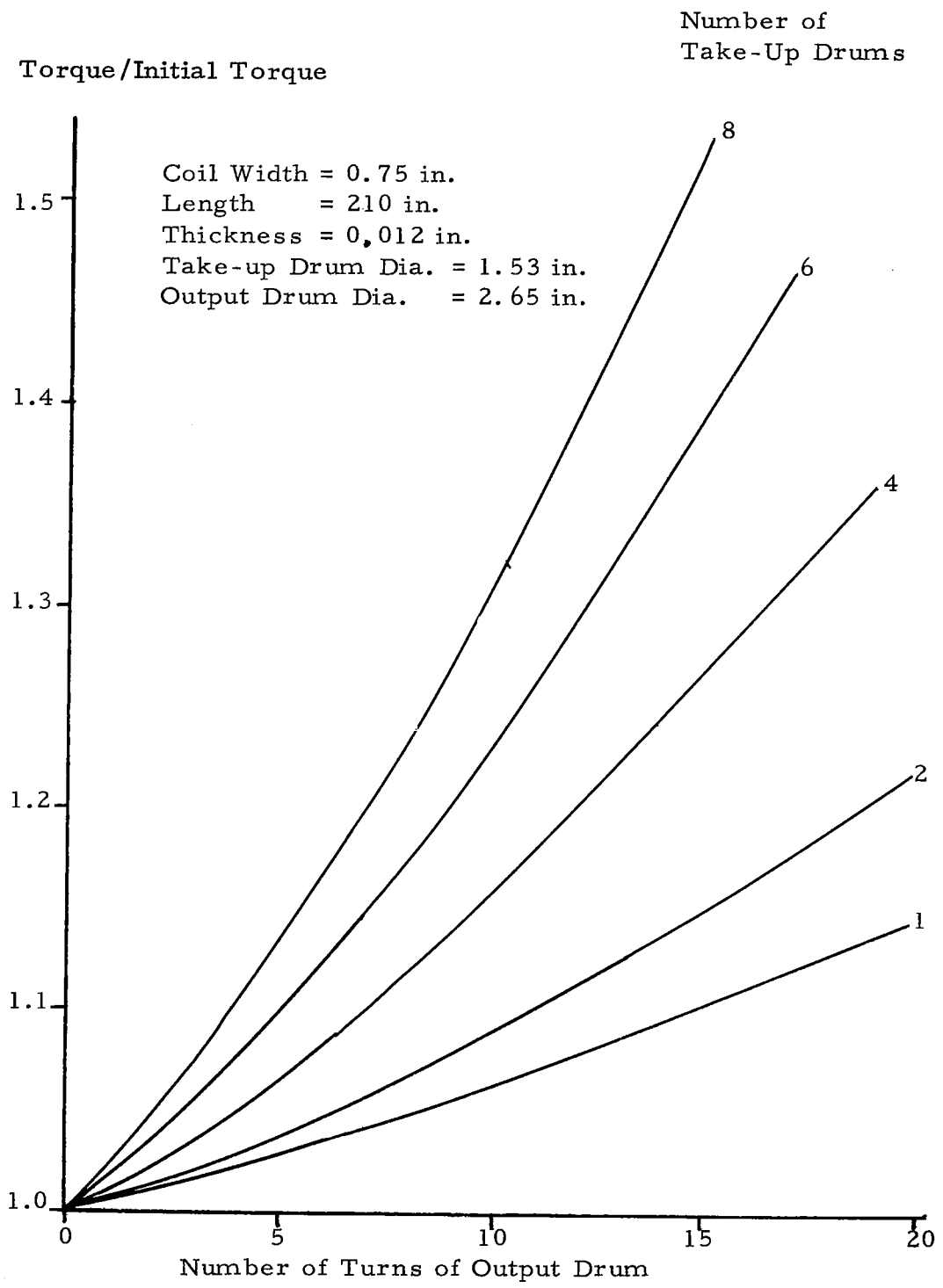

Figure 2.8 - - Torque Characteristics of Torque-Motor

to have the torque constant. It can be seen that as more take-up drums are added to increase torque the torque versus turns characteristic departs further from a constant value. Because of this the torque motor form of negator not considered further. It was decided that simple negator coils mounted back-to-back would provide a more nearly constant force throughout their extension range.

2.2 Fatigue Life Characteristics

2.2.1 Force-to-weight ratio

One of the most important factors affecting the design of the negator units is the fatigue life of the negator coils. The negator coils are highly stressed in order to produce a relatively high force-to-weight ratio, and consequently, they can suffer from very short fatigue lives. The maximum tensile stress in a negator coil when pulled straight is given by;

$$\sigma_{max} = \frac{E}{2} \frac{t}{R_n}$$

a function of t/R_n which is called the stress factor (S_f). One can therefore generate a plot of S_f versus rated fatigue life. Such a curve is shown on the graph of Figure 2.9. Now since the maximum force available from a negator coil is given by

$$F_{max} = \frac{Ewt^3}{24R_n^2} \qquad (2.45)$$

and the weight of the coil is given by

$$\text{weight} = \rho_w wtL \qquad (2.46)$$

The weight/force ratio is

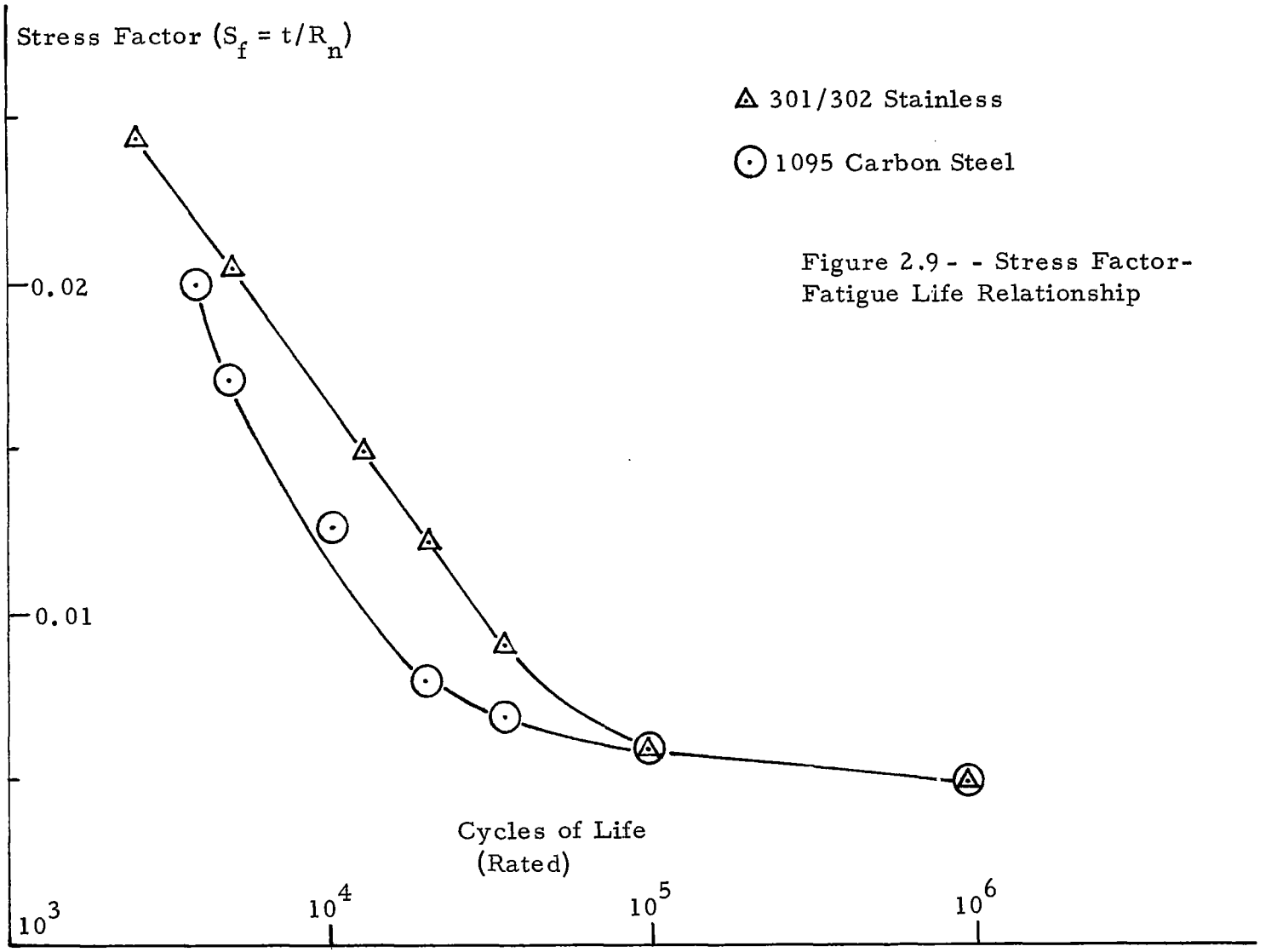

Figure 2.9 - - Stress Factor-Fatigue Life Relationship

$$\text{weight}/F_{max} = \frac{24\rho_w L}{E}\left(\frac{R_n}{t}\right)^2$$

$$= \frac{K}{S_f^2} \quad . \tag{2.47}$$

We see that this ratio is an inverse function of the stress factor squared, and since a low weight to force ratio is desirable, we would like to make S_f as large as possible. But a large stress factor means a low fatigue life. Since $K = \frac{24\rho_w L}{E}$; if we chose a length, L, K will be a function of the material only; and we can make a plot of weight to force ratio versus fatigue life for a given L . Such a plot is shown in Figure 2.10 for two negator coil materials, 1095 carbon steel and 301/202 stainless steel. It is evident that a design trade-off will have to be made between fatigue life and force per unit weight.

2.2.2 Adjustability

The relationship between fatigue life and "adjustability" of negator coils should also be considered. By "adjustability" is meant the change in force for a change in drum diameter or $\frac{\partial F}{\partial R}$. This Equation (2.25) has already been derived:

$$\frac{\partial F}{\partial R} = 2EI\left[\frac{1}{R^3} - \frac{1}{R_n R^2}\right] \tag{2.25}$$

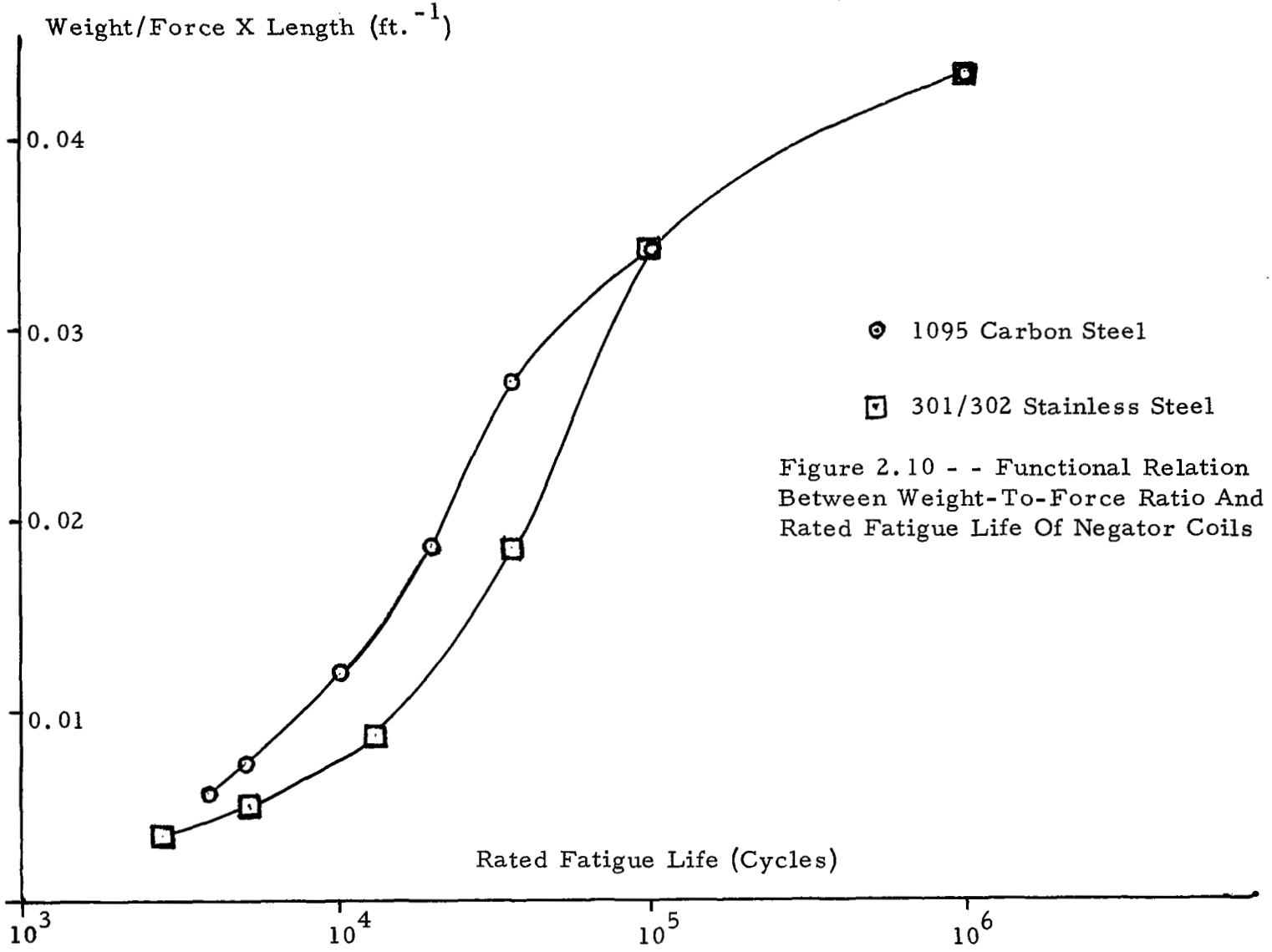

Figure 2.10 - - Functional Relation Between Weight-To-Force Ratio And Rated Fatigue Life Of Negator Coils

Substituting:

$$I = wt^3/12$$

and

$$r = R_n/R$$

we can write

$$\frac{\partial F}{\partial R} = \frac{Ewt^3}{6R_n^3}(r-1)r^2$$

but $t/R_n = S_f$.

So

$$\frac{\partial F}{\partial R} = \frac{Ew}{6} r^2(r-1)(S_f)^3 \quad .$$

It can be seen that $\partial F/\partial R$ is a function of the stress factor cubed. A large value of $\partial F/\partial R$ is desired for good adjustability; therefore, a large value of the stress factor is needed. But a large stress factor means low fatigue life and a design trade-off between the two is indicated. Furthermore, it can be seen that $\partial F/\partial R$ is a function of r , namely $r^2(r-1)$. This function is plotted in Figure 2.11.

The curve has a maximum at a value of $r=2/3$. This is an indication that for maximum adjustability: $r = \frac{R_n}{R}$ should be centered about the value 2/3.

Figure 2.11

Adjustability Function

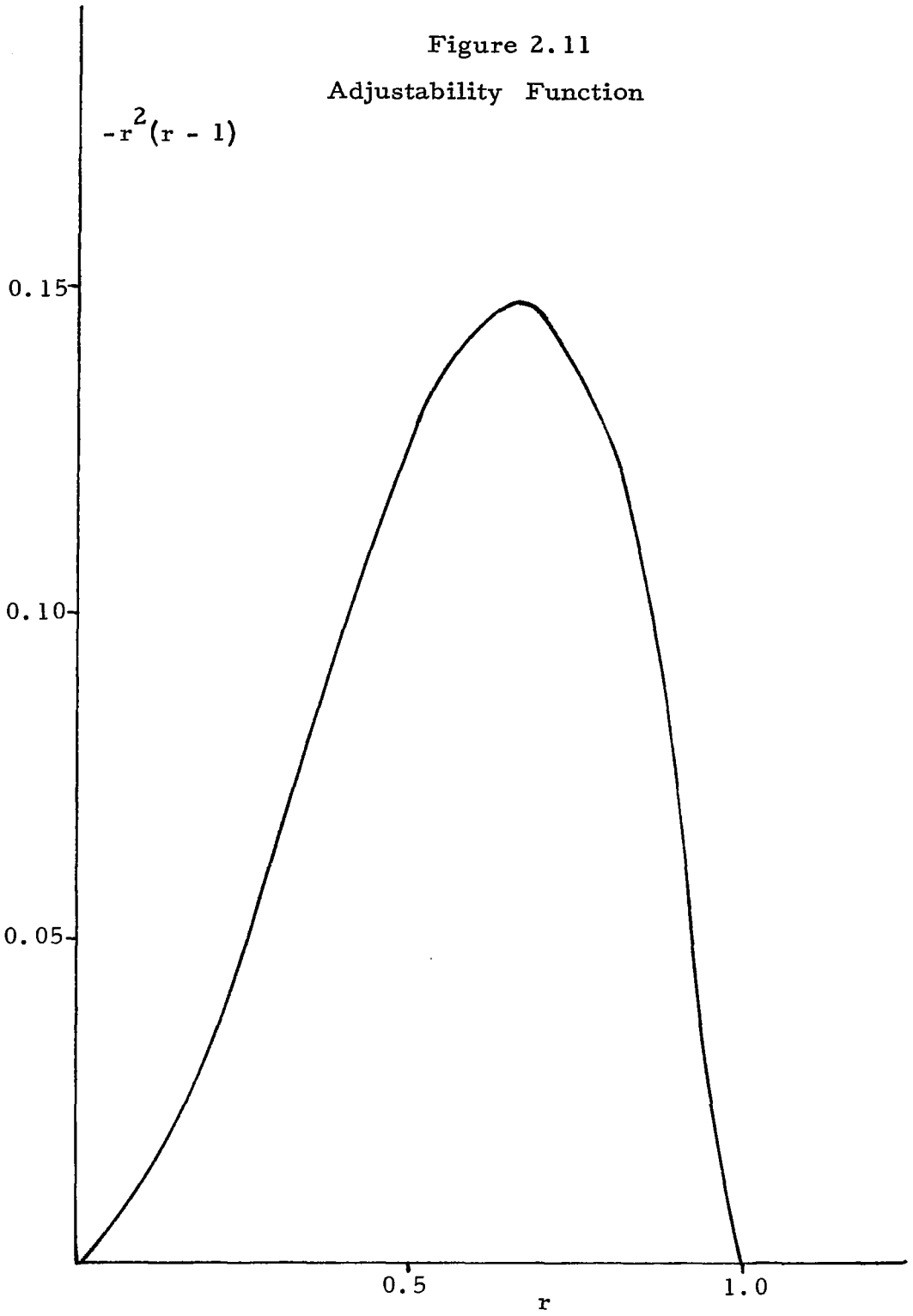

A study of the weight-to-force ratios and adjustability of negator coils indicates that coils of the lowest rated fatigue-life should be used. Limited tests of the fatigue life of negator coils indicated that the coils will last somewhat longer than their rated fatigue life; and, more importantly, their force characteristics do not change with life. Furthermore, should a coil break while in use, it does not pose a safety hazard if the negator coils are always mounted back-to-back. The remaining coil will confine the fractured coil's recoil keeping it well above the test subject. It is therefore recommended that negator coils of the lowest rated fatigue life be used with the lunar gravity simulator.

SIMULATOR DYNAMICS

Introduction

In this section the equations describing the dynamic characteristics of the lunar gravity simulator will be derived. Simple approximate equations and more exact equations which require computer solution are derived. The effects of various parameter changes are studied. The aim is to gain an understanding of dynamic behavior of the simulator and to discover the main factors of design that affect dynamic performance.

3.1 Simple Approximate Solutions

Let us start with the simple system shown below: Two negator coils mounted back-to-back on two spools with a suspended mass.

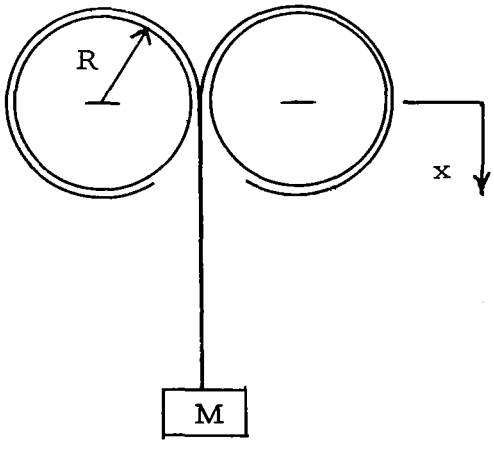

I_s = moment of Inertia of the spool

ρ = mass density of negators

w = width of coils

t = thickness of coils

R = Radius of spools

L = length of coil

Assume that the radius, R, upon which the coils are wrapped is constant and further assume that the force output of the negator unit is such that perfect static simulation is achieved:

$$F = \frac{5}{6} Mg + 2\rho wtxg \quad . \qquad (3.1)^*$$

Writing $f = ma$ for the system:

$$(M + 2\rho wtx)g - F = (M + \frac{I}{R^2} + 2\rho wtx)a \qquad (3.2)$$

where

$$I = 2I_s + 2\rho wt(L-x)R^2 \quad . \qquad (3.3)$$

Solving for the acceleration,

$$a = \frac{(M+2\rho wtx)g - F}{M + \frac{2I_s}{R^2} + 2\rho wtL} \quad . \qquad (3.4)$$

Now using (3.1);

$$a = \frac{1}{6} g[\frac{M}{M + \frac{2I_s}{R^2} + 2\rho wtL}] \quad . \qquad (3.5)$$

We can see immediately that perfect static and dynamic simulation is impossible due to the inertia of the system represented by $2I_s/R^2$ and $2\rho wtL$.

*For this simple analysis, Lunar gravity will be assumed equal to $\frac{1}{6}$ g, which is very close to the true value.

From Equation (3.5), we can see that the acceleration approaches lunar acceleration as the inertia of the spool and the negator approach zero.

Or if we let the static force output of the negator be;

$$F = \frac{5}{6} Mg + 2\rho wtxg - \frac{1}{6} M_n g - \frac{1}{6} \frac{2I_s}{R^2} g \qquad (3.6)$$

where $M_n = 2\rho wtL$

then the acceleration will be:

$$a = \frac{1}{6}g\left[\frac{M+M_n + {}^{2I_s}/_{R^2}}{M+M_n + {}^{2I_s}/_{R^2}} \right] = \frac{1}{6}g \quad . \qquad (3.7)$$

This results in perfect dynamic simulation, but now the static force will be off by an amount

$$\Delta F = \frac{1}{6}g \left(M_n + \frac{2I_s}{R^2}\right) \quad . \qquad (3.8)$$

Therefore, for good simualtion, it would be advantageous to keep the ratio $\Delta F/F$ as small as possible.

3.2 One-Dimensional Simulator Dynamics

In this section a more accurate mathematical model will be formulated to describe the dynamic behavior of the simulator. The analysis will be limited to a consideration of the motion for a jump straight up. The system to be considered is shown in the following sketch:

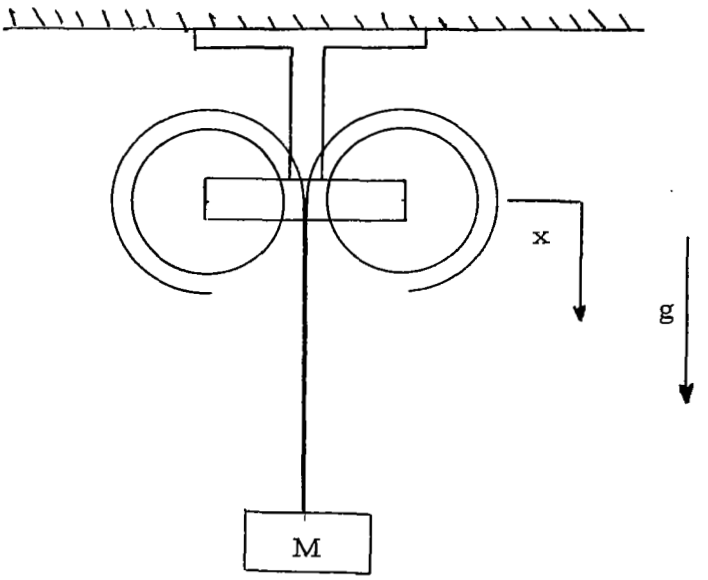

The method of Lagrange will be used to analyze the above system: We can write the kinetic energy of the spools as:

$$T_s = \frac{1}{2} I\omega^2 \tag{3.9}$$

where

$$I = 2I_s + 2I_c \tag{3.10}$$

I_s = moment of inertia of one spool

I_c = moment of inertia of the coiled portion of the negator coil.

$$I_c = \int r^2 dm \qquad r = (R_o^2 + \frac{tl}{\pi})^{1/2}$$

$$dm = \rho wtdl$$

$$I_c = \int_0^{L-x} (R_o^2 + \frac{tl}{\pi})\rho wtdl = \rho wtR_o^2(L-x) + \frac{\rho wt^2}{2\pi}(L-x)^2 \tag{3.11}$$

and since $\omega = \dot{x}/r$, we have:

$$T_s = \frac{1}{2} \frac{\{2I_s+2[\rho wtR_o^2(L-x)+\rho wt^2/_{2\pi}(L-x)^2]\}\dot{x}^2}{R_o^2 + \frac{t}{\pi}(L-x)} \quad . \tag{3.12}$$

The kinetic energy of the extended portion of the negator coils can be written:

$$T_n = \rho wtx\dot{x}^2 \quad . \tag{3.13}$$

The kinetic energy of the mass is: $T_m = \frac{1}{2} M\dot{x}^2$. (3.14)

The generalized force Q_x can be written:

$$Q_x = (2\rho wtx+M)g-F \quad . \tag{3.15}$$

The total kinetic energy of the system is:

$$T = T_s+T_n+T_m$$

$$T = \frac{1}{2} \frac{\{2I_s+2[\rho wtR_o^2(L-x)+\frac{\rho wt^2}{2\pi}(L-x)^2]\}\dot{x}^2}{} + \rho wtx\dot{x}^2+\frac{1}{2}M\dot{x}^2 \tag{3.16}$$

Lagranges equation is:

$$\frac{d}{dt}\left(\frac{\partial T}{\partial \dot{x}}\right) - \frac{\partial T}{\partial x} = Q_x \quad . \tag{3.17}$$

Differentiating (3.16) with respect to $\dot{x}$:

$$\frac{\partial T}{\partial \dot{x}} = \frac{\{2I_s + 2\rho wtR_o^2(L-x) + \frac{\rho wt^2}{\pi}(L-x)^2\}\dot{x}}{R_o^2 + \frac{t}{\pi}(L-x)}$$

$$+ 2\rho wtx\dot{x} + M\dot{x} \quad . \tag{3.18}$$

$$\frac{d}{dt}\left(\frac{\partial T}{\partial \dot{x}}\right) = (2I_s + 2\rho wtR_o^2(L-x) + \frac{\rho wt^2}{\pi}(L-x)^2)$$

$$(\dot{x}^2(R_o^2 + \frac{t}{\pi}(L-x))^{-2}\frac{t}{\pi} + \ddot{x}(R_o^2 + \frac{t}{\pi}(L-x))^{-1})$$

$$+(\dot{x}(R_o^2 + \frac{t}{\pi}(L-x))^{-1})(-2\rho wtR_o^2\dot{x} - \frac{2\rho wt^2}{\pi}(L-x)\dot{x})$$

$$+2\rho wt(\ddot{x}x + \dot{x}^2) + M\ddot{x} \tag{3.19}$$

$$\frac{\partial T}{\partial x} = \rho wt\dot{x}^2 + [\frac{1}{2}\dot{x}^2(2I_s + 2\rho wtR_o^2(L-x) + \frac{\rho wt^2}{\pi}(L-x)^2)]$$

$$[(\frac{t}{\pi})(R_o^2 + \frac{t}{\pi}(L-x))^{-2}]$$

$$+[R_o^2 + \frac{t}{\pi}(L-x)]^{-1}[\frac{1}{2}\dot{x}^2(-2\rho wtR_o^2 - \frac{2\rho wt^2}{\pi}(L-x)] \quad . \tag{3.20}$$

Substituting (3.15), (3.19), and (3.20) into (3.17) and collecting terms we obtain:

$$\ddot{x}[(2I_s + S_2 + S_3)/S_1 + 2\rho wtx + M]$$

$$+ \dot{x}^2[\rho wt + \frac{1}{2}\frac{t}{\pi}(2I_s + S_2 + S_3)/S_1^2 - (\rho wtR_o^2 + \frac{\rho wt^2}{\pi}(L-x))/S_1]$$

$$= (2\rho wtx + M)g - F \qquad (3.21)$$

where $$S_1 = R_o^2 + \frac{t}{\pi}(L-x) \qquad (3.22a)$$

$$S_2 = 2\rho wtR_o^2(L-x) \qquad (3.22b)$$

$$S_3 = (\frac{\rho wt^2}{\pi})(L-x)^2 \quad . \qquad (3.22c)$$

The complexity of Equation (3.21) demanded that a numerical solution be made. A computer program was written to numerically integrate Equation (3.21) using a Runge-Kutta 4th order numerical integration technique.[12] A copy of the developed program is included in appendix B.

The input to the program is an initial upward velocity of the mass. The output of the program gives the trajectory of the mass and its vertical acceleration during the ensuing motion. Figure 3.1 shows a typical simulator jump compared to a true lunar jump with the same initial conditions. The vertical acceleration is also included on the same plot. The"simulator trajectory" is very close to the lunar trajectory in this case.

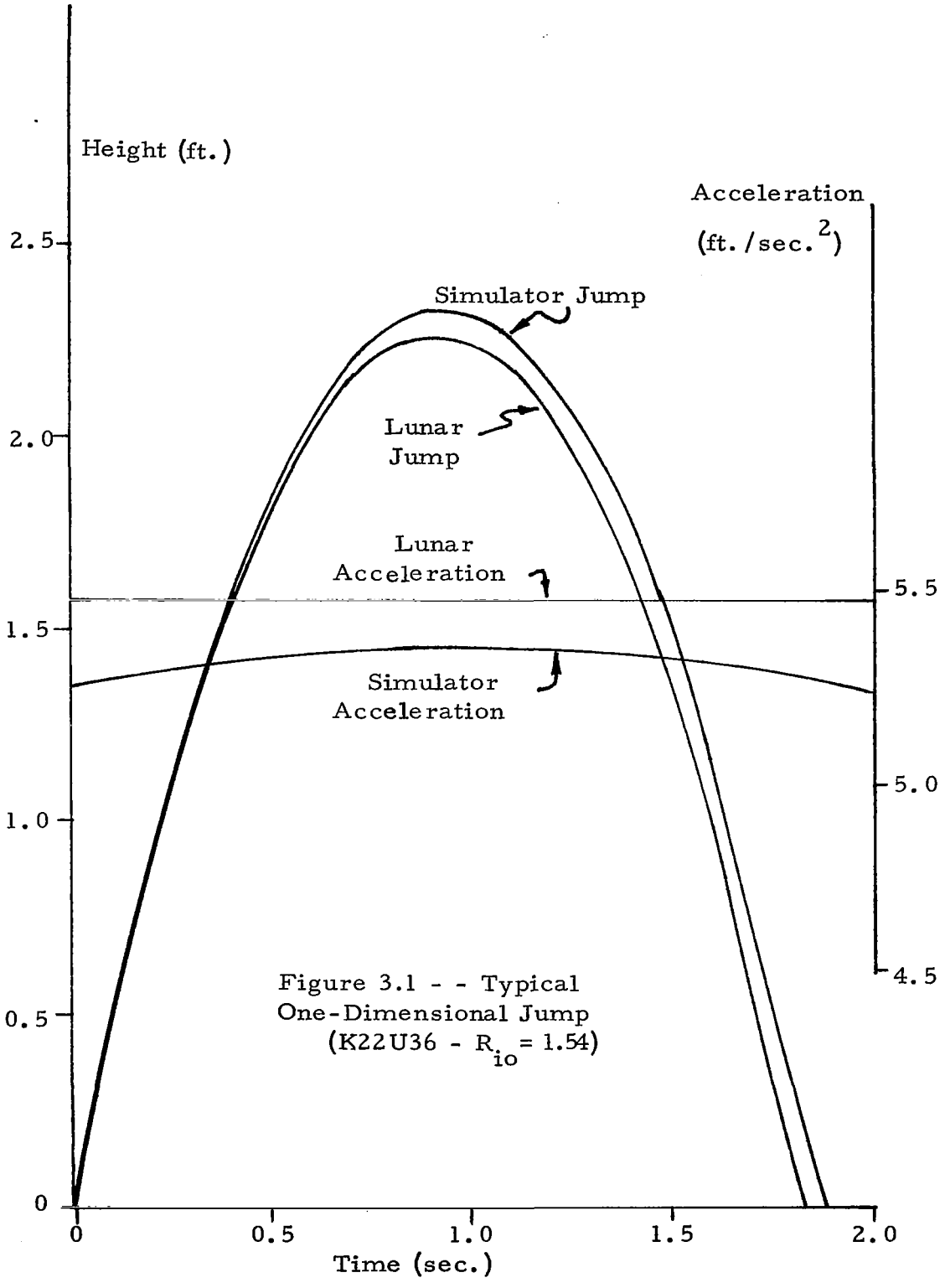

Figure 3.1 - - Typical
One-Dimensional Jump
(K22U36 - R_{io} = 1.54)

As the rated fatigue life of a negator coil increases, the force to weight ratio decreases. To determine quantitatively the effects of using negator coils of different fatigue lives several computer runs were made. The results of these runs are shown in Figure 3.2, together with a lunar jump. It can be seen by observing the trend 1 → 5 that as longer fatigue lives are demanded, the simulation tends to get worse. The "jumper" overshoots by more and more as the weight of the negator coils increases. This is reasonable because the moving parts of the system now have more inertia and thence more energy at a given initial velocity.

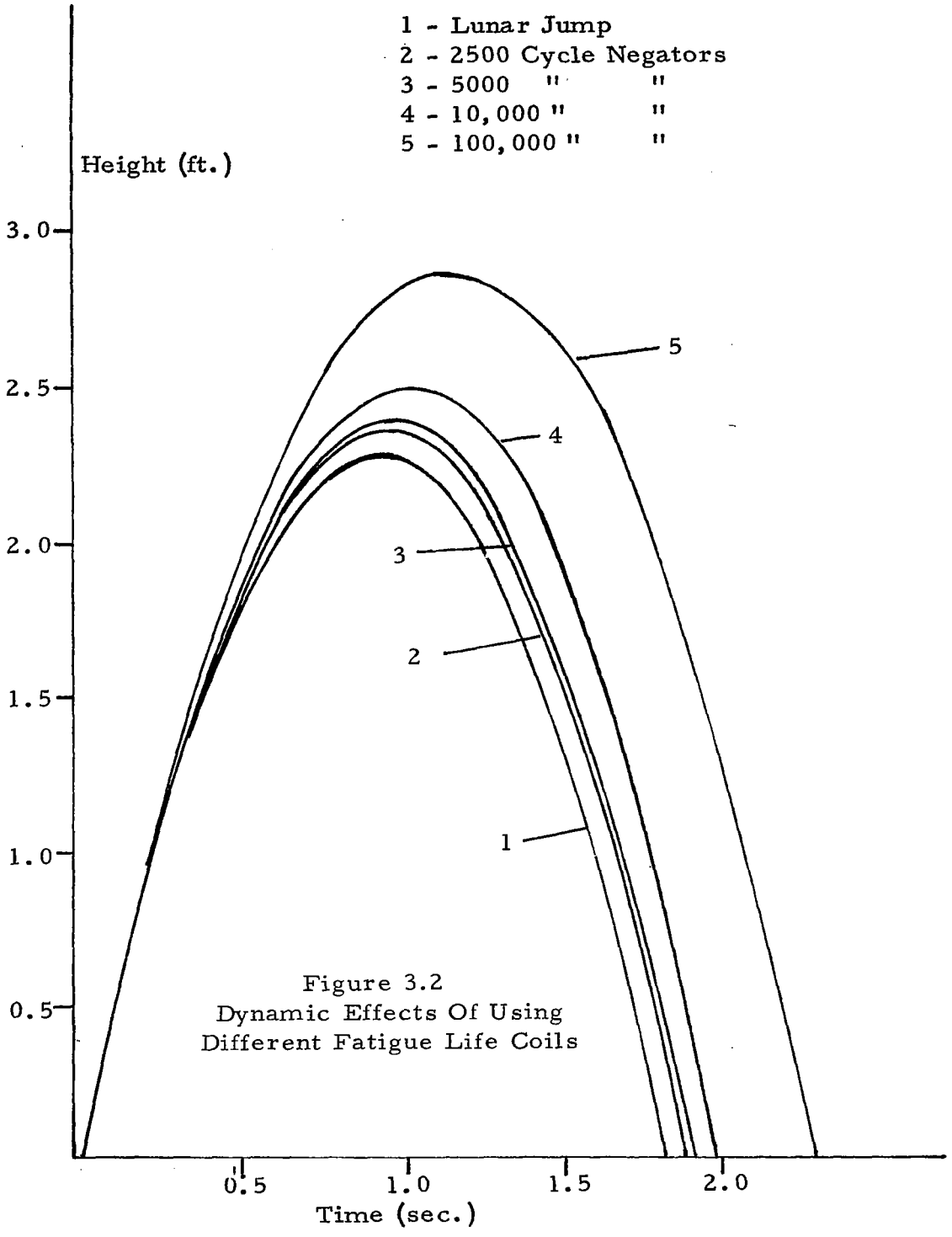

Figure 3.2
Dynamic Effects Of Using
Different Fatigue Life Coils

3.3 Two-Dimensional Simulator Dynamics

In this section the dynamic behavior of the simulator is investigated. The model used to represent the simulator is shown in Figure A1 in appendix A. The analysis of this model was completed (by Millett) in an earlier report.[2] and is included in the appendix. The equations that resulted from this analysis were very complex and required a numerical computer solution. A computer program utilizing the method of Milne[12] was developed to solve these equations. The output of this program gives the trajectory of a man in the simulator with given initial conditions. A typical trajectory is shown in Figure 3.3 together with a lunar trajectory with the same initial conditions. The motion of the overhead air pad is also shown lagging behind the subject at first and then catching up and passing him near the end of the jump.

The effect of using negator coils of greater and greater fatigue life was investigated. Computer runs were made using coils ranging from 2500 cycle rated life to 100,000 cycle rated life. The resulting trajectories for the 2500 cycle and 100,000 cycle negator coils are shown in Figure 3.4 together with the trajectory for a lunar jump. The trajectories for the 2500 and 100,000 cycle negators do not appear to vary appreciably in this plot, but the graph is somewhat

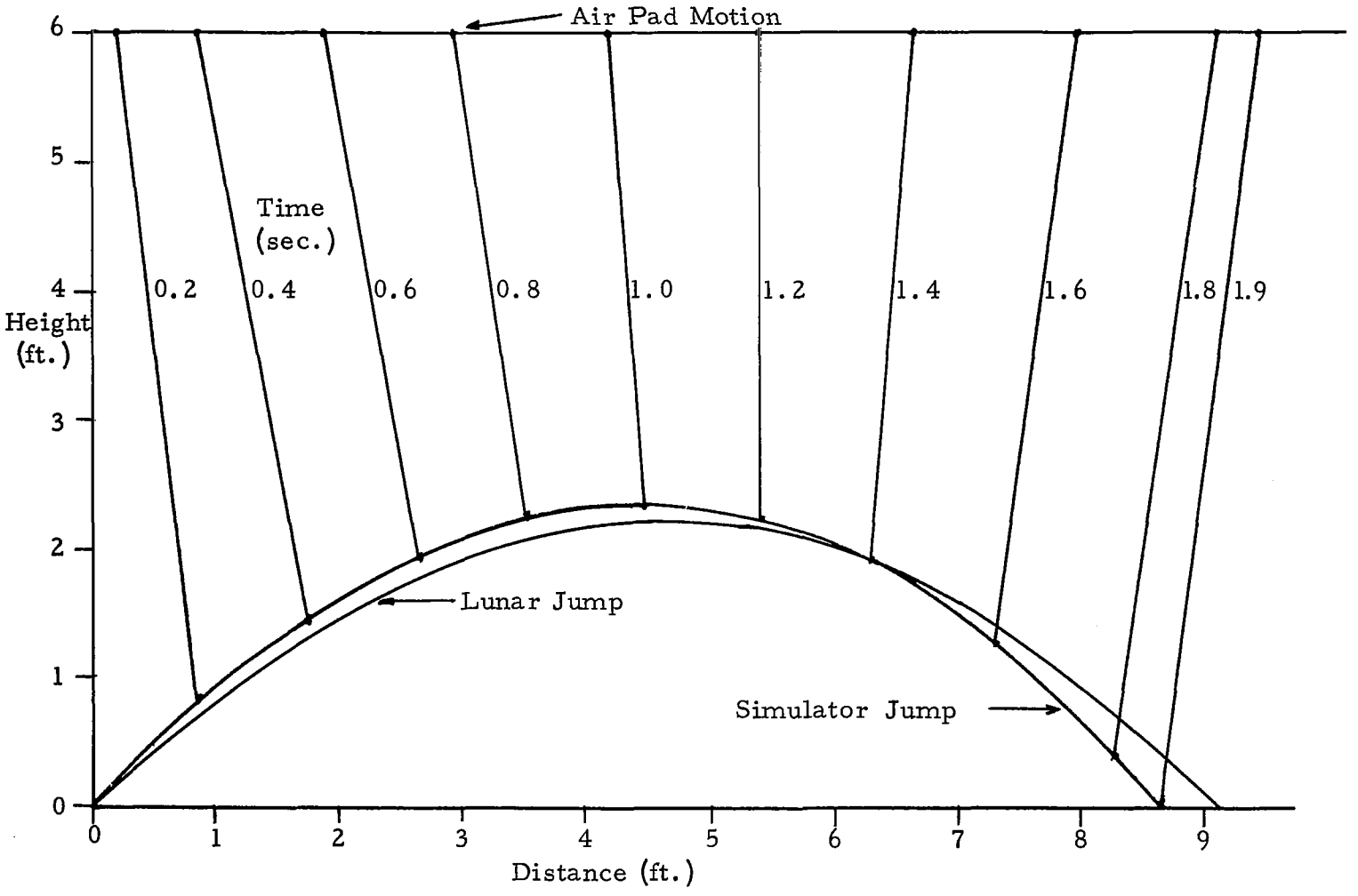

Figure 3.3 - - Two-Dimensional Dynamic Jump Showing Air Pad Motion

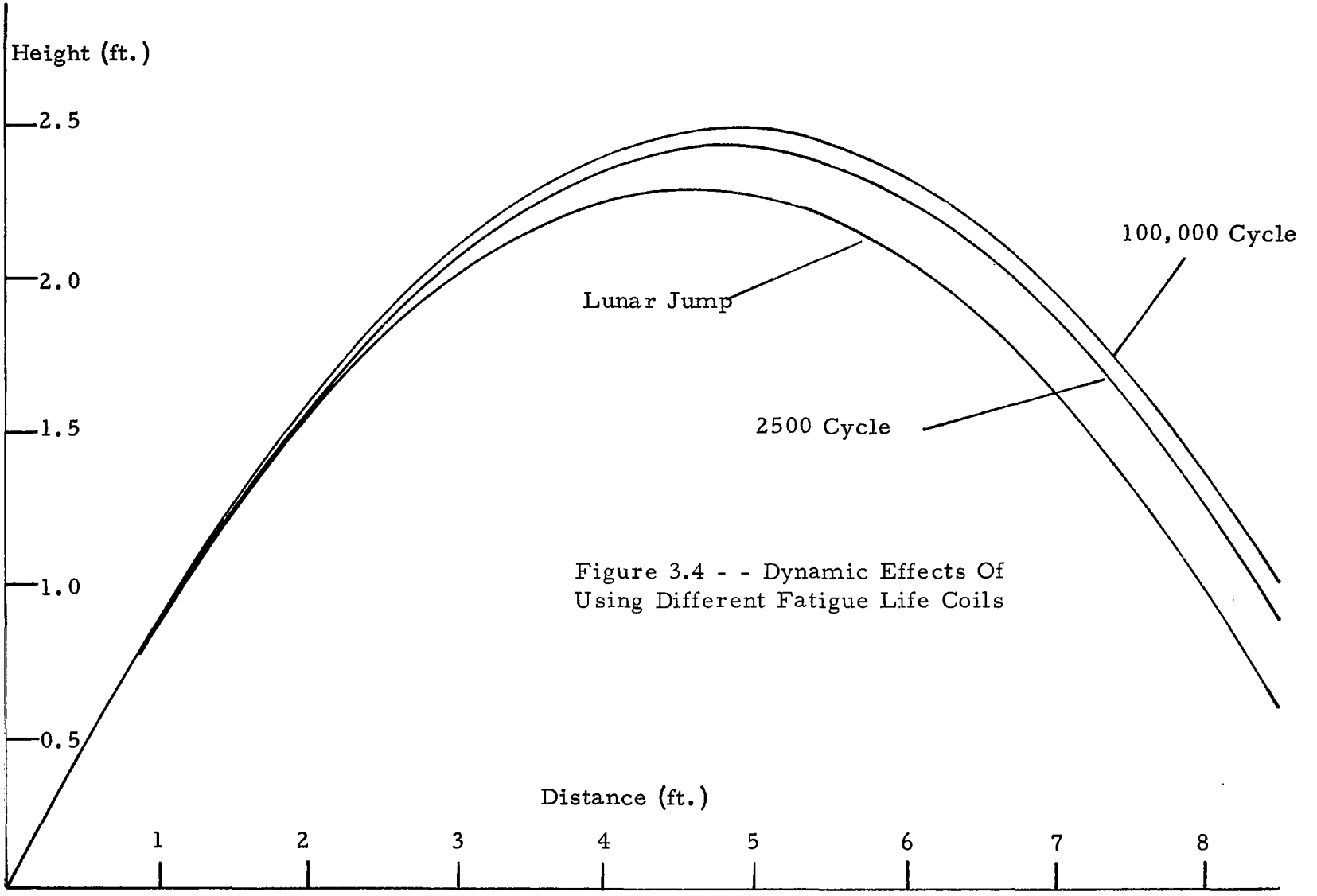

Figure 3.4 - - Dynamic Effects Of
Using Different Fatigue Life Coils

misleading in that time is not included. The subject using 100,000 cycle coils will fall far behind in time compared to the subject using 2500 cycle coils. An indication of this can be seen by observing the time trajectories as shown in Figure 3.2.

The effect of increasing the overhead weight (air pad plus negator housing) was also investigated. For the investigation only the weight of the air pad was varied. The negator housing weight was made negligible so as not to affect the results. Computer runs were made for increasing air pad weight. The results are plotted in Figure 3.5. It is apparant that as the air pad weight is increased the "jumper" begins to fall farther and farther behind the lunar jump trajectory. Figure 3.5 gives a quantitive measurement of this effect. In this Figure, the mass of the air pad is given as a percentage of the mass of the subject.

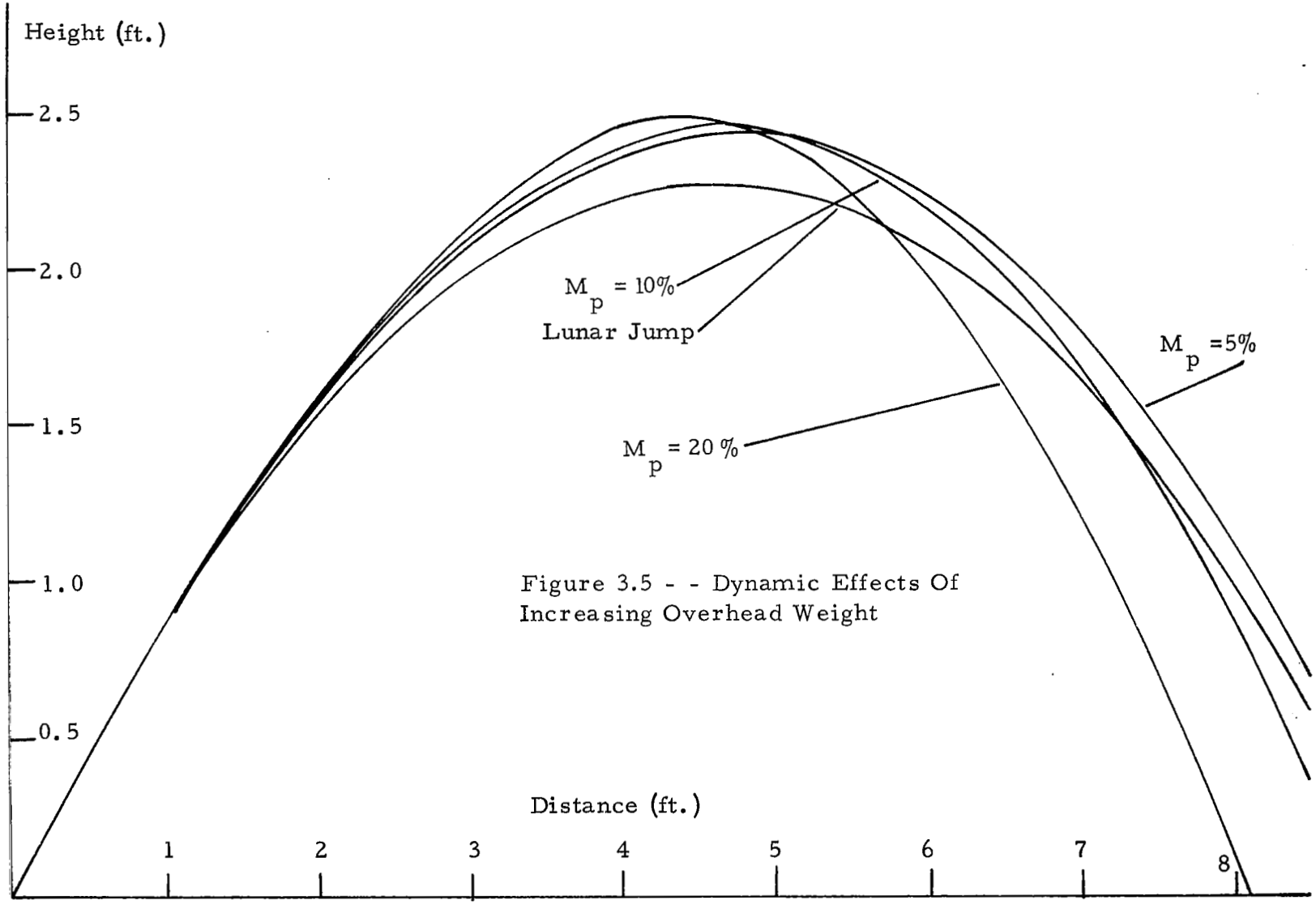

Figure 3.5 - - Dynamic Effects Of Increasing Overhead Weight

NEGATOR UNIT DESIGN

Introduction

The preceding sections indicate that the main factors to be considered in designing the negator units are as follows:

1) The force output of the negator coils is not constant but normally has a slightly positive force-extension gradient.

2) The weight of the negator coils and housing should be a minimum for good dynamic performance.

In addition, it would be desirable to have negator units which are continuously adjustable, at least over a limited range. It has already been shown that the above considerations indicate that negator coils of the lowest rated fatigue life should be used for two reasons:

1) Coils with the lowest rated fatigue life have the lowest weight-to-force ratios (see Figure 2.10).

2) Best adjustability is achieved with the lowest rated fatigue life coils.

In this section various design techniques are discussed, and an optimum design of an adjustable negator unit using two negator coils mounted back-to-back is considered.

4.1 Design Techniques

Negator springs are desirable for this application because of their relatively high force output and low weight. While the negators have been described as constant force spring elements, it has been shown that the force output of a negator coil ordinarily has a slight positive force-deflection gradient. There are several ways to deal with this problem.

4.1.1 Width alteration

One method of producing a constant force negator spring unit involves altering the width of the negator spring coil.[3] The force output of a negator coil is a function of the coil dimensions and the extension of the spring band. The functional relationship can thus be written:

$$F = F(w,x) \quad .$$

x ▫ extension
w = width

The form of this equation is known and can be written:

$$F = f_1(w) \cdot f_2(x) \quad .$$

Both $f_1(w)$ and $f_2(x)$ can be determined by analysis and experiment. Once this is done the width can be altered in such

a way so as to make:

$$f_1(w) \cdot f_2(x) = \text{constant} = F_c \ .$$

Analysis of the negator coil yields the following relations:

$$f_1(w) = K_1 w \qquad \text{where } K_1 = \text{constant}$$

$$f_2(x) = \frac{2}{R_n\left(R_{io}^2 + \frac{t}{\pi}(L-x)\right)^{1/2}} - \frac{1}{R_{io}^2 + \frac{t}{\pi}(L-x)}$$

therefore:

$$w = \frac{F_c}{K_1\left[\frac{2}{R_n\left(R_{io}^2 + \frac{t}{\pi}(L-x)\right)^{1/2}} - \frac{1}{R_{io}^2 + \frac{t}{\pi}(L-x)}\right]} \ .$$

In practive it would probably be easier to determine $f_2(x)$ experimentally. Experiment indicates that $f_2(x)$ is a linear function of x as a good approximation. This means that the width should vary linearly from one end of the coil to the other.

4.1.2 Backwound coils

Another method of producing a more nearly constant force using negator coils involves backwinding them. Analysis and experiment indicate that the force characteristics of negator coils when backwound are markedly different from the frontwound characteristics, (see Figure 2.7). The force output tends to become more nearly constant throughout the

extension range. Some negator coils demonstrate a negative force-extension gradient when backwound. Therefore, when two such coils are mounted back-to-back, one backwound and one frontwound, the total force output tends to be constant throughout the extension range.

4.1.3 Adjustment

It would be highly desirable to have constant force units that are adjustable. The variations in weights of human subjects will probably be significant, but if enough adjustability could be built into the negator spring units, one set might suffice for subjects with a wide range of different weights.

One method of achieveing this adjustability involves keeping a large number of negator coils on hand with different force ratings to accommodate a range of test subject weights.

Another possible way of achieving adjustability would be to vary the diameter on which the negator coil is wound. This could be accomplished by mounting the negator coils back-to-back on opposing conical drums. This type of design is considered in detail in the following section.

4.2 Optimum Conical Drum Design

For a back-to-back adjustable negator unit design, one like that shown in Figure 4.1 is proposed. In this section the stresses and failure modes of the conical unit will be determined.

Consider a length of negator coil held in equilibrium at a certain radius R , by a uniform internal pressure, P.

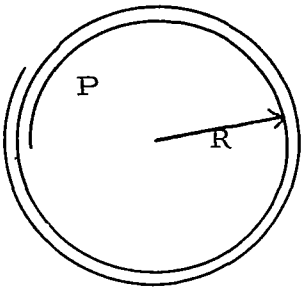

The strain energy contained in the coil is given by:

$$\mathcal{E} = \frac{M^2 L}{2EI} \quad . \tag{4.1}$$

Substituting

$$M = EI\left(\frac{1}{R_n} - \frac{1}{R}\right) \quad . \tag{4.2}$$

We get

$$\mathcal{E} = \frac{EIL}{2}\left(\frac{1}{R_n} - \frac{1}{R}\right)^2 \quad . \tag{4.3}$$

Now considering the work done by the pressure:

$$\mathcal{E} = \int_{R_n}^{R} 2\pi w P R \, dR \quad . \tag{4.4}$$

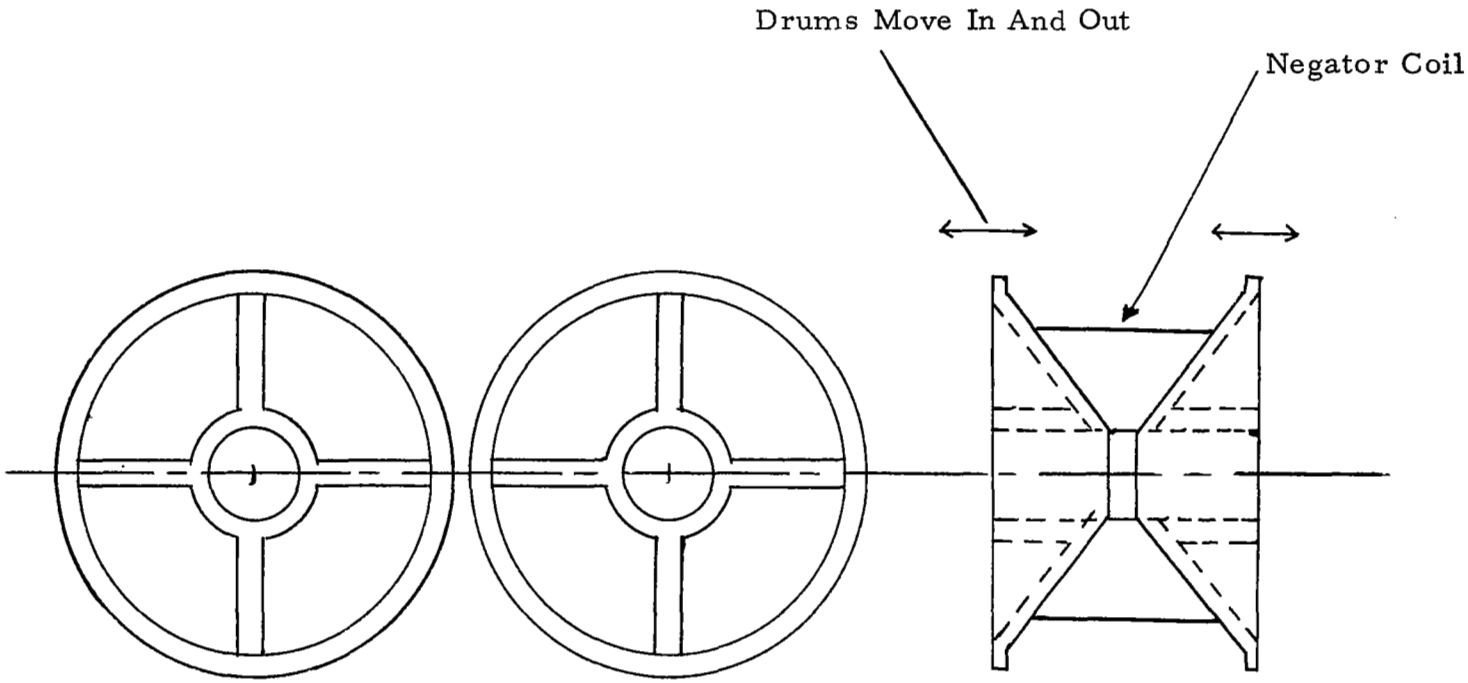

Figure 4.1 - Adjustable Conical
Drum Negator Unit Design

or:

$$\frac{d\mathcal{E}}{dR} = 2\pi wPR \quad . \tag{4.5}$$

Differentiating (4.3)

$$\frac{d\mathcal{E}}{dR} = EIL \left(\frac{1}{R_n} - \frac{1}{R}\right) \frac{1}{R^2} \tag{4.6}$$

setting (4.6) equal to (4.5) we have

$$P = \frac{EIL}{2\pi wR^3} \left(\frac{1}{R_n} - \frac{1}{R}\right) \quad . \tag{4.7}$$

Now, if instead of a uniform pressure there is a force per unit length (f) acting on each edge of the coil, this force per unit length is given by

$$f = \frac{Pw}{2} \quad . \tag{4.8}$$

So we have

$$f = \frac{EIL}{4\pi R^3} \left(\frac{1}{R_n} - \frac{1}{R}\right) \quad . \tag{4.9}$$

Consider now the following situation

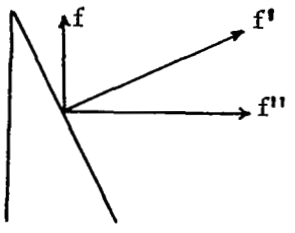

If the frictional force is negligible, only the normal force, f' , can act to produce the component, f . The component, f" , will also be produced. From geometry:

$$f' = f/\sin(\alpha) \tag{4.10}$$

$$f'' = f\ \mathrm{ctn}(\alpha) \tag{4.11}$$

There is in addition to the wrapping force a force produced by the pull of the negator coils. This equation (for two coils) has already been derived:

$$F = EI\left[\frac{2}{R_n R} - \frac{1}{R^2}\right] \quad . \tag{4.12}$$

The force acting on one conical section will be

$$F_c = \frac{F}{4} = \frac{EI}{4}\left[\frac{2}{R_n R} - \frac{1}{R^2}\right] \quad . \tag{4.13}$$

The stresses acting on the spokes will be considered first. Two possible types of failure modes are bending stress failure or compression buckling.

Consider the forces acting at the tip of one spoke:

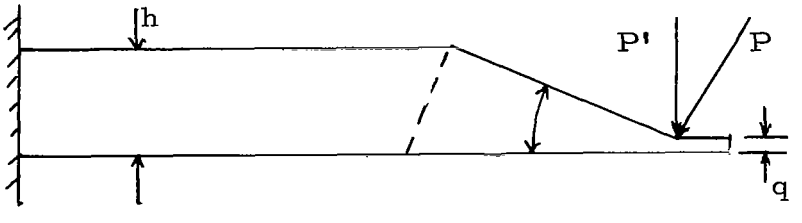

here

$$P = f'l + F_c/\sin(\alpha) \tag{4.14}$$

where

$$l = \frac{2R}{N} \quad . \tag{4.15}$$

Look at the section where the tip indicated by the dotted line:

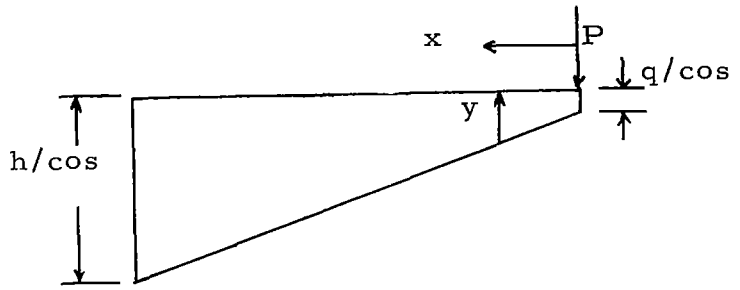

The bending moment will be given by:

$$M = Px \quad . \tag{4.16}$$

The moment of inertia of the section can be approximated by:

$$I = \frac{by^3}{12} \quad . \tag{4.17}$$

The maximum stress is given by:

$$\sigma_{ml} = \frac{My}{2I} \quad . \tag{4.18}$$

Substituting (4.16) and the equation;

$$y = q/\cos(\alpha)+x \tan(\alpha) \tag{4.19}$$

we get

$$\sigma_{ml} = \frac{6Px}{b[\frac{q}{\cos(\alpha)} + \tan(\alpha)]^2} \quad . \tag{4.20}$$

To find the point of greatest stress it is necessary to take the derivative of (4.20):

$$\frac{\partial \sigma_{ml}}{\partial x} = \frac{6P}{b}\left[\frac{-2x\tan(\alpha)}{(\frac{q}{\cos(\alpha)} + x\tan(\alpha))^3} + \frac{1}{(q/\cos(\alpha) + x\tan(\alpha))^2}\right]. \tag{4.21}$$

Setting (4.21) equal to zero results in:

$$x = \frac{q}{\sin(\alpha)} \quad . \tag{4.22}$$

Substituting into (4.20) results in

$$\sigma_{ml} = \frac{3P}{bq}\,\frac{\cos(\alpha)}{\tan(\alpha)} \quad . \tag{4.23}$$

The shear stress at the tip is given by

$$\tau = \frac{P\cos(\alpha)}{bq} \quad . \tag{4.24}$$

Taking the ratio of maximum fiber stress to maximum shear stress, we get

$$\frac{\sigma_{ml}}{\tau} = \frac{3}{\tan(\alpha)} \quad . \tag{4.25}$$

If $\tan(\alpha) = 1/2$; $\sigma_{max}/\tau = 6$

which means that the fiber stress will be greater by a factor of 6.

The maximum bending stress at the far end of the spoke is given by:

$$\sigma_{m2} = \frac{Mh}{2I} \tag{4.26}$$

where

$$M = P'R \tag{4.27}$$

$$P' = f''l + F_c \operatorname{ctn}(\alpha) \tag{4.28}$$

$$I = \frac{bh^3}{12} \quad . \tag{4.29}$$

Substitution of (4.27-4.29) into (4.26) results in

$$\sigma_{m2} = \frac{6P'R}{bh^2} \quad . \tag{4.30}$$

The compressive buckling of the spoke must also be considered. The buckling model to be used is shown below

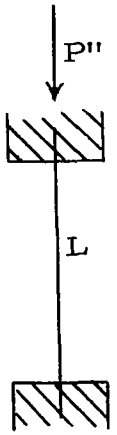

For this case

$$P''_{cr} = \frac{4\pi^2 E_m I}{L^2} \tag{4.31}$$

for the spoke

$$I = \frac{hb^3}{12} \tag{4.32}$$

$$L = R \tag{4.33}$$

$$P'' = fl + F_c \tag{4.34}$$

so we have

$$\frac{P''_{cr}}{P''} = \frac{4\pi^2 E_m hb^3}{12L^2(fl + F_c)} = \frac{1}{\beta} \quad . \tag{4.35}$$

Next, the loading of the conical section is to be considered. It will suffice to consider one section between two spokes as shown below

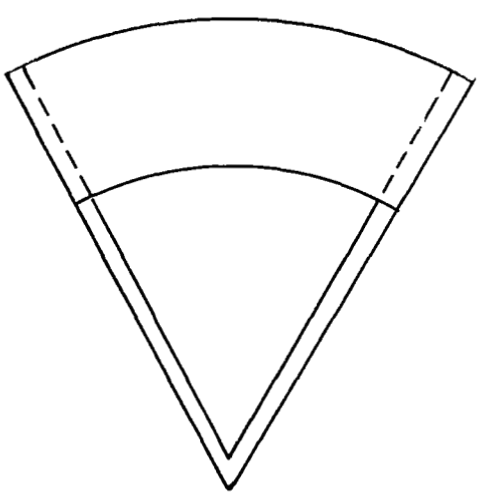

An exact model for this section would be too complicated, so for purposes of maximum stress calculation, the section is represented by a straight rectangular beam as shown below:

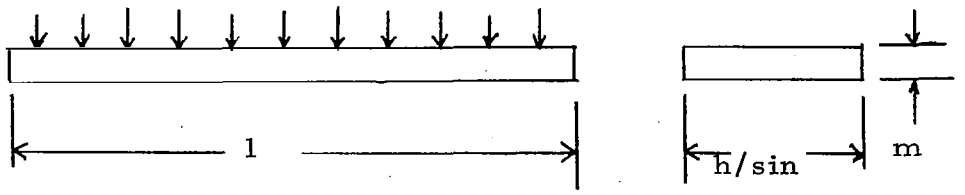

If it is assumed that the total distributed load is concentrated as a point load P" at the center of the beam; the maximum stress will be given by

$$\sigma = \frac{P'' \sin(\alpha)}{hm^2} \quad . \tag{4.36}$$

Where P" is given by

$$P'' = f'l + F_c/\sin(\alpha) \quad . \tag{4.37}$$

This model does not fit the actual situation very well but it does generate a parametric equation (4.36) which can be used for design purposes.

For the design of the spoked conical section, the parameters that must be chosen are the cone angle, α the spoke width, b, and width of the conical section, m. The largest radius, R, is chosen to meet the desired force requirements of the negator unit.

The purposed procedure is to determine R from the force requirements, choose α somewhat arbitrarily, and then determine the physical dimension of the conical section by a consideration of the forces and stresses.

A material and a suitable working stress must be chosen. In addition, the buckling load must be kept below the critical buckling load by some factor, β .

In summary, then, after the working stress, σ_w, and the buckling load factor, β , have been chosen we have the following equations for determining h,b,m, and q.

$$bq = \frac{3P\cos(\alpha)}{\sigma_w \tan(\alpha)} \tag{4.38}$$

$$bh^2 = \frac{6P'R}{\sigma_w} \tag{4.39}$$

$$hb^3 = \frac{3L^2(fl + F_c)}{\beta\pi^2 E_m} \tag{4.40}$$

$$F_c = \frac{EI}{4}\left[\frac{2}{RR_n} - \frac{1}{R^2}\right] \tag{4.41}$$

$$hm^2 = \frac{(fl + F_c)l}{\sigma_w} \tag{4.42}$$

$$l = \frac{2\pi R}{N} \tag{4.43}$$

$$f = \frac{EIL}{4\pi R^3}\left[\frac{1}{R_n} - \frac{1}{R}\right] \tag{4.44}$$

A computer program which used the above equations was written to provide rapid and accurate design data. As the equations stand there may be more than one constraint on some of the dimensions, so the computer program was written to choose the dimension which results in a lower stress. The program was written so that it automatically chooses the values of the cone angle and spoke number which result in an optimum force-to-weight ratio. A copy of the program is included in appendix B.

Using the developed program, the conical spoked section was optimized with respect to force-to-weight ratio. For a given material and working stress, this can be accomplished by varying the cone angle and the number of spokes until a maximum force-to-weight ratio is realized.

Two negator units using two different stock negator coils were optimized in order to demonstrate the feasibility of the procedure. Both units use two coils mounted back-to-back on adjustable conical drums. Coil number SH31U58 was chosen because the force produced is approximately the force necessary to negate the torso weight of an average man. The other coil (SL31U69) was chosen because the negator material has the same width and thickness as SH31U58. SH31U58 is a 2500 cycle fatigue life coil and SH31U69 is a 20,000 cycle coil.

Figures 4.2-4.5 represent the results of applying the computer design procedure to the above two coils. The results are always plotted versus the working stress because the stress may vary widely depending on the particular alloy that is used.

The curves in Figure 4.2 show the force-to-weight ratios that can be obtained using 3 different materials with a buckling factor, β , of 0.5. These represent the optimum force-to-weight ratios that are attainable using two SH31U58 coils mounted back-to-back. Figure 4.3 shows how the optimum cone angle and optimum number of spokes varies with the value of working stress chosen. For the range of working stress for these 3 materials the optimum number of spokes varies from only 6 to 8. The optimum angle, however, is a strong function of the working stress value.

Figures 4.4 and 4.5 show corresponding curves for the 20,000 cycle fatigue life coil (SL31U69). The force-to-weight ratios attainable are much lower than with the 2500 cycle coils, owing largely to the fact that the 20,000 cycle coils are not as highly stressed and therefore have a lower inherent force-to-weight ratio(see Figure 2.10).

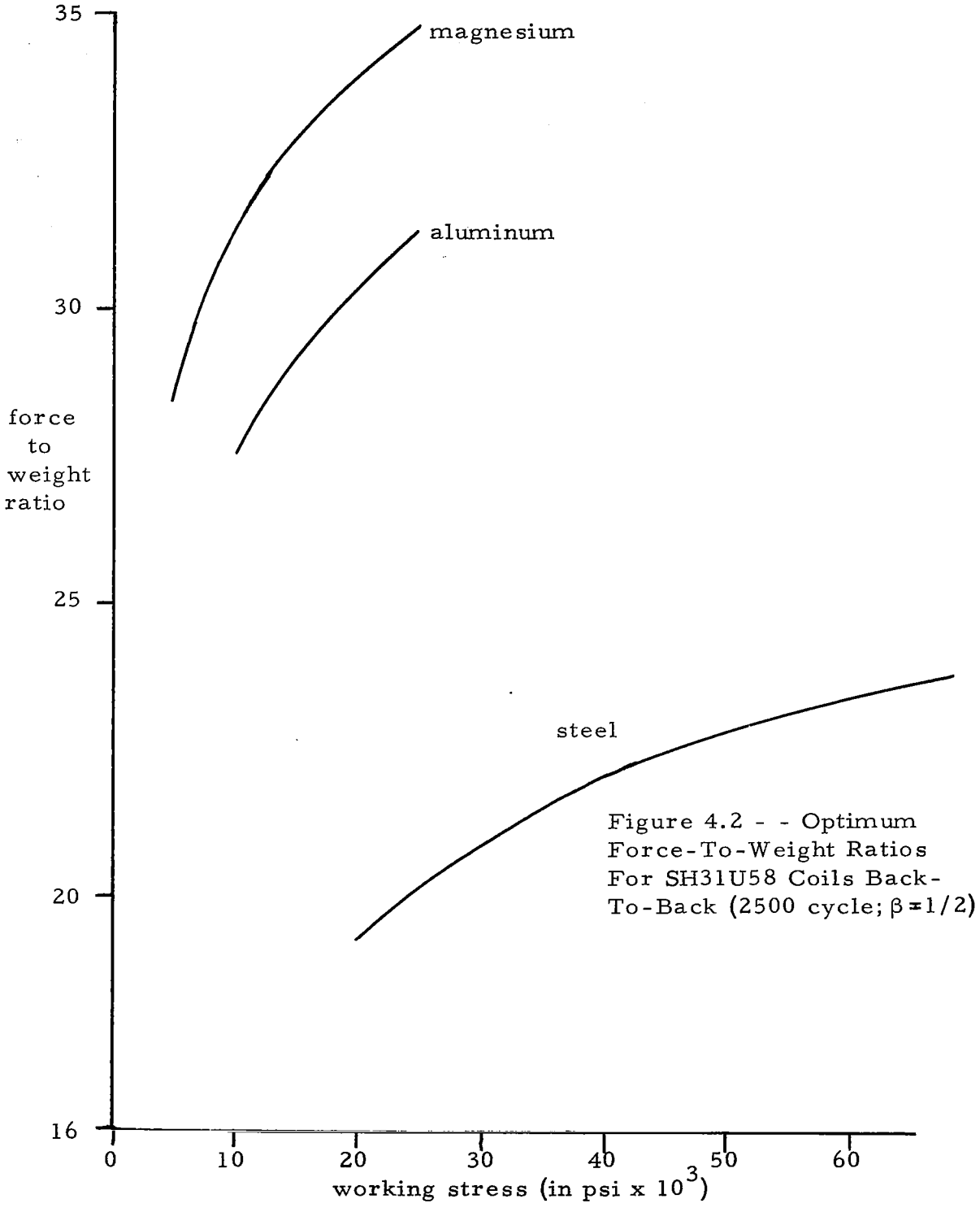

Figure 4.2 - - Optimum Force-To-Weight Ratios For SH31U58 Coils Back-To-Back (2500 cycle; $\beta = 1/2$)

Figure 4.3
Optimum Curves - SH31U58
Coil (2500 cycle, $\beta = 1/2$)

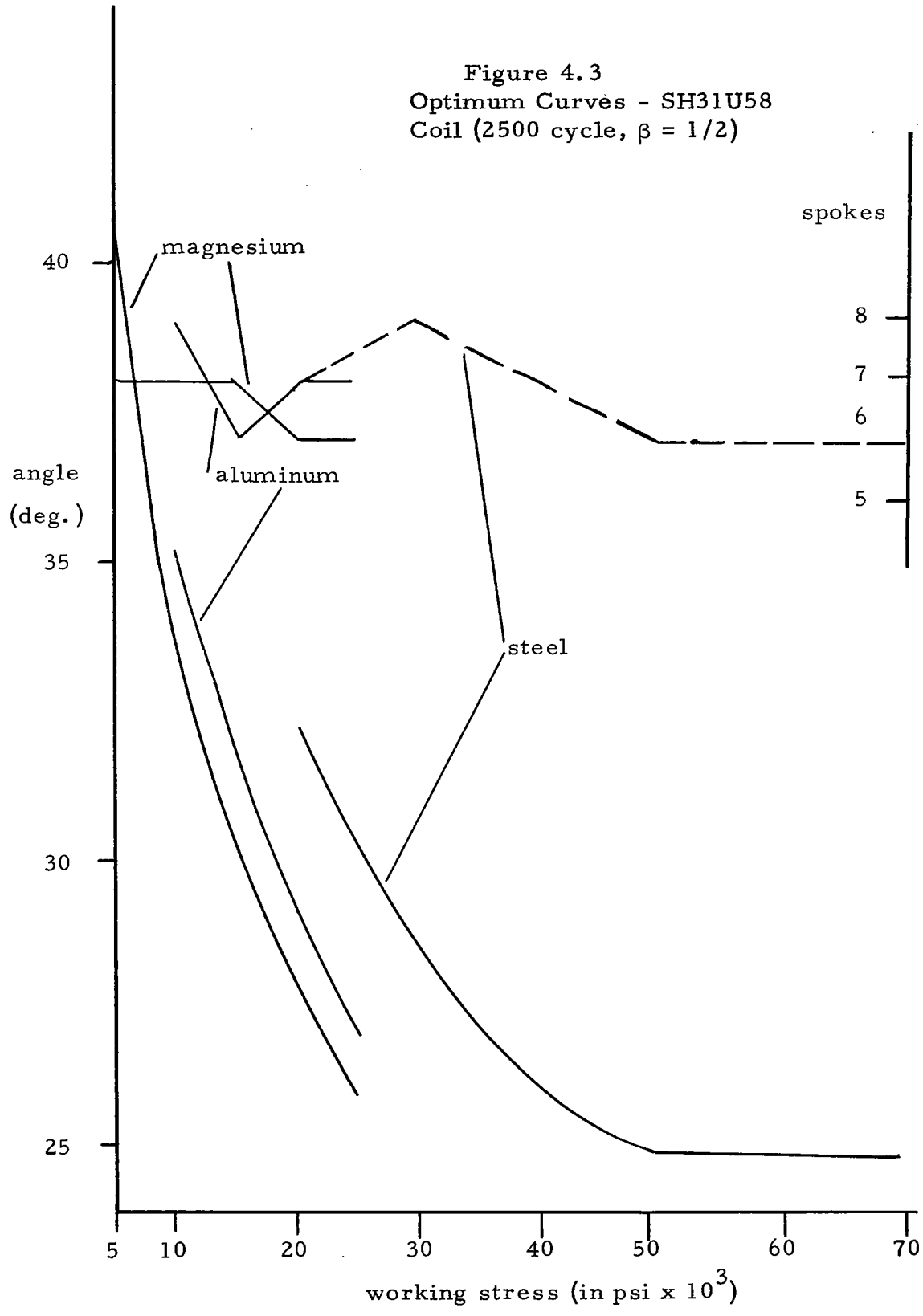

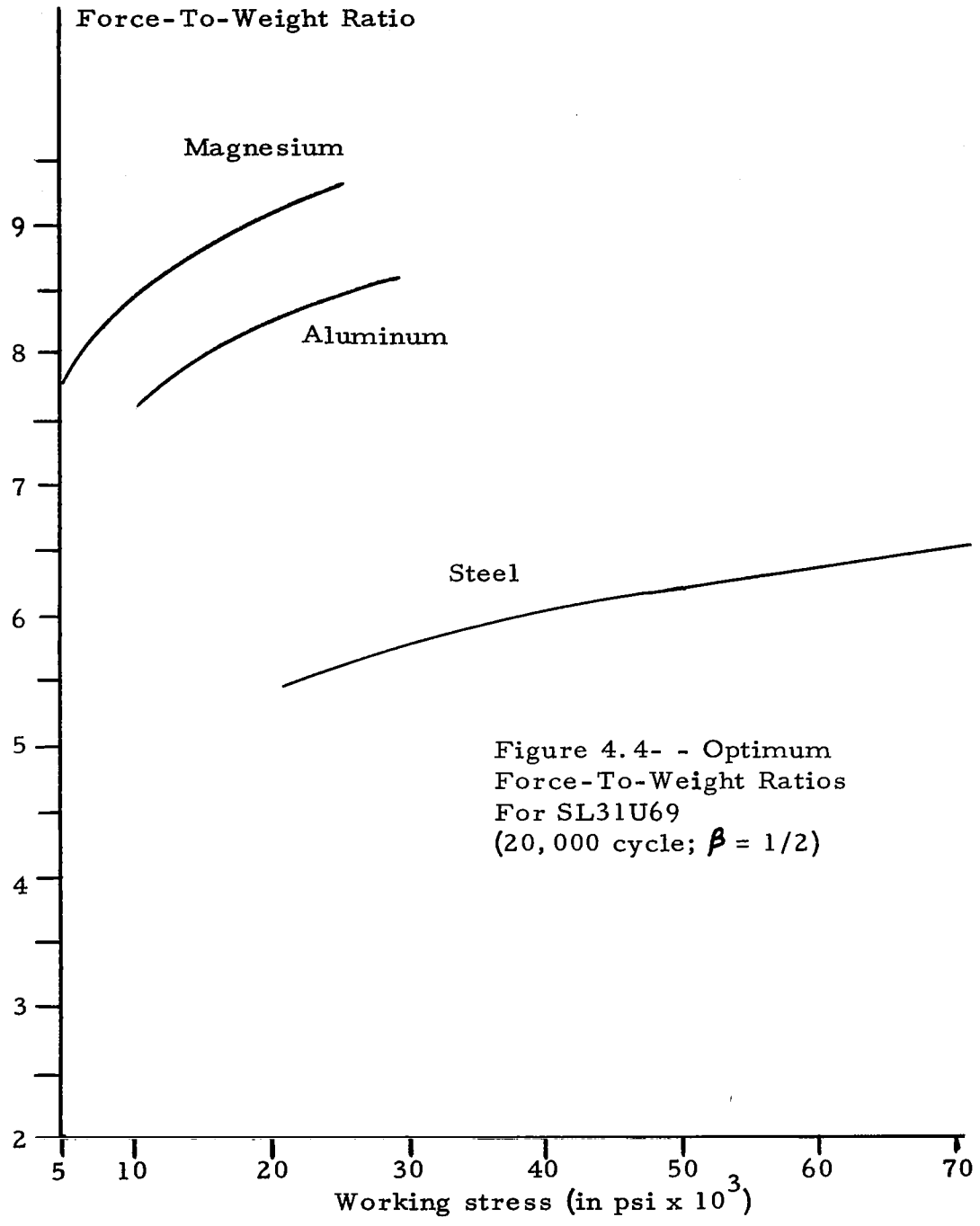

Figure 4.4- - Optimum Force-To-Weight Ratios For SL31U69 (20,000 cycle; $\beta = 1/2$)

Figure 4.5
Optimum Curves For
SL31U69 Coil
(20,000 cycle; $\beta = 1/2$)

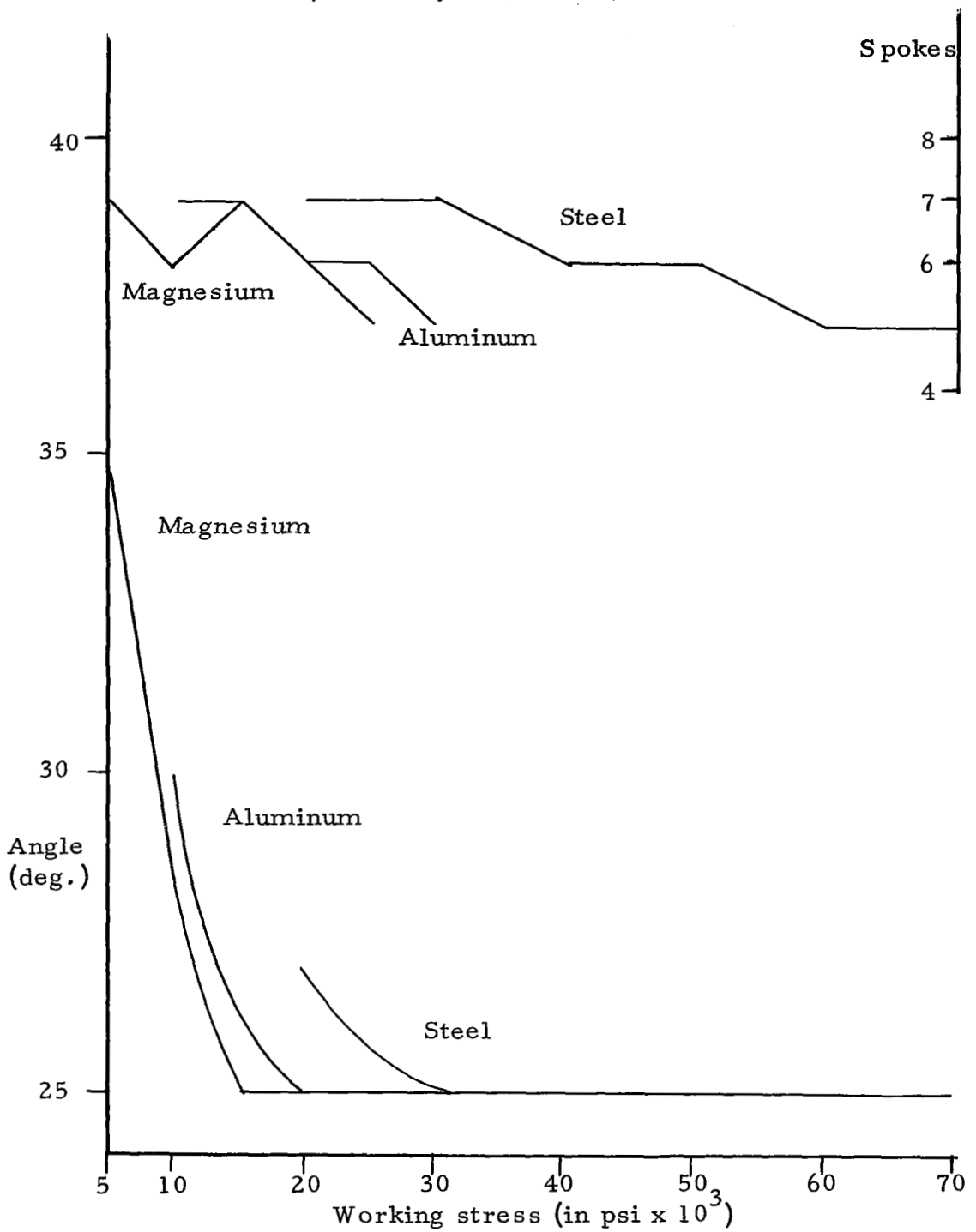

Figures 4.3 and 4.5 give the optimum values of cone angle and number of spokes as a function of the working stress value that is chosen. The top portion of the graph gives the optimum number of spokes and the bottom portion the optimum cone angle for 3 different materials. For example, if we desire to use steel stressed to 30,000 psi as the material for designing a negator unit with two SH31U58 coils (Figure 4.3), we proceed as follows:

1) Find 30,000 psi on the horizontal axis.
2) Move vertically till the optimum angle curve for steel is reached and read 28° on the left as the optimum angle.
3) Continue vertically till the optimum spoke curve for steel is reached and read 8 spokes on the right.

Computer runs for several other stock 2500 cycle negator coils were made (using DESIO, appendix B). The results indicate that the optimum number of spokes is almost invariably 6 or 7 and the optimum cone angle almost always falls somewhere between 25 and 30 degrees (the angle is constrained to be between 25 and 40 degrees). Furthermore, the force-to-weight ratio is not a strong function of N or α near the optimum. It is therefore recommended that negator units using 2500 cycle negator coils be designed with 6 spokes and any convenient angle between 25 and 30 degrees.

HARNESS DESIGN

In the following sections analyses of various suspension systems for limbs and torso are presented. For purposes of suspension and negation, the body is divided into 3 sections: 1) legs, 2) arms, and 3) torso and head.

5.1 Cable Suspension Analysis

There are two proposed methods for negating the torso:

1) 4-point torso suspension

2) "L-C" brace torso suspension

The torso would be held more or less rigid in a harness which consists of a bicycle-like seat with straps to and around the shoulders, and also includes a fiber-glass molded shell to support the front of the torso.

It is observed that while the center of gravity of the human body varies appreciably during normal body movements a large part of this variation occurs as a result of leg and arm movements.[13] While there is no reliable data to support this assumption, it is also felt that the center of gravity of the torso and head combination changes very little over a wide range of movements. This assumption, if true, leads to the conclusion that the torso can be effectively negated and supported by considering it a rigid body with a fixed center of mass.

5.1.1 4-point torso suspension

The 4-point torso suspension system includes 4 suspension points; two on either side of the hips, and two just in front of the shoulders. If the center of mass of the torso is known, it is a simple matter to size the negating force at the various take-up points. Consider the sketch below:

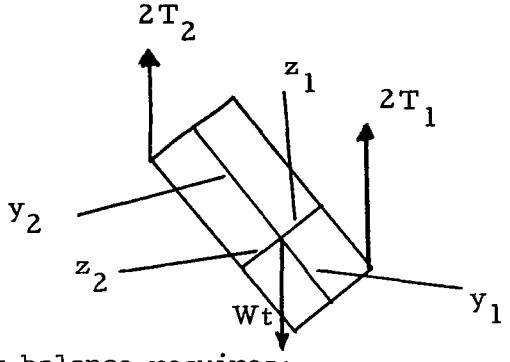

Moment balance requires:

$$T_2(z_2 \sin(\theta)+y_2 \cos(\theta)) = T_1(z_1 \sin(\theta) + y_1 \cos(\theta)). \quad (5.1)$$

For equilibrium at any value of θ we have the two equations:

$$T_2 z_2 = T_1 z_1 \quad (5.2)$$

$$T_2 y_2 = T_1 y_1 \quad . \quad (5.3)$$

Also for lunar gravity simulation:

$$2T_1 + 2T_2 = \frac{5}{6} Wt \quad (5.4)$$

5.1.2 "L-C" brace torso suspension

Because of the difficulty in achieving good balance with the 4-point suspension system and because of the cable

interference problems a second torso negation system was proposed. It was felt that if the torso were held more or less rigid a gimbaled C-brace with pivot points passing through the center of mass of the torso would be suitable. This "L-C" brace system is shown in Figure 1.3. There are bearing pivot points at both sides and at the rear of the subject. The attachment points are adjustable in two directions for fine adjustment.

5.1.3 Limb suspension

In this section an analysis of limb suspension systems is presented.

The analysis for the legs and arm is similar inasmuch as the two extremities are similar. For purposes of analysis, the leg is divided into two sections: 1) upper leg and 2) lower leg and foot. The arm is similarly divided: 1) upper arm and 2) lower arm and hand.

The limb (either leg or arm) is then represented as shown in the following sketch.

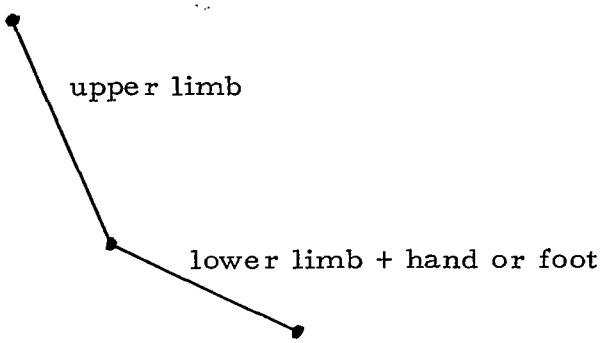

It is proposed that the whole limb be supported at a point below the joint with a force F_2.

First, the condition for perfect simulation must be established. The limb is shown in the arbitrary position below in a lunar gravity environment.

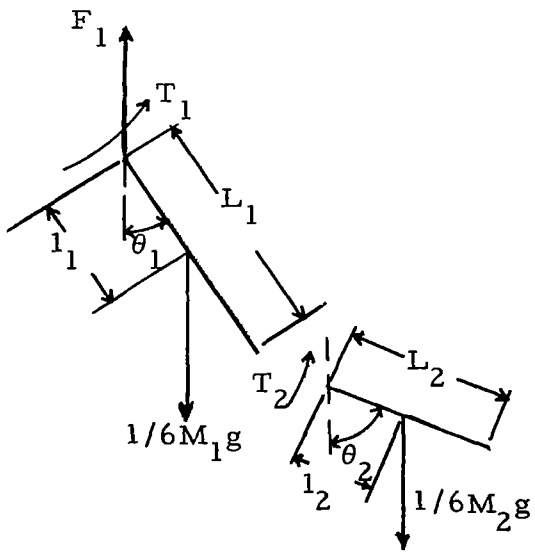

The condition of F_1 , T_1, and T_2 must be established. Force balance requires that:

$$F_1 = \frac{1}{6} g(M_1 + M_2) \quad . \tag{5.5a}$$

Moment balance on the lower section of the limb requires that:

$$T_2 = \frac{1}{6} M_2 g l_2 \sin(\theta_2) \quad . \tag{5.5b}$$

Moment balance on the upper limb requires:

$$T_1 = \frac{1}{6} M_1 g l_1 \sin(\theta_1) + \frac{1}{6} M_2 g(L_1 \sin(\theta_1) + l_2 \sin(\theta_2))$$

$$T_1 = \frac{1}{6} g(M_1 l_1 + M_2 L_1)\sin(\theta_1) + \frac{1}{6} g M_2 l_2 \sin(\theta_2) \quad . \tag{5.5c}$$

Now the limb is put into earth (1g) gravity and for a start we try to simulate lunar gravity by applying a force F_2 to the lower section of the limb at a distance a from the joint in an attempt to simulate lunar gravity, as shown in the following sketch:

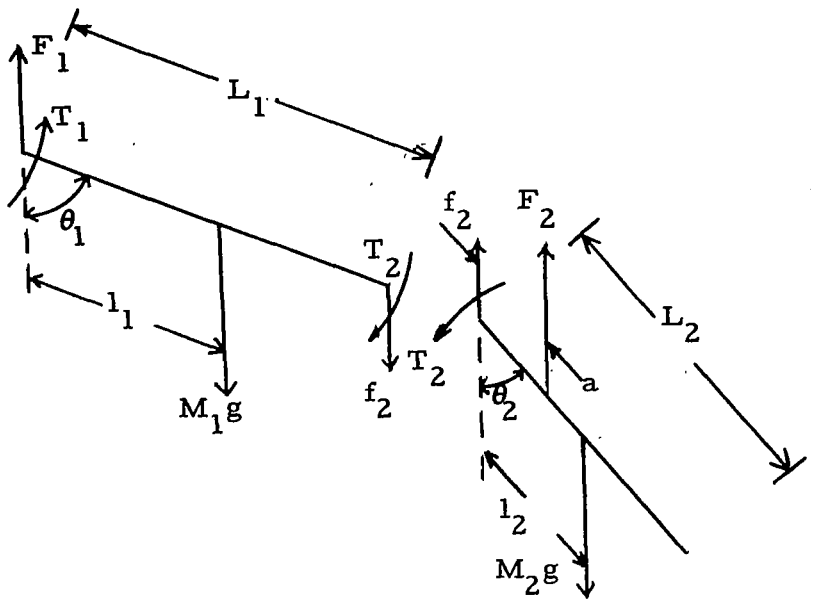

We can write:

Force balance on upper section:

$$F_1 = M_1 g + f_2 \quad . \tag{5.6a}$$

Moment balance:

$$T_1 = M_1 g l_1 \sin(\theta_1) + T_2 + f_2 L_1 \sin(\theta_1) \quad . \tag{5.6b}$$

For the lower section:

Force balance:

$$f_2 = M_2 g - F_2 \quad . \tag{5.6c}$$

Moment balance:

$$T_2 + F_2 a \sin(\theta_2) = M_2 g l_2 \sin(\theta_2) \quad . \tag{5.6d}$$

Rewriting Equation (5.5d)

$$T_2 = (M_2 g l_2 - F_2 a) \sin(\theta_2)$$

in order to satisfy (5.6b):

$$M_2gl_2-F_2a = \frac{1}{6} M_2gl_2$$

or

$$F_2a = \frac{5}{6} M_2gl_2 \qquad (5.7a)$$

substituting (5.6c) into (5.6a) and (5.6b) we have:

$$F_1 = M_1g + M_2g-F_2 \qquad (5.6a)$$

and

$$T_1 = M_1gl_1\sin(\theta_1)+ \frac{1}{6} M_2gl_2\sin(\theta_2)+(M_2g-F_2)L_1\sin(\theta_1) \qquad (5.6b)$$

for (5.5a) to be satisfied:

$$(M_1 + M_2)g-F_2 = \frac{1}{6}(M_1 + M_2)g$$

or

$$F_2 = \frac{5}{6}(M_1 + M_2)g \quad . \qquad (5.7b)$$

We now check to see if T_1 is satisfied.

$$T_1 = [\ \frac{1}{6}M_2gl_1+M_1g(l_1- \frac{5}{6}L_1)]\sin(\theta_1)+ \frac{1}{6}M_2gl_2\sin(\theta_2) \ . \qquad (5.7c)$$

Comparison with Equation (5.5c) indicates that the only way (5.5c) can be satisfied is if:

$$\frac{1}{6}l_1 = l_1 - \frac{5}{6}L_1$$

or

$$L_1 = l_1 \quad .$$

This is physically impossible so we conclude that this type of support is not suitable without some modification. One way to accomplish the simulation would be to add another attachment point above the joint, but, to avoid this complication, let us instead negate some fraction (α) of the weight of the upper section of the limb at the upper joint. We now have the following situation.

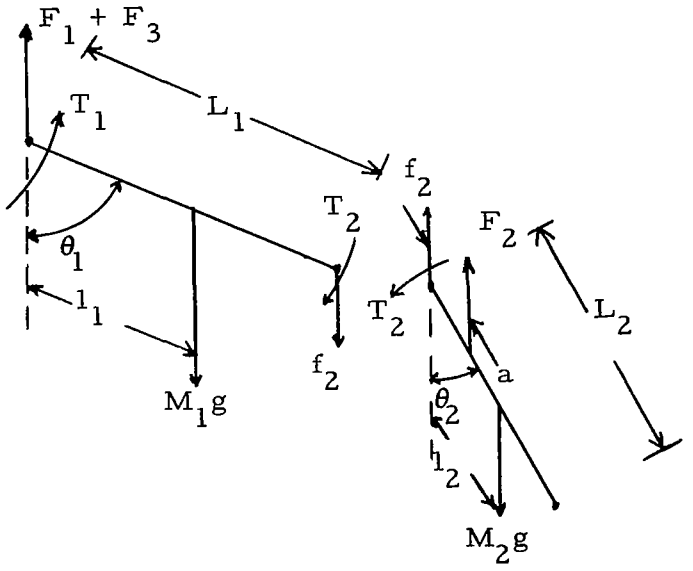

The reaction force at the upper joint is shown as two forces $F_1 + F_3$ to clarify the simulation technique.

We can now write:

For the upper section:

Force Balance:

$$F_1 + F_3 = M_1 g + f_2 \quad . \qquad (5.8a)$$

Moment balance:

$$T_1 = M_1 g l_1 \sin(\theta_1) + f_2 L_1 \sin(\theta_1) + T_2 \quad . \qquad (5.8b)$$

For the lower section:

Force balance:

$$f_2 + F_2 = M_2 g \quad . \qquad (5.8c)$$

Moment balance:

$$T_2 + F_2 a \sin(\theta_2) = M_2 g l_2 \sin(\theta_2) \quad . \qquad (5.8d)$$

We also have:

$$F_3 = \alpha\left[\frac{5}{6} M_1 g\right] \quad . \qquad (5.8e)$$

Solving (5.8d) and comparing it to (5.5b) results in the condition:

$$F_2 a = \frac{5}{6} M_2 g l_2 \quad . \qquad (5.9a)$$

Substituting (5.8c) into (5.8a) and (5.8b) yields:

$$F_1 = M_1 g - F_3 + M_2 g - F_2 \qquad (5.8a)$$

and

$$T_1 = M_1 g l_1 \sin(\theta_1) + (M_2 g - F_2) L_1 \sin(\theta_1) + \frac{1}{6} M_2 g l_2 \sin(\theta_2) \qquad (5.8b)$$

Substituting (5.8e) into (5.8a) and comparing with (5.5a) results in

$$(M_1 + M_2)g - \frac{5}{6} \alpha M_1 g - F_2 = \frac{1}{6} g (M_1 + M_2)$$

or

$$F_2 + \frac{5}{6} M_1 g = \frac{5}{6}(M_1 + M_2)g \quad . \tag{5.9a}$$

Substituting (5.9b) into (5.8b) results in:

$$T_1 = M_1 g l_1 \sin(\theta_1) + (M_2 g - \frac{5}{6}(M_1 + M_2)g + \frac{5}{6} M_1 g) L_1 \sin(\theta_1)$$

$$+ \frac{1}{6} M_2 g l_2 \sin(\theta_2) \quad . \tag{5.8b}$$

Comparing this with (5.5c) reveals the condition

$$\alpha = 1 - l_1/L_1 \quad . \tag{5.9c}$$

Equations (5.9a, b, c) constitute the conditions on F_2, α, and a. Reiterating, we have then the three conditions:

1) $\alpha = 1 - l_1/L_1$

2) $F_2 = \frac{5}{6} g (M_2 + \frac{l_1}{L_1} M_1)$

3) $a = M_2 l_2 / (M_2 + \frac{l_1}{L_1} M_1)$.

The preceding analysis applies to both arms and legs. The results indicate that if a fraction of the upper arm or upper leg weight is added to the torso weight, the rest of the limb's weight can be negated by one attachment point below the joint.

It is obvious that one attachment point above the joint could never satisfy the simulation condition. It is also obvious that two suspension points for each limb could satisfy

the simulation condition. One attachment point would be a much simpler arrangement for limb negation.

5.2 Segment Weight Determination

In order to achieve accurate lunar gravity simulation by negating the body components separately, it is necessary to accurately determine the weight and location of the center of mass of the body segments. Barter[1] developed a set of regression equations for calculating the weight of body segments:

both upper arms	=	0.08W - 2.9 lbs.
both lower arms + hands	=	0.06W - 1.4 lbs.
both upper legs	=	0.18W + 3.2 lbs.
both lower legs + feet	=	0.13W - 0.5 lbs.

In the above formulas W is the man's total weight. Lay and Fisher[9] report that the fraction of the body weight contained in each body segment is as follows:

trunk and head----0.530
both arms---------0.125
both thighs-------0.215
both lower legs---0.130

Contini and Drillis[4] calculate a body build index which is a function of both height and weight given by:

$$c = H/W^{1/3}$$

where H = height in inches

and W = weight in pounds .

They present formulas which are a function of the body build index for calculating the weights of the various body segments. They have also collected data from other sources for determining the location of the centers of mass of the various body

segments. Formulas (which are a function of c) for the average density of the limbs are also presented.

Most of the data in the literature is presented statistically; in terms of averages, standard deviations, etc. For the lunar gravity simulation work, exact data are needed for relatively few subjects. Methods were therefore developed to determine the mass and centers of mass of the torso and limbs of living human subjects.

The volume of a particular segment can be determined by water immersion. Then if the density is somehow known the mass of the limb segment can be easily found. However, it is very difficult to determine the density of a segment of the living body. In fact, determining both the mass and center of mass of any body segment is possible only with cadavers. But if it is assumed that the density is a function of total height and weight as reported by Contini and Drillis the segment's mass and center of mass can be determined as follows:

1) The volume of the segment is determined by water immersion. "Knowing" the density the mass can then be calculated.

2) The center of mass of the segment can be found by measuring the reaction forces on a balance board.

A modified version of the water immersion method for finding the volume is used. The subject immerses his limb in a tank of water and the level is noted. The limb is withdrawn

and enough water added from a known volume of water to bring the level back to its original position. The volume of water necessary to do this is the volume of the segment. Volume measurements are not made; instead the supply bucket is weighed before and after adding the necessary volume of water (see Figure 5.1). The segment density is estimated by using the following equations taken form Contini and Drillis[4]. The equations are modified to include the hand or foot with the lower arm or lower leg:

$c = HW^{-1/3}$ (H in inches) (W in lbs.)

$d = 2.17c + 38.1\ lb/ft^3$

$dUA = 0.82bd + 13.5\ lb/ft^3$ (upper arm)

$dLA = 1.29d - 14.6\ lb/ft^3$ (lower arm + hand)

$dUL = 0.775d + 14.2\ lb/ft^3$ (upper leg)

$dLL = 0.912d + 12.5\ lb/ft^3$ (lower leg + foot)

Having an estimate of the density, it is then a simple matter to calculate the segment weight.

To determine the center of mass of the limb the subject first lays flat on a balance board while the reaction force, F_2, is measured and the raises the limb to some angle, θ , while the reaction force, F_2' , is again measured:

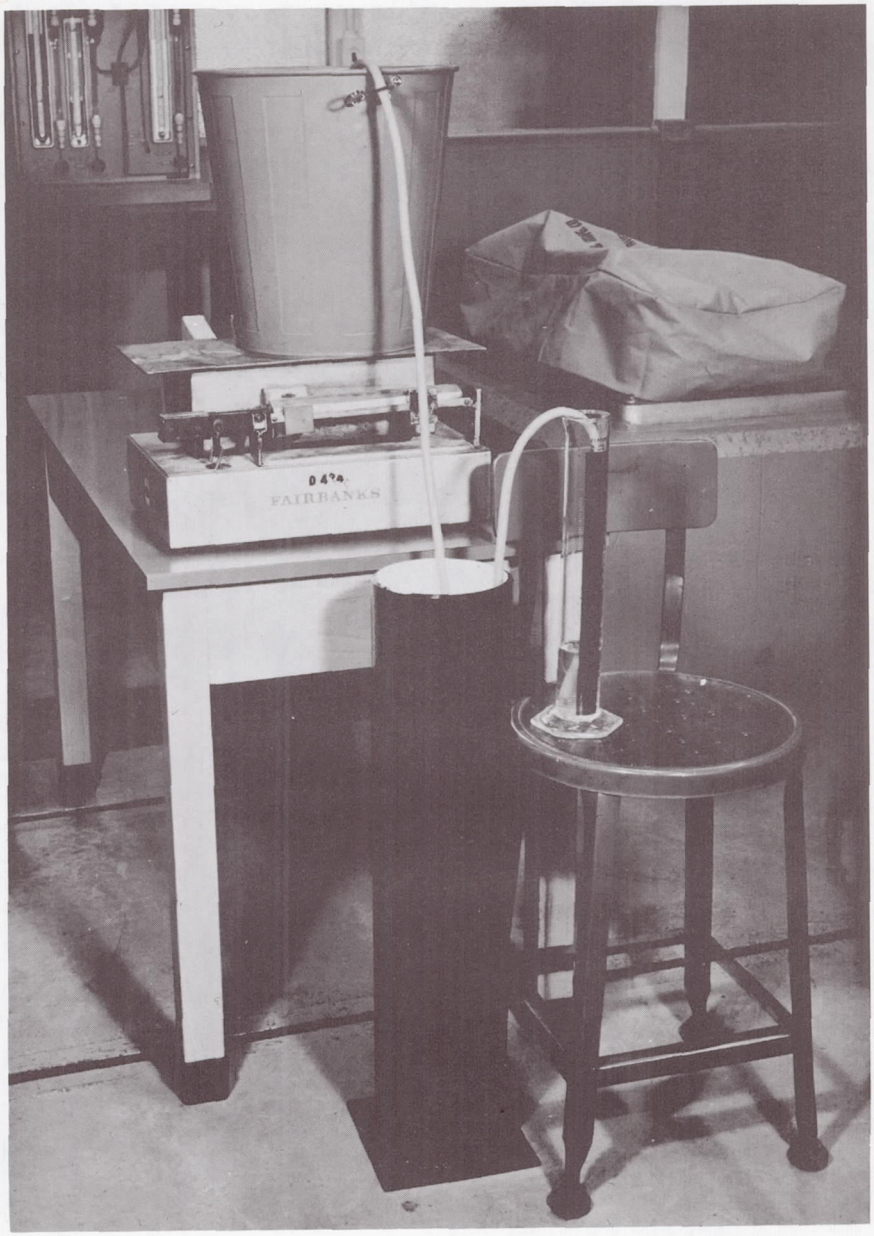

Figure 5.1
Segment Weight Determination:
Arm Immersion Tank

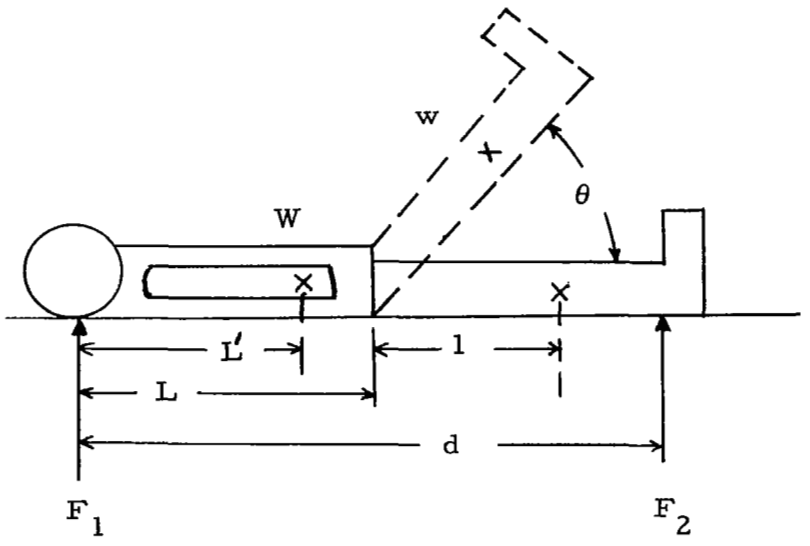

(See also Figures 5.2 and 5.3).

Moment balance yields the following equations:

$$WL' + w(L + l) = F_2 d \qquad (5.11)$$

$$F_2' d = WL' + w(L + l\cos(\theta)) \qquad (5.12)$$

where w = weight of limb

W = weight of rest of body .

Solving for l yields:

$$l = \frac{(F_2 - F_2')d}{w(1-\cos(\theta))} \quad .$$

After the mass and location of the center of mass is known for the limbs, it is easy to calculate the location of the center of mass of the torso-head combination. The

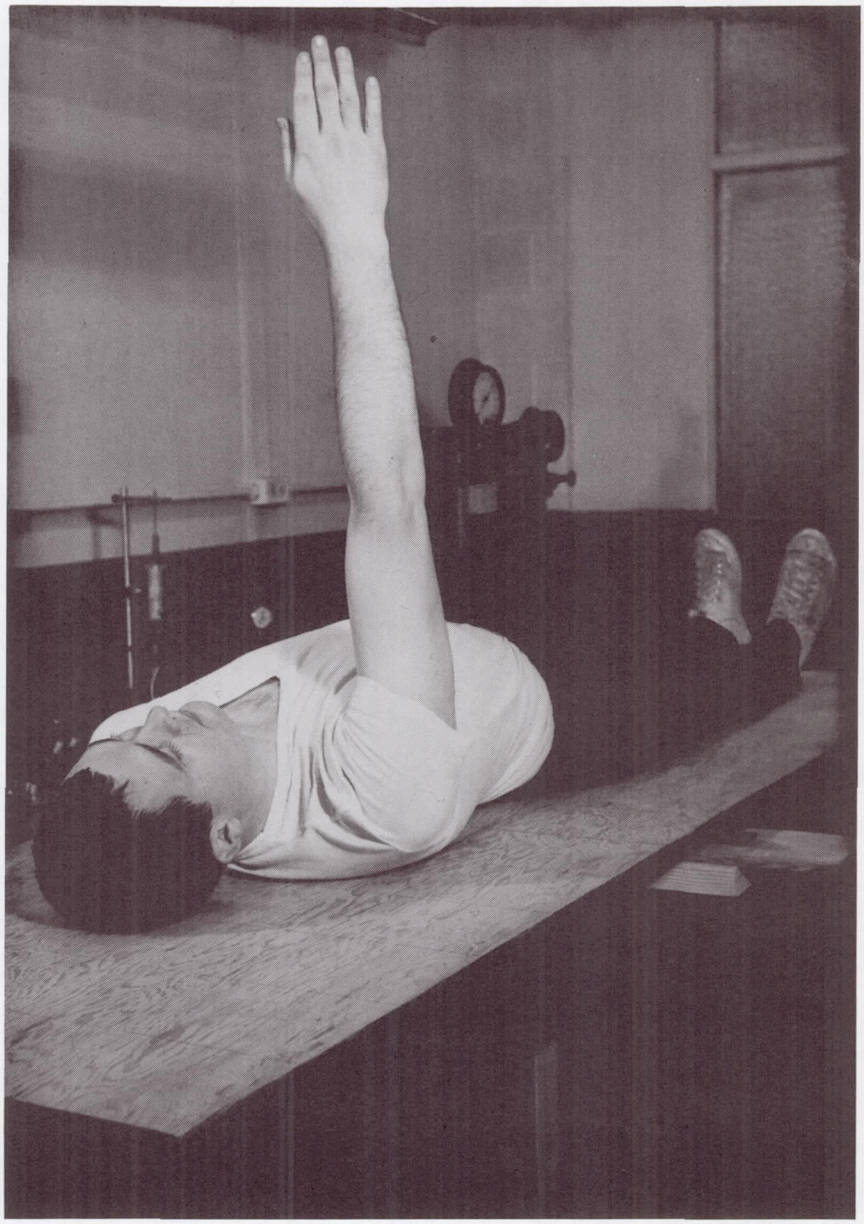

Figure 5.2

Segment Weight Determination: Balance Board

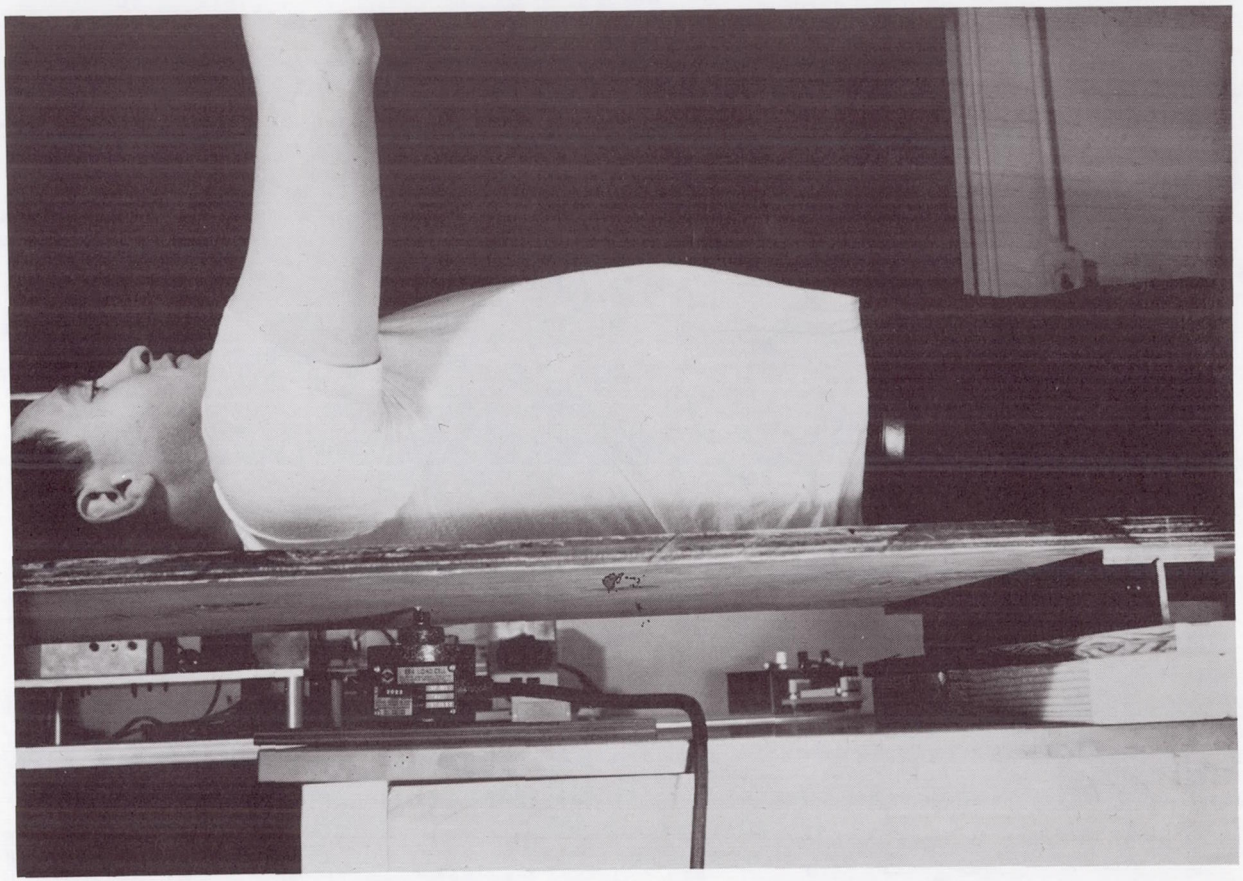

Figure 5.3 - - Balance Board Showing Load Cell and Pivot

center of mass of the total body can be found using the balance board. Moment balance will yield the location of the center of mass of the torso-head combination.

The distance of the center of mass from the posterior body plane is difficult to determine experimentally; however, Swearingen[13] has provided experimental data that can be used to estimate this distance. He reports that the total body center of mass is 4 inches (±1 inch) from the posterior body plane for a standing (arms at sides) position. This data is for normal, young, adult males. It is assumed that the center of mass of the torso is about the same distance from the posterior body plane.

PROTOTYPE SYSTEM

6.1 Negator Units

Several back-to-back conical drum adjustable negator units were designed and built. They were similar in design to those considered in section 4.2 except that they had no spokes but were solid instead. Each conical unit was designed as shown in the following sketch with the dimensions shown in the table below:

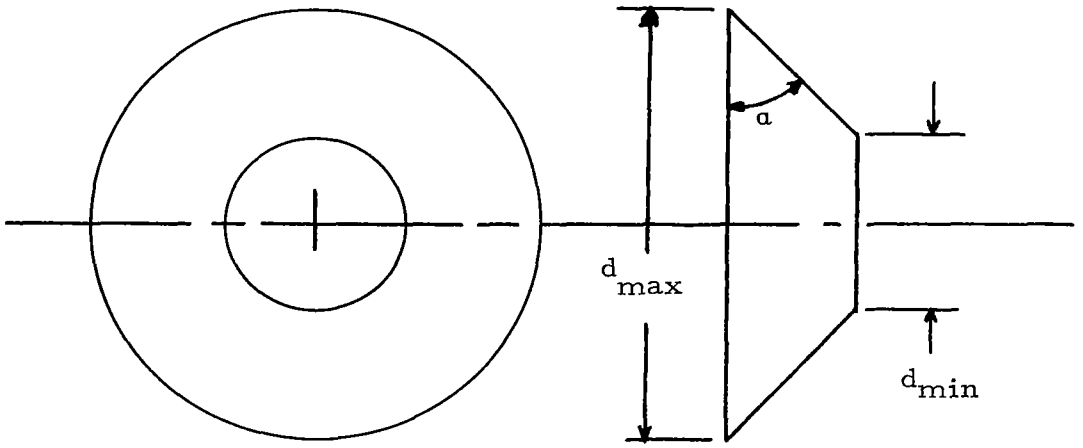

Design No.	Coil No.	α(deg)	dmin(in)	dmax(in)
1	SH31U58	45	2.26	4.71
2	SH25U48	26.5	1.82	4.18
3	SH20R47	26.5	1.47	3.75
4	SH16P38	26.5	1.16	3.4

Design no. 1 (see Figure 6.1) is used to provide negating force for the main torso harness. (This unit is shown in the photograph of Figure 6.1). This design produces approximately 60-80 pounds of force. Design no. 2 is used as a leg

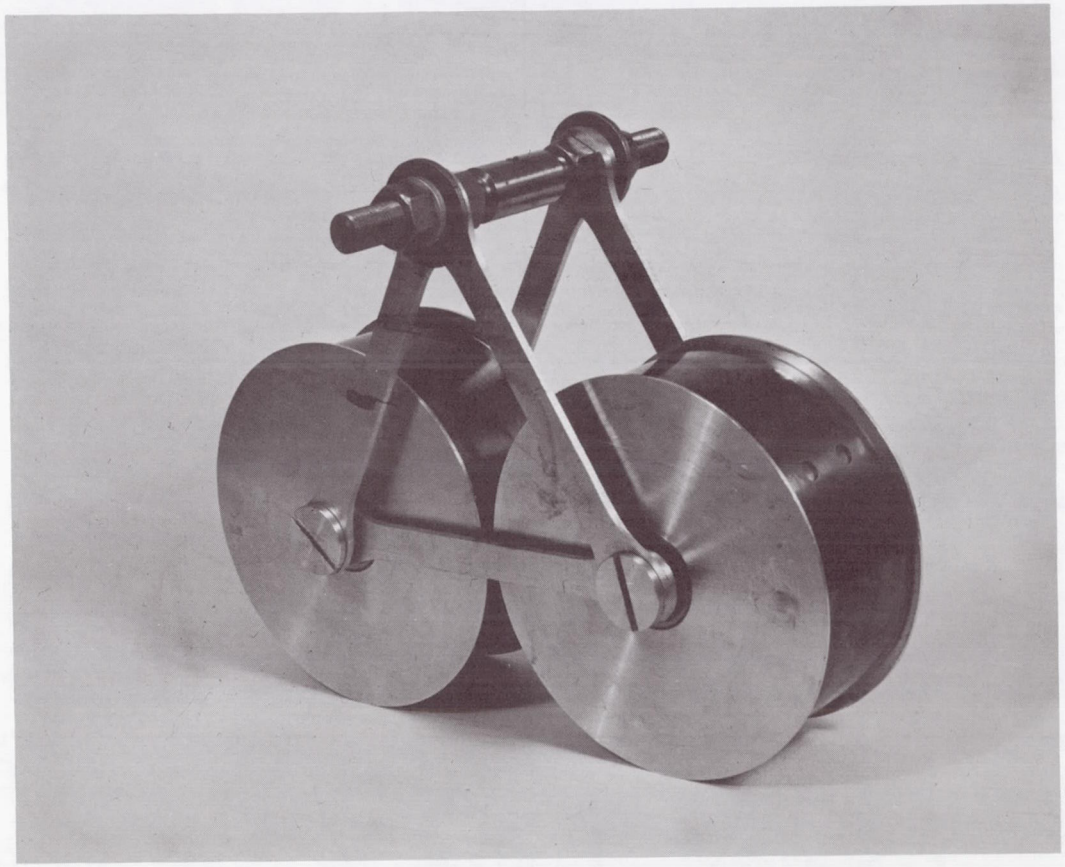

Figure 6.1 - - Prototype Back-To-Back
Adjustable Conical Drum Negator Unit
(Design No. 1)

negator with the cable going straight up the side of the subject rather than being attached to the torso harness. Two other negator units were constructed for use in negating the arms. These used two SH16P38 coils which had their width reduced to 1/2 inch. Their force output was about 10 pounds each. All the negator units used in the prototype simulator were equipped with safety devices to prevent the coils from coming completely unwound from the drums.

6.2 Magnetic Air Pads

Ten prototype magnetic air pads were designed and constructed using the preliminary design of reference 10. Each pad used an eight-pole permanent alnico V magnet rated at 70 pounds and weighing 0.7 pounds. The pads are 4 inches in diameter, machined from magnesium, and assembled with epoxy. The central orifice in each pad is 3/16 inches in diameter. When used with a supply pressure of 80 psig, the pads exhibit a breakaway force of approximately 55 pounds. A photograph of the design is shown in Figure 6.2.

Six of the prototype magnetic air pads arranged in a ring are used to support the main torso harness; one each is used for the arms and legs. The main cluster is shown in Figure 6.3.

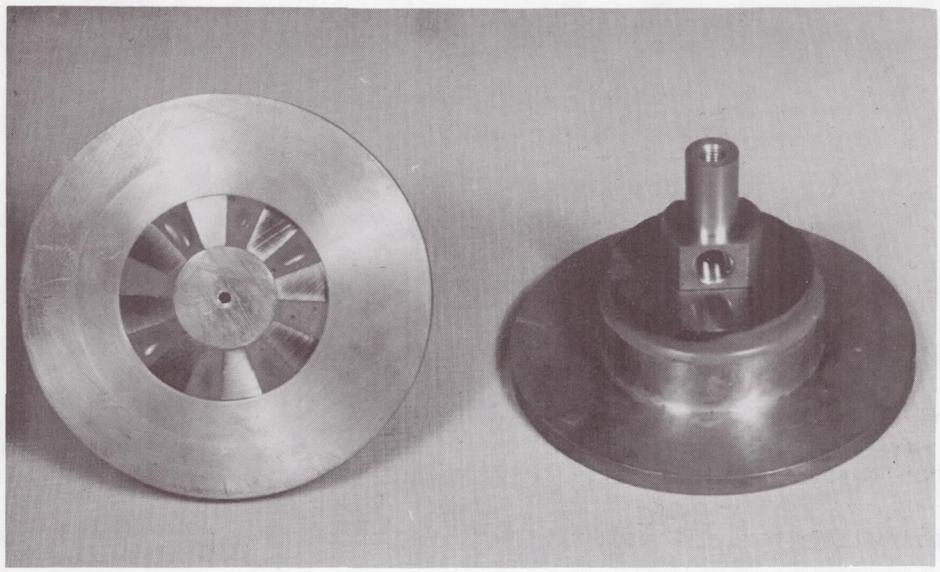

Figure 6.2 - - Magnetic Air Pad

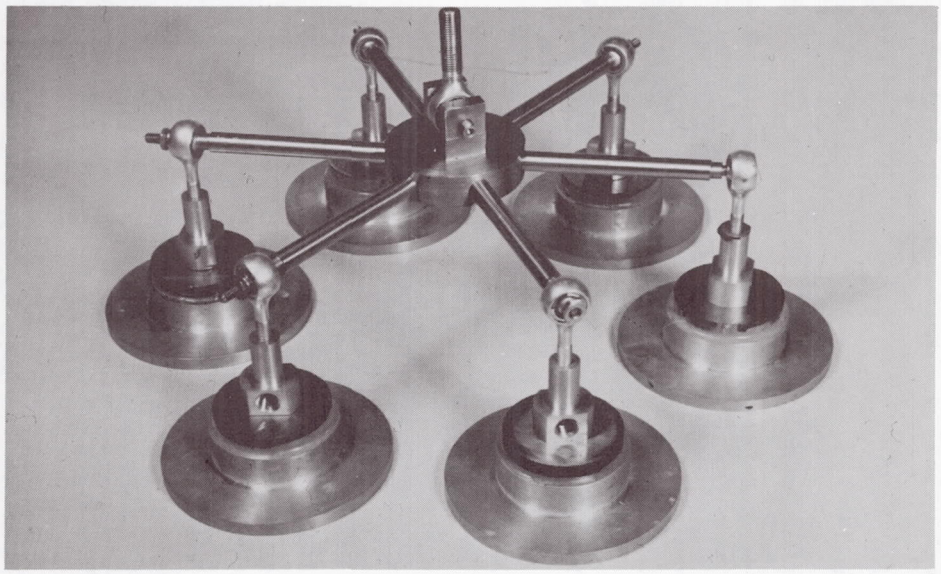

Figure 6.3 - - Magnetic Air Pad Cluster

6.3 Prototype Harness

The harness used with the prototype simulator is shown in several views in Figures 6.4 - 6.7. The subject is supported on a bicycle-like seat and held firmly in place with a foam-padded molded figerglass shell at the front of the torso. The bearing pivot points at the side and back allow for forward and sideways rotation (see Figures 6.8 and 6.9). The harness is constructed mainly of welded square tubular aluminum. Its total weight is about 20 pounds. The attachment points on either side of the harness are adjustable to accommodate subjects of different sizes. (see Figure 6.9).

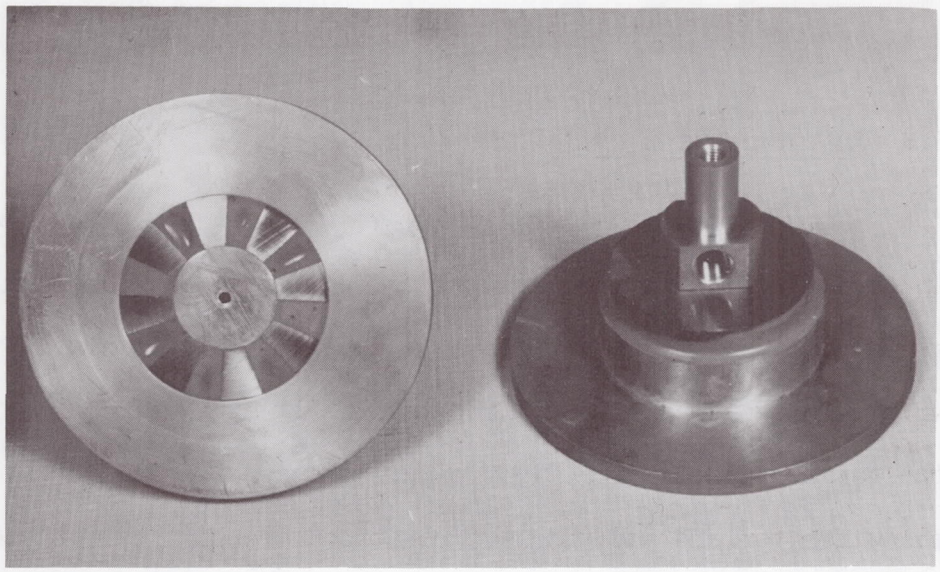

Figure 6.2 - - Magnetic Air Pad

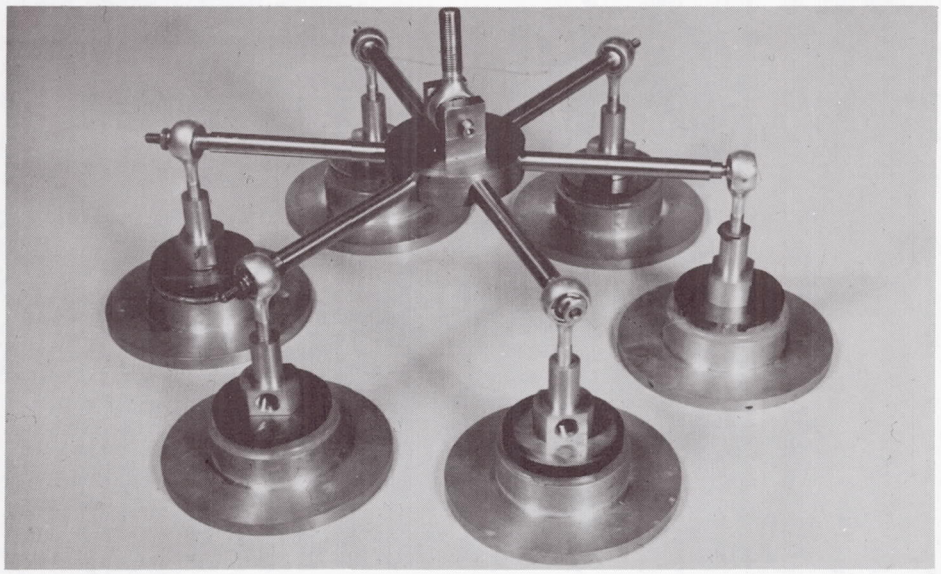

Figure 6.3 - - Magnetic Air Pad Cluster

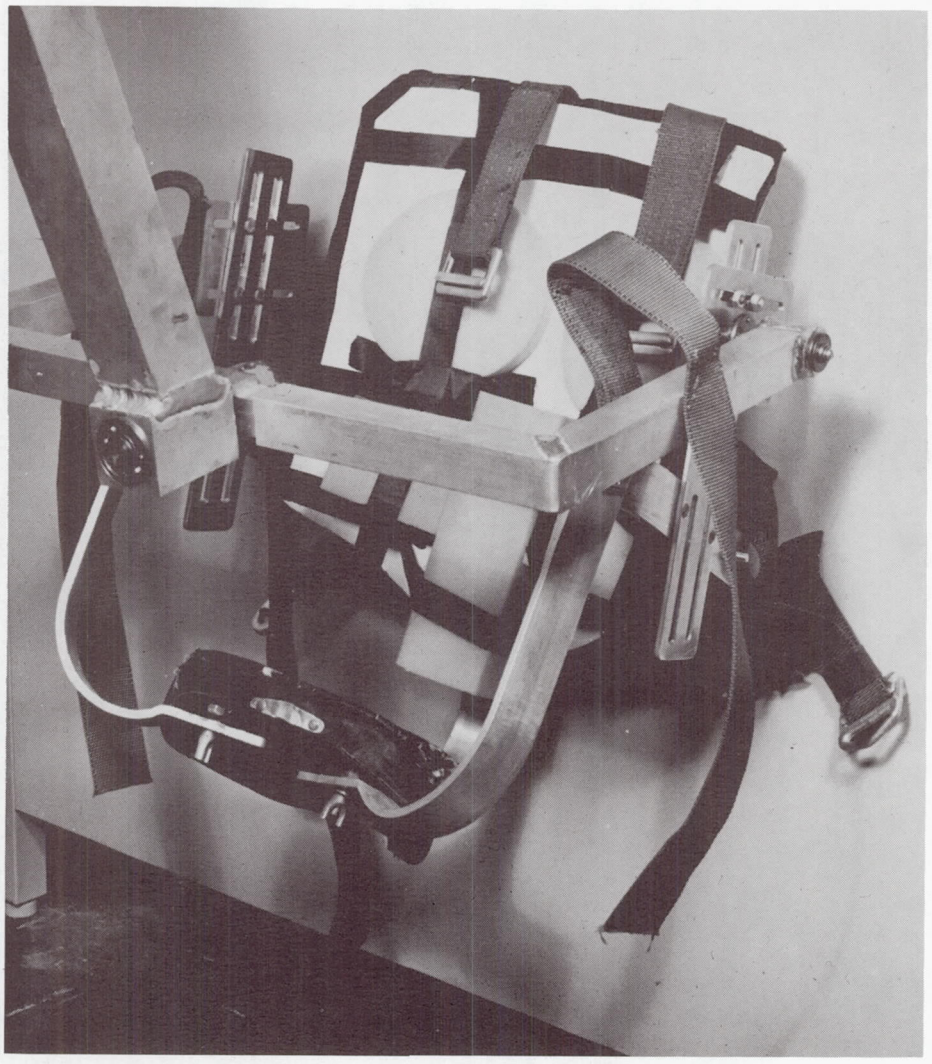

Figure 6.5 - - Prototype Harness

Figure 6.6 - - Prototype Harness

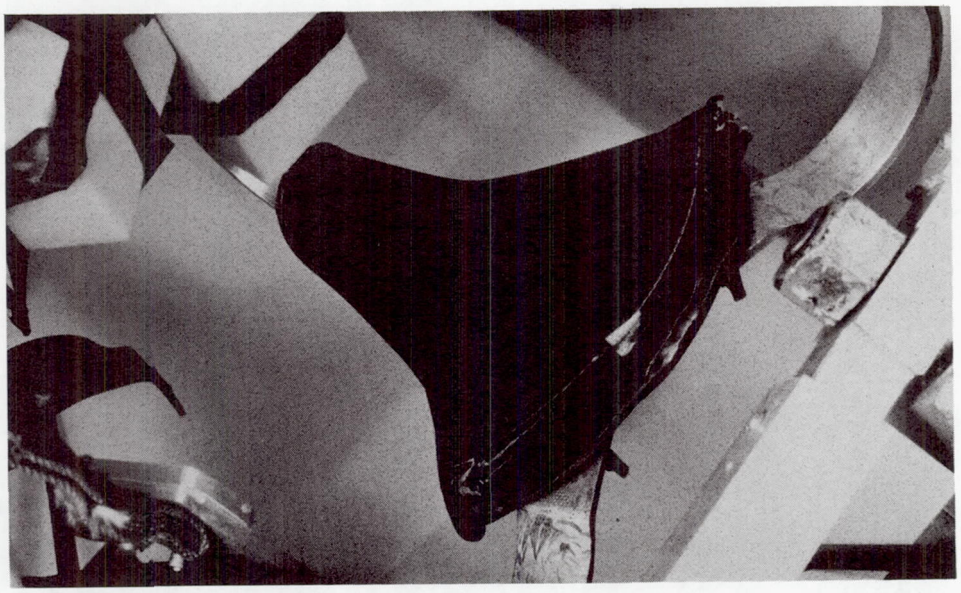

Figure 6.7 - - Prototype Harness: Seat

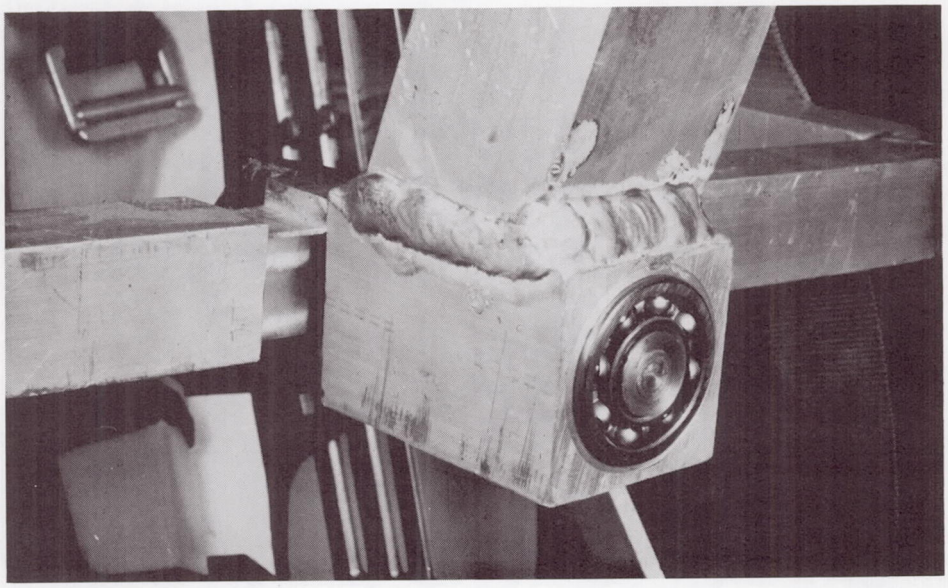

Figure 6.8 - - Prototype Harness: Rear Bearing Pivot Point

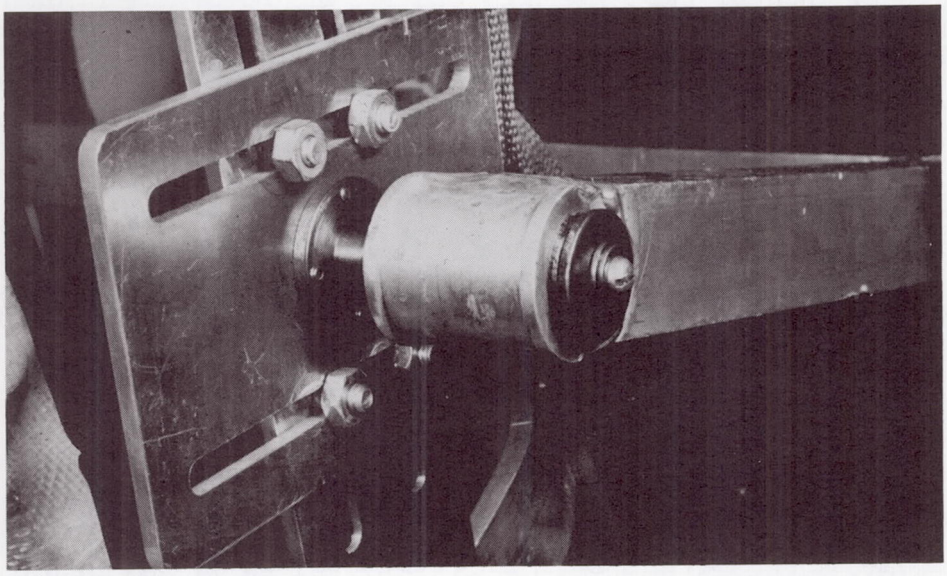

Figure 6.9 - - Prototype Harness: Side Bearing Pivot Point

REFERENCES

1. Barter, J. T., "Estimation of the Mass of Body Segments," WADC Tech. Report 57-260, ASTIA Document No. 118222, April, 1957.

2. Case Institute of Technology, "Prototype Studies in Lunar Gravity Simulation," Report No. EDC 8-66-1, NASA Contract NAS 1-4449, Cleveland, Ohio, February, 1966.

3. Chironis, N.P., "New Springs Do More Jobs," Product Engineering, April 11, 1966.

4. Drillis, R. and Contini, R., "Body Segment Parameters," Technical Report No. 1166.03, Office of Vocational Rehabilitation, Dept of HEW Contract No. R886, New York University, School of Engineering and Science, University Heights, New York, September, 1966.

5. Dubois, J., Omoto, C., and Santschi, W. R., "Moments of Inertia and Centers of Gravity of the Living Human Body," USAF Tech. Documentary Report No. AMRL-TDR-63-36,May, 1963.

6. Hertzberg, H. T., Daniels, E., and Churchill, E., "Anthropometry of Flying Personnel," 1950, USAF, WADC, Tech. Report 52-321, 1954.

7. Hewes, D.E. and Spady, H. A., "Evaluation of a Gravity-Simulation Technique for Studies of Man's Self-Locomotion in Lunar Environment," NASA-TN-D-2176, Langley Research Center, Hampton Va., March, 1964.

8. King, B. G., Patch, C. T., and Shinkman, P. G., "The Center of Mass of Man," ASME Paper No. 60-WA-306, ASME Winter Annual Meeting, Nov.27 - Dec.2, 1964, New York, N.Y.

9. Lay, W. E. and Fisher, L. C., "Riding Comfort and Cushions," Soc.Auto Eng.J., Vol.47, No.5, 1940, pp 482-496.

10. Millett, D. A., "The Design of a Magnetic Air Bearing for Use in a Lunar Gravity Simulator," M.S. Thesis, Case Institute of Technology, Cleveland, Ohio, June, 1967; also published as NASA CR-1235.

11. Northrop Space Laboratories, "A Study of Man's Physical Capabilities on the Moon," NASA Contract No. NAS 1-4449, Hawthorne, California, 1966.

12. Ralston, A. and Wilf, H. S., Mathematical Methods for Digital Computers, John Wiley and Sons, Inc., New York, 1965.

13. Swearingen, J. J., "Determination of Centers of Gravity of Man," Aeromedical Research Division, Civil Aeromedical Research Institute, Oklahoma City, Oklahoma, August, 1962.

14. Timoshenko, S., Strength of Materials, pt. 2 Second Edition, D. Van Nostrand Company, Inc. New York, 1941, p 120.

15. Timoshenko, S.and CacCullough, G. H., Elements of Strength of Materials, Second Edition, D. Van Nostrand Company, Inc., New York, 1940, p 114.

16. Timoshenko, S. and Woinowsky-Krieger, S., Theory of Plates and Sheels, Second Edition, McGraw-Hill, New York, 1959, pp 37-39.

17. Timoshenko, S., Theory of Elastic Stability, Second Edition, McGraw-Hill Book Co., New York, 1936.

18. Votta, F. A., Jr., "The Theory and Design of Long-Deflection Constant-Force Spring Elements," ASME Trans., May, 1952, pp 439-450.

19. Wudell, A. E. and Lewis, D. A., "Comparison of Lunar Simulation Techniques," Martin-Marietta Corp., Report No. M-66-41, October, 1966, Denver, Colorado.

APPENDIX A

Introduction

This appendix contains an abbreviated version of an analysis of the dynamic behavior of a vertical suspension type simulator. The system to be analysed is shown in Figure A1.

The system components consist of one magnetic air pad, a back-to-back negator spring assembly and the subject mass. The subject mass will be considered to be inanimate. The negator spring assembly housing is attached to the air pad by a ball joint. If the system is confined to move in a plane perpendicular to the ceiling, its position can be defined by three generalized coordinates; namely, the position of the air pad center of gravity, the angle between the extended nagator springs and the vertical, and the distance from the ball joint to the subject mass. An important assumption must be made, however, before these three coordinates can correctly determine the position of the system. This is that the extended portion of the negator spring does not bend in the plane of motion. This is probably a valid assumption for the orientation of the negator springs shown in Figure A1.*

* Note that the width of the negator spring is parallel to the plane of motion.

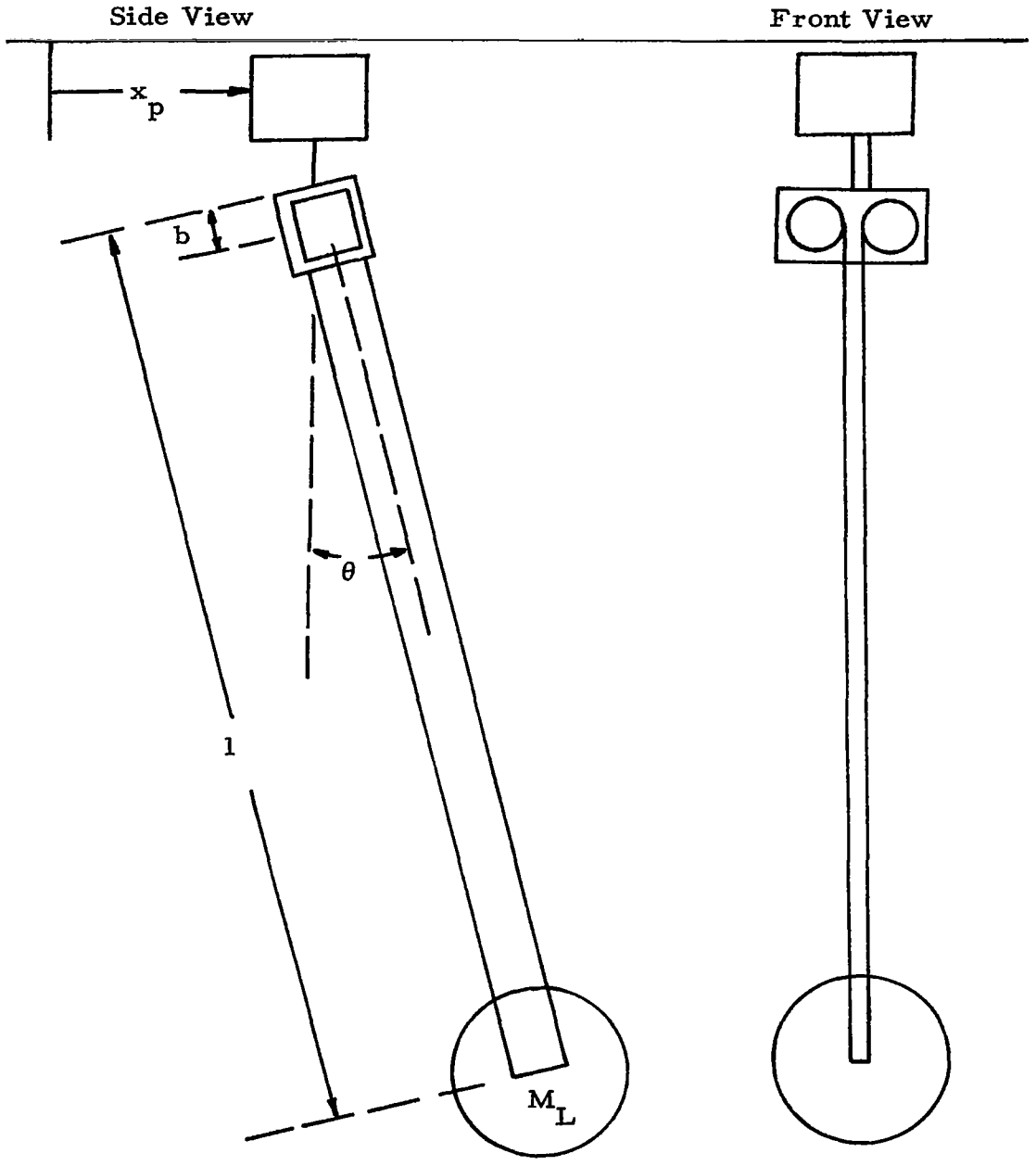

Figure A1
Lunar Gravity Simulator Model

If, however, the negator spring assembly were rotated through 90 degrees, the width of the negator springs would be perpendicular to the plane of motion. Due to the very low rigidity of the negator springs in this direction, the assumption would no longer apply and the three coordinates would not suffice in locating the system.

The following are the assumptions which will be made in the derivation of the dynamic equations:

1. The extended portion of the negator spring is rigid and inextensible.
2. The air pad moves with negligible friction.
3. The up-and-down dynamics of the air pad are so small that they can be neglected.
4. The ball joint has negligible friction.
5. The air drag on the system is negligible.
6. The motion of the system is planar.
7. The negator spring system has a constant force for any elongation.

The parameters used in the analysis are defined as follows:

x_p Location of the center of gravity of the air pad.

θ Angle that the extended portion of the negator spring makes with the vertical.

l The distance from the ball joint to the center of gravity of the subject mass.

a The distance from the center of gravity of the air pad to the ball joint.

b	The distance from the ball joint to the center of gravity of the negator spring spools and housing.
r_s	Radius of a negator spring spool.
R	Radius of the coiled portion of negator spring.
W	Width of the negator spring.
t	Thickness of the negator spring.
L	Total length of a negator spring.
D_{cg}	The center of gravity of the system of masses suspended from the ball joint measured from that point.
λ	A distance parallel to any point on the extended portion of the negator spring.
x	Horizontal distance from a reference point.
y	Vertical distance from a reference point.
M_L	Mass of the subject.
M_p	Mass of the air pad.
M_h	Mass of the negator spring housing.
M_s	Mass of a negator spring spool containing bearings.
M_e	Mass of the extended portion of one negator spring.
M_c	Mass of the coiled poriton of one negator spring.
ρ	The density of the negator spring material.
$I_{s\theta}$	Moment of inertia of one spool about the ball joint.
$I_{c\theta}$	Moment of inertia of the coiled portion of one negator spring about the ball joint.
$I_{h\theta}$	Moment of inertia of the negator spring housing about the ball joint.
$I_{s\alpha}$	Moment of inertia of one spool about its axis of rotation.

I_c Moment of inertia of the coiled portion of one negator spring about the axis of rotation.

F The force output of both negator springs.

T The kinetic energy of the system.

Q A generalized force.

D_m Damping coefficient.

τ A torque.

τ_f Coulamb bearing friction torque.

Kinetic Energy of the Extended Portions of Negator Springs

With reference to Figure A1, the position of any element of mass along the extended portion of the negator spring can be written

$$x = x_p + \lambda \sin(\theta)$$

$$y = -a - \lambda \cos(\theta) .$$

The component velocities of any element of mass can be found by differentiating the above positions with respect to time.

$$\dot{x}_\lambda = \dot{x}_p + \dot{\lambda} \sin(\theta) + \lambda \dot{\theta} \cos(\theta)$$

$$\dot{y}_\lambda = -\dot{\lambda} \cos(\theta) + \lambda \dot{\theta} \sin(\theta)$$

The kinetic energy of the extended portions of both negator springs can be written as

$$T_e = \rho w t \int_b^l (\dot{x}_\lambda^2 + \dot{y}_\lambda^2)\, d\lambda \quad .$$

Upon substitution of the squares of the component velocities into the above expression, the kinetic energy can be written

$$T_e = \rho w t \int_b^l (\dot{x}_p^2 + \dot{\lambda}^2 + \lambda^2 \dot{\theta}^2 + 2\dot{x}_p \lambda \sin(\theta) + 2\dot{x}_p \lambda \dot{\theta} \cos(\theta))\, d\lambda \quad .$$

It should be noted that $\dot{\lambda}$ is a constant over the integration which takes place at any instant of time. In addition, $\dot{\lambda}$ must be equal to $\dot{l}$ due to physical constraint. Upon completing the integration and making the above-mentioned substitution, the kinetic energy of the extended portion of both negator springs can be expressed as follows:

$$T_e = \rho w t \{[\dot{x}_p^2 + \dot{l}^2 + 2\dot{x}_p \dot{l} \sin(\theta)][l - b] + \frac{\dot{\theta}^2}{3}[l^3 - b^3] + \dot{x}_p \dot{\theta} \cos(\theta)[l^2 - b^2]\} \quad .$$

Kinetic Energy of the Subject Mass

For the sake of simplicity, the mass M_L will be assumed concentrated at a point. The coordinates of this point are

$$x_L = x_p + l \sin(\theta)$$

$$y_L = -a - l \cos(\theta) \quad .$$

$$\dot{x}_L = \dot{x}_p + \dot{l}\sin(\theta) + l\,\dot{\theta}\cos(\theta)$$

$$\dot{y}_L = -\dot{l}\cos(\theta) + l\,\dot{\theta}\sin(\theta) \quad .$$

The kinetic energy of the mass can be written

$$T_L = \frac{1}{2} M_L(\dot{x}_L^2 + \dot{y}_L^2) \quad .$$

Upon making the appropriate substitutions, the kinetic energy of the subject mass is

$$T_L = \frac{1}{2} M_L(\dot{x}_p^2 + \dot{l}^2 + l^2\dot{\theta}^2 + 2\dot{x}_p\,\dot{l}\sin(\theta)$$

$$+ 2\dot{x}_p\, l\,\dot{\theta}\cos(\theta)) \quad .$$

Kinetic Energy of the Negator Spring Housing

The coordinates of the center of gravity of the negator spring housing are

$$x_h = x_p + b\sin(\theta)$$

$$y_h = -a - b\cos(\theta) \quad .$$

The velocities are

$$\dot{x}_h = \dot{x}_p + b\,\dot{\theta}\cos(\theta)$$

$$\dot{y}_h = b\,\dot{\theta}\sin(\theta) \quad .$$

The kinetic energy of the housing can then be written as

$$T_h = \frac{1}{2} M_h(\dot{x}_p^2+b^2\dot{\theta}^2+2\dot{x}_p b\ \dot{\theta}\ \cos(\theta))+ \frac{1}{2} I_{hcg}\dot{\theta}^2 \quad .$$

Using the parallel axis theorem, the moment of inertia of the housing about the ball joint is

$$I_{h\theta} = I_{hcg} + M_h\ b^2 \quad .$$

Substituting this equation into the expression for kinetic energy yields the following:

$$T_h = \frac{1}{2} M_h(\dot{x}_p^2 + 2\dot{x}_p b\ \dot{\theta}\ \cos(\theta))+ \frac{1}{2} I_{h\theta}\dot{\theta}^2 \quad .$$

Kinetic Energy of Both Negator Spring Spools

The coordinates of the center of gravity of the two-spool combination are

$$x_s = x_p + b\ \sin(\theta)$$

$$y_s = -a -b\ \cos(\theta) \quad .$$

The corresponding velocities of this center of mass are

$$\dot{x}_s = \dot{x}_p + b\ \dot{\theta}\ \cos(\theta)$$

$$\dot{y}_s = b\ \dot{\theta}\ \sin(\theta) \quad .$$

The spools rotate with an angular velocity $\dot{\alpha}$. This angular velocity is a function of both $\dot{l}$ and l, and can be

expressed as

$$\dot{\alpha} = \frac{\dot{l}}{R} \qquad R = \sqrt{\frac{t}{\pi}(L + b - l) + r_s^2}$$

where R is the varialbe radius of a coil. The expression for R is derived in the next section.

Solving for the kinetic energy due to translation of the center of mass plus that due to rotation about the center of mass gives

$$T_s = M_s[x_p^2 + 2x_p b\ \theta\ \cos(\theta)] + I_{s\theta}\theta^2 + I_s\ \alpha \frac{\dot{l}^2}{[\frac{t}{\pi}(L + b - l) + r_s^2\ ]} \quad .$$

Kinetic Energy of the Coiled Portions of Both Negator Springs

The coordinates of the center of mass of the coil are

$$x_c = x_p + b \sin(\theta)$$

$$y_c = -a - b \cos(\theta) \quad .$$

It should be noted that these coordinates are not a function of the variable l.

The velocities of the center of mass are

$$\dot{x}_c = \dot{x}_p + b\ \dot{\theta} \cos(\theta)$$

$$\dot{y}_c = b\ \dot{\theta} \sin(\theta) \quad .$$

The kinetic energy of the coil can be expressed as

$$T_c = M_c(\dot{x}_p + 2\dot{x}_p b\,\dot{\theta}\cos(\theta)) + I_{c\theta}\dot{\theta}^2 + I_{\alpha c}\frac{\dot{l}^2}{R^2} \quad .$$

The parameters M_c, $I_{c\theta}$, and $I_{\alpha c}$ are functions of the distance l. It can be easily seen that the mass of one coil is

$$M_c = \rho w t\,(L + b - l) \quad .$$

The radius of the coil can be found from the evaluation of the following integral:

$$\int_{r_s}^{R} r\,dr = \int_{o}^{C} \frac{t}{2\pi}\,ds \quad .$$

Where C is the length of the coiled negator spring and ds is an element of arc length:

$$C = L + b - l \quad .$$

Upon evaluation of the above integral, R is found:

$$R = \sqrt{\frac{t}{\pi}(L + b - l) + r_s^2} \quad .$$

The moment of inertia of one coil about its cylindrical axis is

$$I_{\alpha c} = \frac{\pi}{2}\,\rho w[R^4 - r_s^4] \quad .$$

The moment of inertia of a coil about an axis perpendicular to the axis of symmetry through the ball joint is

$$I_{\theta c} = m_c\left[\frac{(R^2 - r_s^2)}{4} + \frac{W^2}{12} + b^2\right] \quad .$$

Making the appropriate substitutions, the kinetic energy of both coils is found.

$$T_c = \rho wt(L + b - l)(\dot{x}_p^2 + 2\dot{x}_p b \dot{\theta} \cos(\theta)$$

$$+ \rho wt(L + b - l)\left[\frac{t}{4\pi} (L + b - l) + \frac{W^2}{12} + b^2 \right] \dot{\theta}^2$$

$$+ \frac{1}{2} \rho wt(L + b - l) \frac{\left[\frac{t}{\pi}(L + b - l) + 2r_s^2 \right] \dot{l}^2}{\left[\frac{t}{\pi}(L + b - l) + r_s^2 \right]}$$

Kinetic Energy of the Air Pad

The kinetic energy of the air pad can be simply expressed by

$$T_p = \frac{1}{2} m_p \dot{x}_p^2 \quad .$$

Kinetic Energy of the System

The kinetic energy of the system is the summation of the kinetic energies of the component masses:

$$T = T_e + T_l + T_h + T_s + T_c + T_p \quad .$$

Generalized Forces

Because of the negligible air drag assumption, the generalized force due to a variation in x_b is

$$Q_{x_b} = 0 \quad .$$

Using the assumptions of negligible air drag and friction in the ball joint, the generalized force due to the variation of θ is

$$Q_\theta = -g(M_L + M_h + 2M_g + 2M_c + 2M_e)D_{cg} \sin(\theta) \quad .$$

Where D_{cg} is the center of mass of the system suspended below the ball joint.

$$D_{cg} = \frac{b(2M_s+M_h)+lM_L+2\rho wtbL+\rho wt(l - b)^2}{M_L+M_h+2M_s+2M_c+2M_e}$$

Q_θ can now be expressed as

$$Q_\theta = -g[b(2M_s+M_L)+lM_L+2\rho wtbL+ \rho wt(l - b)^2] \sin(\theta) \quad .$$

In calculating the generalized force due to a variation in l, the frictional torque in the bearings of one negator spring spool is assumed to be of the form

$$\tau = -(D_m \dot{\alpha} + \frac{\dot{\alpha}}{|\dot{\alpha}|} \tau_f) \quad .$$

The frictional torque contains a viscous friction term and a coulomb friction term. It will be assumed that these are independent of the load applied to the bearing because the variation in the bearing load should be small.

The frictional force due to this torque can be written $f = \frac{2\pi}{R}$ making the substitution $\dot{\alpha} = \frac{\dot{l}}{R}$.

The frictional force due to the bearings in the spools is

$$f = -2(D_m \frac{\dot{l}}{R^2} + \frac{\dot{l}}{|\dot{l}|} \frac{\tau_f}{R}) \quad .$$

The generalized force due to a variation in l is

$$Q_l = (2M_e + M_l)g \cos(\theta) - 2(D_m \frac{\dot{l}}{R^2} + \frac{\dot{l}}{|\dot{l}|} \tau_f) - F \quad .$$

Substituting the expressions for M_e and R into the above equation, Q_l is found in terms of the generalized coordinates.

$$Q_l = [2\rho wt(l-b)+M_L]g \cos(\theta) - \frac{2[D_m \dot{l} + \frac{\dot{l}}{|\dot{l}|} \tau_f \sqrt{\frac{t}{\pi}(L+b-l)+r_s^2}]}{\frac{t}{\pi}(L+b-l)+r_s^2} - F$$

Derivation of Dynamic Equations

Using the method of Lagrange, three dynamic equations will be derived. There will be one equation for each generalized coordinate or degree of freedom.

The first equation of motion for the system is

$$\frac{d}{dt}\left(\frac{\partial T}{\partial \dot{x}_p}\right) - \frac{\partial T}{\partial x_p} = Q_{xp}$$

$$\frac{\partial T}{\partial x} = 0 = Q_{xp} \quad .$$

Then $\frac{d}{dt}\left(\frac{\partial T}{\partial \dot{x}_p}\right) = 0$.

It is seen that the coordinate x_p can be ignored from the standpoint of the dynamics of the system. Furthermore, the above equation is immediately integrable and has the form

$$\frac{\partial T}{\partial \dot{x}_p} = \text{const.}$$

Since the quantity $\frac{\partial T}{\partial \dot{x}_p}$ is the momentum associated with the coordinate $\dot{x}_p$, the previous equation is a statement of conservation of momentum in the x_p direction.

Carrying out the required differentiation, this equation becomes

$$(M_p+M_h+2M_s+2\rho wtL+M_L)\dot{x}_p+(M_h+2M_s+2\rho wtL)b\,\dot{\theta}\cos(\theta)$$

$$+M_L(\dot{l}\sin(\theta)+l\,\dot{\theta}\cos(\theta)+\rho wt[(l-b)^2\,\dot{\theta}\cos(\theta)$$

$$+2(l-b)\dot{l}\sin(\theta)] = \text{const.}$$

The second equation of motion for the system is

$$\frac{d}{dt}\left(\frac{\partial T}{\partial \dot{\theta}}\right) - \frac{\partial T}{\partial \theta} = Q_\theta \quad .$$

Performing the required differentiations yields:

$$\ddot{\theta}\left[\frac{2}{3}\rho wt(l^3-b^3)+M_L l^2+I_{h\theta}+2I_{s\theta}+\rho wt(L+b-l)\left(\frac{t}{4\pi}(L+b-l)+\frac{r_s^2}{2}+\frac{w^2}{12}+b^2\right)\right]$$

$$+\dot{\theta}\dot{l}\left[2\rho wtl^2+2M_L l-2\rho wt\left(\frac{t}{2\pi}(L+b-l)+\frac{r_s^2}{2}+\frac{w^2}{12}+b^2\right)\right]$$

$$+\ddot{x}_p\left[\rho wt\cos(\theta)(l^2-b^2)+M_L l\cos(\theta)+2b\cos(\theta)\right.$$

$$\left.\left(\frac{1}{2}M_h+M_s+\rho wt(L+b-l)\right)\right]+g\left[b(2M_s+M_L)+lM_L+2\rho wtbL+\rho wt(l-b)^2\right]$$

$$\sin(\theta)=0$$

The third equation of motion for the system is

$$\frac{d}{dt}\left(\frac{\partial T}{\partial \dot{l}}\right)-\frac{\partial T}{\partial l}=Q_l$$

The evaluation of this equation yields:

$$\ddot{l}\left\{2\rho wt(l-b)+M_L+\frac{2I_{s\alpha}+\rho wt(L+b-l)\left[\frac{t}{\pi})L+b-l)+2r_s^2\right]}{\frac{t}{\pi}(L+b-l)+r_s^2}\right\}$$

$$+\ddot{x}_p\left[2\rho wt\sin(\theta)(l-b)+M_L\sin(\theta)\right]$$

$$+\frac{t}{\pi}\dot{l}^2\left\{\frac{I_{s\alpha}+\frac{1}{2}\rho wt(L+b-l)\left[\frac{t}{\pi}(L+b-l)+2r_s^2\right]}{\left[\frac{t}{\pi}(L+b-l)+r_s^2\right]^2}\right\}$$

$$+\dot{\theta}^2\left\{\rho wt\left[\frac{t}{2\pi}(L+b-l)+\frac{w^2}{12}+\frac{r_s^2}{2}+b^2\right]-\rho wtl^2-M_L l\right\}$$

$$=\left[2\rho wt(l-b)+M_L\right]g\cos(\theta)-F-\frac{2\left[D_m\dot{l}+\tau_f sgn(\dot{l})\sqrt{\frac{t}{\pi}(L+b-l)+r_s^2}\right.}{\frac{t}{\pi}(L+b-l)+r_s^2}$$

APPENDIX B - COMPUTER PROGRAMS

In this appendix is a listing of three fortran computer programs: JUMP1, DESIO, and JUMP2.

JUMP1 is the name of the computer program that was developed to solve the equations derived in section 3.2. The inputs to the program are as follows:

mass of subject	UM
length of negator coils	UL
thickness of negator coils	T
width of negator coils	W
natural radius of curvature of negator coils	RNO
radius of drums that the negator coils were wrapped on	RIO
initial upward velocity of subject	X20

The output of the program is the height and acceleration of the subject at selected time intervals. The corresponding lunar height is also printed out.

DESIO is the name for the program that was developed to use the equations derived in Section 4.2. The program automatically chooses the optimum values of cone angle and spoke number that will result in a minimum weight design. The inputs are as follows:

width of negator coils	W
length of negator coils	UL
thickness of negator coils	T
natural radius of curvature of negator coils	RNO
minimum radius that negator coils are wrapped on	RIO
change in radius that is desired	DELR

density of material	RHOS
Young's modulus of material	EM
Working stress	SIGMA
buckling load factor (see section 4.2)	BETA

The output of the program is the cone angle and number of spokes to be used plus all the dimensions such as spoke width, etc. These symbols are defined in section 4.2.

JUMP2 used the equations that were derived in Appendix A. The inputs are the same as JUMP1 except that the thickness of the negator coil is TT and the input velocities are YODOT upward and XODOT sideways. UMP is the mass of the air pad. The output of the program gives the position and acceleration in both dimensions of the subject together with the corresponding position for a lunar "jumper."

```
LST
FOR JUMP1
  1 FORMAT()
  2 FORMAT(2X17HTOTAL COIL WEIGHT)
  3 FORMAT(2XF12.3)
 10 FORMAT(9X 4HTIME 11X 6HHEIGHT 9X 12HLUNAR HEIGHT 3X 5HACCEL)
 11 FORMAT(4F15.3)
 12 FORMAT(2X 28HYOU HAVE GONE THRU THE FLOOR)
 13 FORMAT(2X 37HTHE SPRING DIMENSIONS, IN INCHES, ARE)
 14 FORMAT(8X 3HRNO 7X 3HRIO 7X 1Hw 9X 1HT)
 15 FORMAT(2X 4F10.3)
 16 FORMAT(2X 44HTHE INITIAL VELOCITY UPWARD, IN FT./SEC., IS)
 17 FORMAT(12X F10.1)
    J=99
    Y=(28.0E6)*144.0
    UL=6.0
    RHO=0.283*1728.0/32.2
    READ(5,1)(W,T,RNO,RIO)
    WRITE(6,13)
    WRITE(6,14)
    WRITE(6,15) (RNO,RIO,W,T)
    WRITE(6,2)
    CWT=2.0*0.283*UL*W*T/12.0
    WRITE(6,3)(CWT)
    W=W/12.0
    T=T/12.0
    RO=RIO/12.0
    RNO=RNO/12.0
    PI=3.14159
    RH1=(0.07/0.283)*RHO
    DIS=W*RH1*PI*RO**3/48.0
    UM=24.0/32.2
    G=32.2
    WL=RHO*W*T
    H=0.001
    ULL=UL+2.0
    X1=UL
    X20=-7.0
    X20=-5.0
    Z=-X20
    WRITE(6,16)
    WRITE(6,17)(Z)
    X2=X20
    WRITE(6,10)
    DO 100 N=1,100000
    J=J+1
    AX1=X1
    AX2=X2
    F1=AX2
    S1=RO**2+(T/PI)*(UL-AX1)
    S2=2.0*WL*RO**2*(UL-AX1)
    S3=WL*(T/PI)*((UL-AX1)**2)
    F=0.8301*UM*G+WL*AX1*G *2.0
```

```
      F2=((2.0*WL*AX1+UM)*G-F-AX2**2*(WL+0.5*(T/PI)*(2.0*UIS+S2+S3)/(S1*
     1*2)-(WL*RO**2+WL*(T/PI)*(UL-AX1))/S1))/((2.0*UIS+S2+S3)/S1+2.0*WL*
     2AX1+UM)
      ACCEL=F2
      Q21=H*F2
      Q11=H*F1
      AX2=X2+0.5*Q21
      AX1=X1+0.5*Q11
      F1=AX2
      S1=RO**2+(T/PI)*(UL-AX1)
      S2=2.0*WL*RO**2*(UL-AX1)
      S3=WL*(T/PI)*((UL-AX1)**2)
      F=0.8301*UM*G+WL*AX1*G *2.0
      F2=((2.0*WL*AX1+UM)*G-F-AX2**2*(WL+0.5*(T/PI)*(2.0*UIS+S2+S3)/(S1*
     1*2)-(WL*RO**2+WL*(T/PI)*(UL-AX1))/S1))/((2.0*UIS+S2+S3)/S1+2.0*WL*
     2AX1+UM)
      Q12=H*F1
      Q22=H*F2
      AX1=X1+0.5*Q12
      AX2=X2+0.5*Q22
      F1=AX2
      S1=RO**2+(T/PI)*(UL-AX1)
      S2=2.0*WL*RO**2*(UL-AX1)
      S3=WL*(T/PI)*((UL-AX1)**2)
      F=0.8301*UM*G+WL*AX1*G *2.0
      F2=((2.0*WL*AX1+UM)*G-F-AX2**2*(WL+0.5*(T/PI)*(2.0*UIS+S2+S3)/(S1*
     1*2)-(WL*RO**2+WL*(T/PI)*(UL-AX1))/S1))/((2.0*UIS+S2+S3)/S1+2.0*WL*
     2AX1+UM)
      Q13=H*F1
      Q23=H*F2
      AX1=X1+Q13
      AX2=X2+Q23
      F1=AX2
      S1=RO**2+(T/PI)*(UL-AX1)
      S2=2.0*WL*RO**2*(UL-AX1)
      S3=WL*(T/PI)*((UL-AX1)**2)
      F=0.8301*UM*G+WL*AX1*G *2.0
      F2=((2.0*WL*AX1+UM)*G-F-AX2**2*(WL+0.5*(T/PI)*(2.0*UIS+S2+S3)/(S1*
     1*2)-(WL*RO**2+WL*(T/PI)*(UL-AX1))/S1))/((2.0*UIS+S2+S3)/S1+2.0*WL*
     2AX1+UM)
      Q14=H*F1
      Q24=H*F2
      Q1=(1.0/6.0)*(Q11+2.0*Q12+2.0*Q13+Q14)
      Q2=(1.0/6.0)*(Q21+2.0*Q22+2.0*Q23+Q24)
      IF(J.NE.100) GO TO 120
      J=0
      TIME=(N-1)*H
      HE=UL-X1
      ULUHE=-X20*TIME-0.5*5.47*TIME**2
      WRITE(6,11) (TIME,HE,ULUHE,ACCEL)
  120 IF(X1.GT.ULL) GO TO 130
      X1=X1+Q1
  100 X2=X2+Q2
  130 WRITE(6,12)
```

```
LST
FOR DESIO
    DIMENSION Y(8,21)
  1 FORMAT( )
  2 FORMAT(40X 6HSPOKES)
  3 FORMAT(2X6HANGLES5X1H39X1H49X1H59X1H69X1H79X1H89X1H99X2H10)
  4 FORMAT(4X I2, 8F10.2)
  5 FORMAT(3X 22HFORCE TO WEIGHT RATIOS)
  6 FORMAT(2X32HOPTIMUM FORCE TO WEIGHT RATIO IS)
  7 FORMAT(15X F10.2)
  8 FORMAT(2X 16HNUMBER OF SPOKES 2X 5HANGLE)
  9 FORMAT(8X 2I10)
 10 FORMAT(2X 21HPARAMETERS VALUES ARE)
 11 FORMAT(8X1HW9X1HB9X1HM9X1HQ)
 12 FORMAT(2X 4F10.3)
 13 FORMAT(2X9HMAX FORCE 10X 9HMIN FORCE10X11HCOIL WEIGHT)
 14 FORMAT(5X 3F15.4)
 15 FORMAT(8X1HW9X1HT9X3HRNO7X3HRIO7X4HDELR6X2HUL8X4HRHOS6X2HEM8X
   15HSIGMA5X4HBETA)
 16 FORMAT(2X 10E10.5)
    READ(5,1)(W,T,RNO,RIO,DELR,UL,RHOS,EM,SIGMA,BETA)
    WRITE(6,15)
    WRITE(6,16)(W,T,RNO,RIO,DELR,UL,RHOS,EM,SIGMA,BETA)
    RHO=0.283
    E=28.0E6
    PI=3.14159
    R=RIO+DELR
    UI=W*T**3/12.0
    FMAX=E*UI*(1.0/(RIO**2)-2.0/(RNO*RIO))*(-1.0)
    FMIN=E*UI*(1.0/(R**2)-2.0/(RNO*R))*(-1.0)
    F=(F*W*T**3/48.0)*(2.0/(R*RNO)-1.0/(R**2))
    SF=(E*UI*UL/(4.0*PI*R**3))*(1.0/RNO-1.0/R)
    DO 100 N=1,21
    A=N
    ALPHA=24.0+A
    ALPHA=ALPHA/57.29578
    TANA=TAN(ALPHA)
    H=DELR*TANA
    DO 90 M=1,8
    C=M
    UN=2.0+C
    SL=2.0*PI*R/UN
    HQ=(3.0*(SF*SL+F))/(SIGMA*((TANA       )**2))
    HB2=6.0*R*(SF*SL+F)/(SIGMA*TANA       )
    HB3=3.0*UL**2*(SF*SL+F)/(PI**2*BETA*EM)
    HM2=(SF*SL+F)*SL/SIGMA
    UM=SQRT(HM2/H)
    B1=HB2/(H**2)
    B2=CBRT(HB3/H)
    B=AMAX1(B1,B2)
    Q=HQ/B
    WT=RHOS*UN*B*H*(RIO+DELR/2.0)*4.0
   1+((RHOS*UM*PI*H/((SIN(ALPHA))*TANA))*(2.0*R*TANA-H))*4.0
```

```
      CWT=2.0*RHO*W*T*UL
      FWT=FMAX/(WT+CWT)
   90 Y(M,N)=FWT
  100 CONTINUE
      WRITE(6,5)
      WRITE(6,2)
      WRITE(6,3)
      DO 110 L=1,21
      LL=L+ 24
  110 WRITE(6,4)(LL,(Y(N,L),N=1,8))
      X=1.0
      K=1
      KK=1
      DO 130 I=1,8
      DO 120 J=1,21
      IF(X.GT.Y(I,J)) GO TO 120
      X=Y(I,J)
      K=I
      KK=J
  120 CONTINUE
  130 CONTINUE
      A=KK
      C=K
      KKW=KK+24
      KW=K+2
      ALPHA=(24.0+A)/57.29578
      UN=2.0+C
      TANA=TAN(ALPHA)
      H=DELR*TANA
      SL=2.0*PI*R/UN
      BQ=(3.0*(SF*SL+F))/(SIGMA*((TANA       )**2))
      BH2=6.0*R*(SF*SL+F)/(SIGMA*TANA       )
      HB3=3.0*UL**2*(SF*SL+F)/(PI**2*BETA*EM)
      HM2=(SF*SL+F)*SL/SIGMA
      UM=SQRT(HM2/H)
      B1=BH2/(H**2)
      B2=CBRT(HB3/H)
      B=AMAX1(B1,B2)
      Q=BQ/B
      WT=RHOS*UN*B*H*(RIO+DELR/2.0)*4.0
     1+((RHOS*UM*PI*H/((SIN(ALPHA))*TANA))*(2.0*R*TANA-H))*4.0
      CWT=2.0*RHO*W*T*UL
      FWT=FMAX/(WT+CWT)
      WRITE(6,6)
      WRITE(6,7)(FWT)
      WRITE(6,8)
      WRITE(6,9)(KW,KKW)
      WRITE(6,10)
      WRITE(6,11)
      WRITE(6,12)(H,B,UM,Q)
      WRITE(6,13)
      WRITE(6,14)(FMAX,FMIN,CWT)
      END
N XQT DESIO
```

```
LST
FOR RAT
      SUBROUTINE RAT(AY,T,F,Z,P1,P5,P8)
      DIMENSION AY(6),T(6)
      COMMON/DAD/UL, B, TP,      RS, WL, UMH, UMS, UML, G, WL2, UIHO,
     1UISO, TT,P1, P2, P3, UISA, DM, TF, P6, P7, F5 ,RNO,A
      Z=ABS(AY(6))
      P1=UL+B-AY(5)
      P3=COS(AY(3))
      P4=SIN(AY(3))
      P5=TP*P1+RS**2
      P6=WL*UL
      P7=UMH+2.0*UMS+2.0*P6
      P8=TP*P1+2.0*RS**2
      P9=AY(5)-B
      F=0.8301*UML*G+WL2*G*AY(5)
      F1=(2.0/3.0)*WL*(AY(5)**3-B**3)+UML*UL**2+UIHO+2.0*UISO
      F2=WL2*AY(5)**2+2.0*UML*AY(5)-WL2*((TT/(2.0*PI))*P1+P2)
      F3=WL*P3*(AY(5)**2-B**2)+UML*AY(5)*P3+2.0*B*P3*(0.5*UMH+UMS+WL*P1)
      F4=G*P4*(B*(2.0*UMS+UML)+AY(5)*UML+WL2*B*UL+WL*P9**2)
      F6=P7*B*P3+UML*AY(5)*P3+WL*P3*P9**2
      F7=UML*P4+WL2*P4*P9
      F8=WL2*P9+UML+(2.0*UISA+WL*P1*P8)/P5
      F9=WL2*P4*P9+UML*P4
      F10=TP*(UISA+0.5*WL*P1*P8)/(P5**2)
      F11=WL*(0.5*TP*P1+P2)-WL*AY(5)**2-UML*AY(5)
      F12=(WL2*P9+UML)*G*P3-F-(2.0*(DM*AY(6)+(TF*AY(6)/Z)*SQRT(P5)))/P5
      F6D=-P7*B*P4*AY(4)+UML*(AY(6)*P3-AY(5)*P4*AY(4))+WL*
     1(-P9**2*P4*AY(4)+P3*2.0*AY(6)*P9)
      F7D=UML*P3*AY(4)+WL2*(P9*P3*AY(4)+P4*AY(6))
      D=F1*F5*F8-F1*F7*F9-F3*F6*F8
      P11=F6D*AY(4)+F7D*AY(6)
      P12=F12-AY(4)**2*F11-AY(6)**2*F10
      P13=F4+AY(4)*AY(6)*F2
      T(1)=AY(2)
      T(2)=(-F1*F8*P11-F1*F7*P12+F6*F8*P13)/D
      T(3)=AY(4)
      T(4)=(-F5*F8*P13+F3*F7*P12+F7*F9*P13+F3*F8*P11)/D
      T(5)=AY(6)
      T(6)=(F1*F5*P12-F6*F9*P13+F1*F9*P11-F3*F6*P12)/D
      RETURN
      END
FOR JUMP2
      COMMON/DAD/UL, B, TP,      RS, WL, UMH, UMS, UML, G, WL2, UIHO,
     1UISO, TT,P1, P2, P3, UISA, DM, TF, P6, P7, F5 ,RNO,A
      DIMENSION Q(6,4),T(6),R(6),YP(6,5), AY(6),Y(6,5),S(6,5),U(6),YN(6)
    1 FORMAT( )
    3 FORMAT(2X 47HTHE SPRING AND SPOOL DIMENSIONS, IN INCHES, ARE)
    4 FORMAT(8X 2HRS 8X 1HW 9X 1HT 9X 3HRNO)
    5 FORMAT(2X 4F10.3)
   10 FORMAT(5X 4HTIME 5X 1HX 8X 3HXLU 6X 1HY 8X 3HYLU 6X 6HVACCEL
     14X 4HXVEL 5X 5HANGLE 4X7HPAD POS 2X5HXPDOT 4X 4HVFOR5X 8HPADACCEL)
   11 FORMAT(12F9.3)
```

```
12 FORMAT(2X 22HYOU HAVE HIT THE FLOOR)
13 FORMAT(2X 26HTHE INITTAL CONDITIONS ARE)
14 FORMAT(2X 19HHORIZONTAL VELOCITY 5X 17HVERTICAL VELOCITY)
15 FORMAT(10X F8.3,F12.3)
16 FORMAT(111X 10HITERATIONS)
17 FORMAT(115X I2)
18 FORMAT(2X 29HOVERHEAD MASSES, IN LBS., ARE)
19 FORMAT(2X 3HPAD 7X 7HHOUSING 3X 11HBOTH SPOOLS 3X 5HTOTAL)
20 FORMAT(2X 4F10.2)
   H=0.002
   I=0
   TF=0.0
   DM=0.0
   READ(5,1)(UMP,TT,RNO,W,RIO)
   UMP=UMP/32.2
   RIO1=RIO
   W1=W
   TT1=TT
   RNO1=RNO
   TT=TT/12.0
   W=W/12.0
   RS=RIO/12.0
   RNO=RNO/12.0
   UML=24.0/32.2
   SMALL=1.0E-8
   G=32.2
   PI=3.14159
   UL=6.0
   RHO=0.283*1728.0/32.2
   RHO=(1.0/8.0)*RHO
   B=1.5*RS
   RH1=(0.07/0.283)*RHO
   WL=RHO*W*TT
   ULL=UL+B
   WL2=2.0*WL
   TP=TT/PI
   UMS=RH1*PI*RS*W/48.0
   UMS=0.01/                                        32.2
   UMH=RH1*RS/288.0
   UMH=0.01/32.2
   UISA=UMS*RS**2
   UIHO=UMH*RS**2
   UISO=UMS*RS**2
   UMS2=64.4*UMS
   UMP1=UMP*32.2
   UMH1=UMH*32.2
   TOTAL=UMP1+UMH1+UMS2
   P2=RS**2/2.0+W**2/12.0+B**2
   P6=WL*UL
   P7=UMH+2.0*UMS+2.0*P6
   P5=UMP+UMH+2.0*UMS+WL2*UL+UML
   Y=(28.0E6)*2.0*144.0
   A=Y*W*TT**3/26.4
   YODOT=5.0
```

```
      XODOT=5.0
      Y(1,1)=0.0
      Y(2,1)=XODOT
      Y(2,1)=0.0
      Y(3,1)=0.0
      Y(5,1)=UL
      Y(4,1)=((XODOT-Y(2,1))*COS(Y(3,1))+YODOT*SIN(Y(3,1)))/Y(5,1)
      Y(6,1)=(XODOT-Y(2,1))*SIN(Y(3,1))-YODOT*COS(Y(3,1))
      WRITE(6,3)
      WRITE(6,4)
      WRITE(6,5) (RIO1,W1,TT1,RNO1)
      WRITE(6,18)
      WRITE(6,19)
      WRITE(6,20)(UMP1,UMH1,UMS2,TOTAL)
      WRITE(6,13)
      WRITE(6,14)
      WRITE(6,15)(XODOT,YODOT)
      WRITE(6,10)
      WRITE(6,16)
      DO 100 N=1,3
      M=N+1
      IF(N.NE.1) GO TO 99
      TIME=(N-1)*H
      X=Y(1,1)+Y(5,1)*SIN(Y(3,1))
      XLU=Y(1,1)
      V=UL-Y(5,1)*COS(Y(3,1))
      YLU=0.0
      XVEL=Y(2,1)+Y(3,1)*Y(5,1)*COS(Y(3,1))+Y(6,1)*SIN(Y(3,1))
      WRITE(6,11) (TIME,X,XLU,V,YLU,VACCEL,XVEL)
   99 DO 999 K=1,6
  999 AY(K)=Y(K,N)
      CALL RAT(AY,T,F,Z,P1,P5,P8)
      DO 88 K=1,6
   88 Q(K,1)=H*T(K)
      DO 78 K=1,6
   78 AY(K)=Y(K,N)+0.5*Q(K,1)
      CALL RAT(AY,T,F,Z,P1,P5,P8)
      DO 89 K=1,6
   89 Q(K,2)=H*T(K)
      DO 79 K=1,6
   79 AY(K)=Y(K,N)+0.5*Q(K,2)
      CALL RAT(AY,T,F,Z,P1,P5,P8)
      DO 90 K=1,6
   90 Q(K,3)=H*T(K)
      DO 80 K=1,6
   80 AY(K)=Y(K,N)+Q(K,3)
      CALL RAT(AY,T,F,Z,P1,P5,P8)
      DO 91 K=1,6
   91 Q(K,4)=H*T(K)
      DO 92 K=1,6
   92 R(K)=(1.0/6.0)*(Q(K,1)+2.0*Q(K,2)+2.0*Q(K,3)+Q(K,4))
      DO 93 K=1,6
   93 Y(K,M)=Y(K,N)+R(K)
  100 CONTINUE
```

```
      J=3
      DO 110 N=4,20000
      I=0
      J=J+1
      DO 81 K=1,6
   81 AY(K)=Y(K,2)
      CALL RAT(AY,T,F,Z,P1,P5,P8)
      DO 44 K=1,6
   44 YP(K,2)=T(K)
      DO 82 K=1,6
   82 AY(K)=Y(K,3)
      CALL RAT(AY,T,F,Z,P1,P5,P8)
      DO 45 K=1,6
   45 YP(K,3)=T(K)
      DO 83 K=1,6
   83 AY(K)=Y(K,4)
      CALL RAT(AY,T,F,Z,P1,P5,P8)
      DO 46 K=1,6
   46 YP(K,4)=T(K)
      DO 47 K=1,6
   47 Y(K,5)=Y(K,1)+(4.0*H/3.0)*(2.0*YP(K,2)-YP(K,3)+2.0*YP(K,4))
  101 DO 84 K=1,6
   84 AY(K)=Y(K,3)
      CALL RAT(AY,T,F,Z,P1,P5,P8)
      DO 33 K=1,6
   33 S(K,3)=T(K)
      DO 85 K=1,6
   85 AY(K)=Y(K,4)
      CALL RAT(AY,T,F,Z,P1,P5,P8)
      VACCEL=(Y(4,4)**2*Y(5,4)-T(6))*COS(Y(3,4))+(2.0*Y(4,4)*Y(6,4)+T(4)
     1*Y(5,4))*SIN(Y(3,4))
      XPDD=T(2)
      VFORCE=G*(UMP+UMH+2.0*UMS+WL2*P1)+F+2.0*(DM*AY(6)/P5+(AY(6)/Z)
     1*(TF/(SQRT(P5))))-2.0*WL*AY(6)**2+((WL*P1*P8+2.0*UISA)/P5)*T(6)
     2+((WL*P1*P8+2.0*UISA)/(P5**2))+(TT*AY(6)**2/(2.0*PI))
      DO 34 K=1,6
   34 S(K,4)=T(K)
      DO 86 K=1,6
   86 AY(K)=Y(K,5)
      CALL RAT(AY,T,F,Z,P1,P5,P8)
      DO 35 K=1,6
   35 S(K,5)=T(K)
      DO 22 K=1,6
   22 YN(K)=Y(K,3)+(H/3.0)*(S(K,3)+4.0*S(K,4)+S(K,5))
      DO 23 K=1,6
   23 U(K)=ABS(YN(K)-Y(K,5))
      DO 24 K=1,6
      IF(U(K).GT.SMALL) GO TO 102
   24 CONTINUE
      GO TO 103
  102 DO 25 K=1,6
   25 Y(K,5)=YN(K)
      I=I+1
      GO TO 101
```

```
103 DO 26 K=1,6
    DO 27 L=1,3
    LL=L+1
 27 Y(K,L)=Y(K,LL)
 26 CONTINUE
    DO 28 K=1,6
 28 Y(K,4)=YN(K)
    IF(J.NE.50) GO TO 104
    J=0
    TIME=N*H
    X=Y(1,4)+Y(5,4)*SIN(Y(3,4))
    XLU=XODOT*TIME
    YLU=YODOT*TIME-0.5*5.47*TIME**2
    V=UL-Y(5,4)*COS(Y(3,4))
    XVEL=Y(4,4)*Y(5,4)*COS(Y(3,4))+Y(6,4)*SIN(Y(3,4))+Y(2,4)
    WRITE(6,11)(TIME,X,XLU,V,YLU,VACCEL,XVEL,Y(3,4),Y(1,4),Y(2,4),
   1VFORCE,XPDD)
    WRITE(6,17)(I)
104 IF (Y(5,4).GT.ULL) GO TO 120
110 CONTINUE
120 WRITE(6,12)
    END
N XQT JUMP2
 0.48,0.016,0.685,1.25,0.82
 FIN
```

NATIONAL AERONAUTICS AND SPACE ADMINISTRATION
WASHINGTON, D.C. 20546

OFFICIAL BUSINESS

FIRST CLASS MAIL

POSTAGE AND FEES PAI
NATIONAL AERONAUTICS
SPACE ADMINISTRATION

"The aeronautical and space activities of the United States shall be conducted so as to contribute . . . to the expansion of human knowledge of phenomena in the atmosphere and space. The Administration shall provide for the widest practicable and appropriate dissemination of information concerning its activities and the results thereof."

—NATIONAL AERONAUTICS AND SPACE ACT OF 1958

NASA SCIENTIFIC AND TECHNICAL PUBLICATIONS

TECHNICAL REPORTS: Scientific and technical information considered important, complete, and a lasting contribution to existing knowledge.

TECHNICAL NOTES: Information less broad in scope but nevertheless of importance as a contribution to existing knowledge.

TECHNICAL MEMORANDUMS: Information receiving limited distribution because of preliminary data, security classification, or other reasons.

CONTRACTOR REPORTS: Scientific and technical information generated under a NASA contract or grant and considered an important contribution to existing knowledge.

TECHNICAL TRANSLATIONS: Information published in a foreign language considered to merit NASA distribution in English.

SPECIAL PUBLICATIONS: Information derived from or of value to NASA activities. Publications include conference proceedings, monographs, data compilations, handbooks, sourcebooks, and special bibliographies.

TECHNOLOGY UTILIZATION PUBLICATIONS: Information on technology used by NASA that may be of particular interest in commercial and other non-aerospace applications. Publications include Tech Briefs, Technology Utilization Reports and Notes, and Technology Surveys.

Details on the availability of these publications may be obtained from:

SCIENTIFIC AND TECHNICAL INFORMATION DIVISION

NATIONAL AERONAUTICS AND SPACE ADMINISTRATION

Washington, D.C. 20546